LA-UR-20-30408

Approved for public release; distribution is unlimited.

Title: A Virtual Element Method for the Full MHD system

Author(s): Naranjo Alvarez, Sebastian
Bokil, Vrushali A.
Gyrya, Vitaliy
Manzini, Gianmarco

Intended for: Report

Issued: 2020-12-22

A Virtual Element Method for the Full MHD system

S. Naranjo Alvarez [a] , V. Bokil [b] , V. Gyrya [c] , and G. Manzini [d]

[a] *Department of Mathematics, Oregon State University, Corvallis, OR 97331 USA,* e-mail: naranjos@math.oregonstate.edu

[b] *Department of Mathematics, Oregon State University, Corvallis, OR 97331 USA,* e-mail: bokilv@math.oregonstate.edu

[c] *Group T-5, Theoretical Division, Los Alamos National Laboratory, Los Alamos, 87545 NM, USA;* e-mail: vitaliy_gyrya@lanl.gov

[d] *Group T-5, Theoretical Division, Los Alamos National Laboratory, Los Alamos, 87545 NM, USA;* e-mail: gmanzini@lanl.gov

Abstract

In this manuscript we present a novel discretization for the incompressible MHD system. Our approach follows the framework of the Virtual Element Method and offers two main advantages. The method can be implemented in unstructured meshes making it highly versatile and capable of handling a wide array of problems involving interfaces, free-boundaries or adaptive refinements on the mesh. The second advantage involves the divergence of the magnetic field, our approach guarantees that it remains solenoidal. We include a theoretical proof of the condition on the magnetic field as well as energy estimates and a well-posedness study. The latter sheds light as to the stability properties of the method.

Key words: Maxwell equations, resistive MHD, virtual element method, polytopal mesh

1. Introduction

The number of applications involving magnetized fluids has skyrocketed in the modern age. With this interest in mind great efforts have been devoted to predict their behavior. To this end a series of models have been developed. One approach that has withstood the test of time and has become standard goes by the name of Magneto-hydrodynamics (MHD). MHD can be thought of as a coupling between fluid flow and electromagnetics, thus models in MHD are PDE models. In this manuscript we consider one such model. The electromagnetics are modelled using Maxwell's equations while the motion is modelled using conservation principles, namely conservation of momentum and mass. These two are coupled since momentum is influenced by the Lorentz force, simultaneously the fluid velocity influences the electric and magnetic fields which in turn generate the Lorentz force. The details of the model, its derivation and properties are well-understood, readers interested are referred to [17, 31].

The topic of this manuscript is in developing a novel discretization for the aforementioned model. We follow the framework of the Virtual Element Method (VEM). This method came about as a re-framing of the older Mimetic Finite Difference Method (MFD), see [13]. The guiding philosophy of the MFD method relies on coming up with a discrete mimicry of vector and tensor calculus. It is within this discrete version that the differential system can be posed. Thus, MFD discretizations closely resemble the continuous system. Often times this implies that important properties of model have their discrete counterpart. A second advantage involves the mesh. The MFD method was developed with care to guarantee that implementations can be done in a large variety of meshes allowing the cells to have general geometries. The VEM inherits both of these properties while preserving a presentation that is similar to that of the classic Finite Element Method (FEM), thus results and techniques from FEM can be imported over to VEM. These features imply that VEM has important advantages over more classical discretization methods. The generality of on the mesh makes VEM highly versatile. In problems where the boundary deforms in time, as is the case with gases, or in problems where there are oddly shaped material interfaces it is of the utmost importance that the mesh fit these characteristics. There is also the case of adaptive mesh refinement (AMR). In order to make the best of computation resources a commonly used technique involves refining the mesh in the parts of the computational domain where greater accuracy is required while the rest of the domain remains relatively coarse. The process of refining the mesh in this way often times yields meshes with irregular structures requiring that the discretization method be capable of handling these traits. We also note that the numerical dispersion can be greatly reduced on select polygonal meshes, see [18,23]. In these works, the Finite Difference Time Domain (FDTD) method by Yee was applied to a grid of hexagonal prisms and yields much less numerical dispersion and anisotropy than on the grids that are usually considered in the formulation of Yee's method, i.e., regular hexahedral cells. One final advantage that we stress involves the divergence of the magnetic field. As is stated in one of Maxwell's equations, the magnetic field should remain diverge-free. This condition is not an additional equation since it results as a consequence of Faraday's Law. However, care needs to be taken when discretizing the system to make sure that the condition is also preserved at the discrete level, violating this condition will yield fictitious forces that will render simulations unfaithful to the true physics, see [7]. Because we closely resemble the continuous system and such a system satisfies the condition on the divergence of the magnetic field it is the case that a VEM for MHD will provide with solenoidal approximations to the magnetic field automatically. This is a fact that is proven theoretically in Corollary 6.2 and verified numerically in Section 7.1.

The present work builds on [32] where we develop a VEM for the subsystem involving the electromagnetics exclusively. Here, we extend to a VEM that simulates both the electromagnetics and fluid flow. We borrow the definition of the virtual elements from [4, 35]. In the VEM framework when restricted to each cell the functions in the modelling spaces come about as solutions to a system of local differential equations. In principle, one could use a different numerical method to approximate these functions. This would be highly inefficient, the name of the game in VEM is to come up with approximations using only the degrees of freedom. Thus, avoiding having to compute the functions pointwise. To do this the literature introduces a series of projectors onto polynomial spaces, the most important of which is the L^2-orthogonal projector. Unfortunately, this projector is not computable in the spaces used to model the electric field. The general strategy involves an enhancement process, see [1]. This approach has been proven to be useful in problems involving Maxwell's equations, see [11, 12]. However, in our case this enhancement invalidates a De-Rham diagram which turns out to be very important in order for our approximation to the magnetic field to be solenoidal. Here, as in [32], we propose a novel strategy that involves using oblique projectors and avoids the enhancement process altogether.

Moreover, the continuous model involves several non-linearities we also propose a Jacobian-Free Newton-Krylov Method. This approach is very similar to more classic Newton method, the main difference lies in the fact that the Jacobian is approximated using a Newton quotient. By avoiding the computation of the Jacobian we save on computational resources while preserving the quadratic convergence that the classical Newton method yields. This method has been widely studied, see [24] for general exposition and theory and [9] for an application specifically in MHD. Here we also present a proof that each of the linear solves is well-posed. This is done by taking advantage of the saddle-point nature of the problem and is an application of the more general BBL theory. The well-posedness guarantees a degree of stability in our computations but more importantly serves as a basis to come up with efficient preconditioners. The development of such preconditioners is outside the scope of this manuscript and would be an application of the theory presented in [28]. This theory has been successfully applied to MHD systems for a different linearization strategy, see [29]. We also note that other physics-based preconditioners have been developed, see [9, 10].

This manuscript is structured as follows: first, in Section 2 we introduce some important notation. Next, in Section 3 we present both the continuous and discrete models. Although, the modelling spaces are introduced in this section, their formal definition is a topic for Section 4, in this section we also propose the aforemention oblique projector. Our method satisfies a series of important energy estimates that provide evidence as to the stability of the method, these are presented in Section 5. Then, in Section 6, we present the details of the linearization strategy along with a proof that the approximate magnetic field is divergence free and of well-posedness of the linear solve. In Section 7 we present a series of numerical experiments that we wish to perform, they include a convergence test, a model of the well-known cavity problem and a model for magnetic reconnection. Finally, in Section 8 we summarize the findings and expose further work.

2. Notation

This section is dedicated to describing the notation we will use in throughout this article. We consider $\Omega \subset \mathbb{R}^2$ be an open domain with polygonal boundary. At the discrete level we will define Ω_h to be a mesh of Ω with mesh-size $h > 0$. Analysis and development of any finite element method will require a series of functional spaces. We will formally define them below over an open set $\omega \subset \Omega$.

$$L^2(\omega) := \big\{ v : \omega \to \mathbb{R} : \int_\omega |v|^2 < \infty \big\}, \tag{1a}$$

$$L_0^2(\omega) := \big\{ v \in L^2(\omega) : \int_\omega v = 0 \big\}, \tag{1b}$$

$$H^1(\omega) := \big\{ v \in L^2(\omega) : \nabla v \in \left[L^2(\omega) \right]^2 \big\}, \tag{1c}$$

$$H_0^1(\omega) := \big\{ v \in H^1(\omega) : v_{|\partial v} \equiv 0 \big\}, \tag{1d}$$

$$H(\mathbf{rot}; \omega) := \big\{ v \in L^2(\omega) : \mathbf{rot}\, v \in \left[L^2(\omega) \right]^2 \big\} \tag{1e}$$

$$H_0(\mathbf{rot}; \omega) := \big\{ v \in H(\mathbf{rot}; \omega) : v_{|\partial v} \equiv 0 \big\}, \tag{1f}$$

$$H(\mathrm{div}; \omega) := \big\{ \boldsymbol{v} \in [L^2(\omega)]^2 : \mathrm{div}\, \boldsymbol{v} \in L^2(\omega) \big\} \tag{1g}$$

$$L^\infty(\omega) := \{ \boldsymbol{w} : \omega \to \mathbb{R} : \exists\, C > 0\, ; |\boldsymbol{w}| < C \text{ almost everywhere} \} \tag{1h}$$

where $\mathbf{rot}\, v = (\partial v / \partial y, -\partial v / \partial x)^T$. We note that throughout this paper we use the symbol $\triangle$ to denote both the scalar and vector Laplacian. Finally, the space $H^{-1}(\omega)$ to be the topological dual of $H_0^1(\Omega)$, i.e., the space of all continuous linear functionals of $H^{-1}(\omega)$. We note that we use the letter C to denote a positive constants whose value may change from instance to instance. This constant will always be independent of the mesh characteristics and time step.

3. The 2-D MHD Formulation

In this article we consider the resistive MHD system, over the domain Ω, as defined below.

$$\text{Conservation of Momentum :}\quad \frac{\partial}{\partial t}\boldsymbol{u} - R_e^{-1} \triangle \boldsymbol{u} - J \times \boldsymbol{B} + \nabla p = \boldsymbol{f}, \tag{2a}$$

$$\text{Faraday's Law :}\quad \frac{\partial}{\partial t}\boldsymbol{B} + \mathbf{rot}\, E = \mathbf{0}, \tag{2b}$$

$$\text{Ohm's Law :}\quad E + \boldsymbol{u} \times \boldsymbol{B} = J \tag{2c}$$

$$\text{Ampere's Law :}\quad J - R_m^{-1} \mathrm{rot}\, \boldsymbol{B} = \mathbf{0}, \tag{2d}$$

$$\text{Gauss's Law :}\quad \mathrm{div}\, \boldsymbol{B} = 0, \tag{2e}$$

$$\text{Conservation of Mass :}\quad \mathrm{div}\, \boldsymbol{u} = 0. \tag{2f}$$

where the source function $f \in H^{-1}(\Omega)$, the constants R_e and R_m are the viscous and magnetic Reynolds numbers. This system is closed by considering the Dirichlet boundary data and initial conditions

$$\boldsymbol{u}(x, y, 0) = \boldsymbol{u}_0(x, y), \quad \boldsymbol{B}(x, y, 0) = \boldsymbol{B}_0(x, y) \quad \text{in} \quad \Omega, \tag{3a}$$

$$\boldsymbol{u} = \boldsymbol{u}_b, \quad E = E_b \quad \text{on} \quad \partial\Omega. \tag{3b}$$

Where we must assume the compatibility condition

$$\int_{\partial\Omega} \boldsymbol{u}_b \cdot \boldsymbol{n} ds = 0. \tag{4}$$

We note that, in the equation describing conservation of momentum, we have dropped a convective term of the form $(\boldsymbol{u} \cdot \nabla)\boldsymbol{u}$. This is done for the sake of simplicity. This term is quadratic in the velocity field which makes it negligible with respect to the rest when the flow is slow.

The first step in coming up with a compatible discretization is to consider the variational formulation for the system (2). Such a formulation is

Find $(\boldsymbol{u}, \boldsymbol{B}, E, p) \in C^1\left([0,T], \left[H^1(\Omega)\right]^2\right) \times C^1\left([0,T], H(div; \Omega)\right) \times C\left([0,T], H_0(\boldsymbol{rot}; \Omega)\right) \times C\left([0,T], L_0^2(\Omega)\right)$ *such that for any* $(\boldsymbol{v}, \boldsymbol{C}, D, q) \in \left[H_0^1(\Omega)\right]^2 \times H(div; \Omega) \times H_0(\boldsymbol{rot}; \Omega) \times L_0^2(\Omega)$ *it holds*

$$\Big(\frac{\partial}{\partial t}\boldsymbol{u},\boldsymbol{v}\Big)+R_e^{-1}\Big(\nabla\boldsymbol{u},\nabla\boldsymbol{v}\Big)-\Big(J\times\boldsymbol{B},\boldsymbol{v}\Big)-\Big(p,\operatorname{div}\boldsymbol{v}\Big)=\Big(\boldsymbol{f},\boldsymbol{v}\Big), \tag{5a}$$

$$\Big(\operatorname{div}\boldsymbol{u},q\Big)=0, \tag{5b}$$

$$\Big(\frac{\partial}{\partial t}\boldsymbol{B},\boldsymbol{C}\Big)+\Big(\mathbf{rot}\,E,\boldsymbol{C}\Big)=0, \tag{5c}$$

$$\Big(J,D\Big)-R_m^{-1}\Big(\boldsymbol{B},\mathbf{rot}\,D\Big)=0, \tag{5d}$$

$$J=E+\boldsymbol{u}\times\boldsymbol{B},\quad \boldsymbol{u}(\cdot,0)=\boldsymbol{u}_0,\quad \boldsymbol{B}(\cdot,0)=\boldsymbol{B}_0 \text{ with } \operatorname{div}\boldsymbol{B}_0=0. \tag{5e}$$

As is the case in any conforming Galerkin method, we will consider a set of subspaces of $\left[H^1(\Omega)\right]^2$, $H(\mathrm{div};\Omega)$, $H_0(\mathbf{rot};\Omega)$ and $L^2_0(\Omega)$ which we denote as $\mathcal{TV}_h,\mathcal{E}_h,\mathcal{V}_h$ and $\mathcal{P}_{h,0}$ respectively. These spaces depend on the mesh Ω_h and their precise definition of these spaces is the topic of section 4. Viewing the system (2b) as a coupling between the fluid flow and electromagnetics these spaces can be seen as belonging to one of two classes . The spaces that relate to the fluid flow are $\mathcal{TV}_h$ and $\mathcal{P}_h$, they must be carefully selected to guarantee the so-call LLB condition. In One hand, this condition will imply that approximations of the pressure are necessarily of lower order than those of the velocity field. On the other hand, violating this condition is a clear guarantee that the numerical method is unstable. The electromagnetics are approximated using $\mathcal{V}_h$ and $\mathcal{E}_h$. They have to be carefully designed to form a commuting De-Rham diagram. This is done to guarantee that, at the discrete level, the magnetic field remains solenoidal or divergence-free. This is critical in if we are interested in realistically modelling physical phenomena.

The discrete form of the variational formulation (5) is

Find $\left\{(\boldsymbol{u}_h^n,\boldsymbol{B}_h^n)\right\}_{n=0}^N\subset\mathcal{TV}_h\times\mathcal{E}_h$ *and* $\left\{(E_h^{n+\theta},p_h^{n+\theta}))\right\}_{n=0}^{N-1}\subset\mathcal{V}_h\times\mathcal{P}_{h,0}$ *such that for all* $(\boldsymbol{v}_h,\boldsymbol{C}_h,D_h,q_h)\in\mathcal{TV}_{h,0}\times\mathcal{E}_h\times\mathcal{V}_{h,0}\times\mathcal{P}_{h,0}$ *it holds:*

$$\Big(\frac{\boldsymbol{u}_h^{n+1}-\boldsymbol{u}_h^n}{\Delta t},\boldsymbol{v}_h\Big)_{\mathcal{TV}_h}+R_e^{-1}\Big[\boldsymbol{u}_h^{n+\theta},\boldsymbol{v}_h\Big]_{\mathcal{TV}_h}+\underbrace{\Big(J_h^{n+\theta},\mathcal{I}^{\mathcal{V}_h}(\boldsymbol{v}_h\times\Pi^{RT}\boldsymbol{B}_h^{n+\theta})\Big)_{\mathcal{V}_h}}_{(1)}-$$
$$-\Big(\operatorname{div}\boldsymbol{v}_h,p_h^{n+\theta}\Big)_{\mathcal{P}_h}=\Big(\boldsymbol{f}_h,\boldsymbol{v}_h\Big)_{\mathcal{TV}_h}, \tag{6a}$$

$$\Big(\operatorname{div}\boldsymbol{u}_h^{n+\theta},q_h\Big)_{\mathcal{P}_h}=0, \tag{6b}$$

$$\Big(\frac{\boldsymbol{B}_h^{n+1}-\boldsymbol{B}_h^n}{\Delta t},\boldsymbol{C}_h\Big)_{\mathcal{E}_h}+\Big(\mathbf{rot}\,E_h^{n+\theta},\boldsymbol{C}_h\Big)_{\mathcal{E}_h}=0, \tag{6c}$$

$$\big(J_h^{n+\theta},D_h\big)_{\mathcal{V}_h}-R_m^{-1}\big(\boldsymbol{B}_h^{n+\theta},\mathbf{rot}\,D_h\big)_{\mathcal{E}_h}=0, \tag{6d}$$

$$\boldsymbol{u}_h^{n+\theta}=(1-\theta)\boldsymbol{u}_h^n+\theta\boldsymbol{u}_h^{n+1},\quad \boldsymbol{B}_h^{n+\theta}=(1-\theta)\boldsymbol{B}_h^n+\theta\boldsymbol{B}_h^{n+1}, \tag{6e}$$

$$J_h^{n+\theta}=E_h^{n+\theta}+\mathcal{I}^{\mathcal{V}_h}(\boldsymbol{u}_h^{n+\theta}\times\Pi^{RT}\boldsymbol{B}_h^{n+\theta}), \tag{6f}$$

$$\boldsymbol{u}_h^0=\mathcal{I}^{\mathcal{TV}_h}(\boldsymbol{u}_0),\quad \boldsymbol{B}_h^0=\mathcal{I}^{\mathcal{E}_h}(\boldsymbol{B}_0) \text{ with } \operatorname{div}\boldsymbol{B}_0=0. \tag{6g}$$

The term labeled (1) in (6a) comes about from the approximation:

$$-\Big(J\times\boldsymbol{B},\boldsymbol{v}\Big)=\Big(J,\boldsymbol{v}\times\boldsymbol{B}\Big)\approx\Big(J_h,\mathcal{I}^{\mathcal{V}_h}(\boldsymbol{v}_h\times\boldsymbol{B}_h)\Big)_{\mathcal{V}_h} \tag{7}$$

The reason we go through this trouble will become clear in section 5 when we come up with stability energy estimates.

4. The Virtual Elements

In this section we discuss the virtual element methods that we use in the discretization (6). To this end, we first introduce a family of mesh partitions of the computational domain Ω, here denoted by $\{\Omega_h\}_h$. Each mesh Ω_h is a collection of nonoverlapping, closed polygonal cells P with boundary P, area $|\mathsf{P}|$, and diameter h_{P}, such that $\overline{\Omega}=\cup_{\mathsf{P}}\mathsf{P}$, and is labelled by the mesh size parameter $h=\max_{\mathsf{P}}h_{\mathsf{P}}$. We denote each edge of $\partial\mathsf{P}$ by e and its length by $|\mathsf{e}|=h_{\mathsf{e}}$.

The mesh size parameter is assumed to be in the countable set of mesh sizes $\mathcal{H}\subset(0,+\infty)$ that ahs 0 as its unique accumulation point.

According to the "usual" VEM formulation **[Add citations]**, the family of meshes must be *regular* in the sense that the two following conditions hold for some non-negative real number ρ independent of h:

(M1) (*star-shapedness*): every polygonal cell P of every mesh Ω_h is star-shaped with respect to a disk of radius ρh_{P};

(M2) (*uniform scaling*): every edge $\mathsf{e} \in \partial\mathsf{P}$ of cell $\mathsf{P} \in \Omega_h$ satisfies $h_{\mathsf{e}} \geq \rho h_{\mathsf{P}}$.

These assumptions on the mesh regularity are not quite restrictive and allows us to use polygonal elements with very general geometric shapes, as for example nonconvex elements or elements with hanging nodes. It is worth noting that the hypotheses above can even be further relaxed as proposed, for example, in [**?**].

Some important implications of $(\mathbf{M1})$-$(\mathbf{M2})$ are:

(i) every polygonal element is *simply connected*;

(ii) the number of edges of each polygonal cell in the mesh family $\{\Omega_h\}_h$ is uniformly bounded;

(iii) a polygonal element cannot have *arbitrarily small* edges with respect to its diameter $h_{\mathsf{P}} \leq h$ for $h \to 0$.

and inequality $h_{\mathsf{P}}^2 \leq C(\rho)|\mathsf{P}|h_{\mathsf{P}}^2$ holds, with the obvious dependence of constant $C(\rho)$ on the mesh regularity factor ρ. It is worth mentioning that virtual element methods on polygonal or polyhedral meshes possibly containing "small edges" in 2D or "small faces" in 3D have been considered in Ref. [8] for the numerical approximation of the Poisson problem, which extends the results of work in Ref. [2].

We split the rest of the section in two subsection. In the first subsection, we discuss the virtual element spaces $\mathcal{TV}_h$ and $\mathcal{P}_{h,0}$ for the fluid part of the variational form of the MHD model (6), i.e., equations (6a), (6b), and (**??**). In the second subsection, we discuss the virtual element spaces $\mathcal{V}_h$ and $\mathcal{E}_h$ for the electromagnetic part of the variational form of the MHD model (6), i.e., equations (6c), (6d), and (**??**).

4.1. *Fluid flow*

The virtual element space used in the discretization of the Navier-Stokes part of the equations was oiginally proposed in [15, 35]. Here, we consider the "enhanced" formulation introduced in [14], which allows us to compute the L^2 orthogonal projection onto the polynomial subspace of the virtual element space Such operator is used in the construction of the approximate mass matrices.

4.1.1. *Vertex Space*

Let P be a mesh element and consider the finite dimensional space defined on $\partial\mathsf{P}$ as:

$$\mathbb{B}\left(\partial\mathsf{P}\right) := \left\{ v \in C^0(\partial\mathsf{P}) : v_{|\mathsf{e}} \in \mathbb{P}_2(\mathsf{e}) \ \forall \mathsf{e} \in \partial\mathsf{P} \right\}. \tag{8}$$

The local virtual element space for the fluid velocities is defined on P as

$$\mathbf{V}^h(\mathsf{P}) := \Big\{ \boldsymbol{v}_h \in \left[H^1(\mathsf{P})\right]^2 \ : \ \boldsymbol{v}_{h|\partial\mathsf{P}} \in \left(\mathbb{B}\left(\partial\mathsf{P}\right)\right)^2, \mathrm{div}\,\boldsymbol{v}_h \in \mathbb{P}_0(\mathsf{P}), \ -\triangle\boldsymbol{v}_h - \nabla s = \mathbf{0} \ \text{for some } s \in L^2_0(\mathsf{P}) \Big\}. \tag{9}$$

The following degrees of freedom are unisolvent for the vector-valued fields $\boldsymbol{v}_h \in \mathbf{V}^h(\mathsf{P})$:

- $(\mathbf{D_1})$: pointwise evaluations of $\boldsymbol{v}_h$ at the vertices of P;
- $(\mathbf{D_2})$: pointwise evaluations at $\boldsymbol{v}_h$ at the midpoint of the edges of $\partial\mathsf{P}$.

According to the enhancement strategy in [14], we modify the definition of the space $\mathbf{V}^h(\mathsf{P})$ as follows. First, we introduce the spaces:

$$\mathcal{G}_2\left(\mathsf{P}\right) := \nabla\mathbb{P}_3(\mathsf{P}), \quad \mathcal{G}_2^{\perp}\left(\mathsf{P}\right) := \Big\{ \boldsymbol{g}^{\perp} \in [\mathbb{P}_2(\mathsf{P})]^2 : \forall \boldsymbol{g} \in \mathcal{G}_2\left(\mathsf{P}\right) \quad \Big(\boldsymbol{g}^{\perp}, \boldsymbol{g}\Big) = 0 \Big\}, \tag{10}$$

and

$$\mathbf{U}^h(\mathsf{P}) := \Big\{ \boldsymbol{v}_h \in \left[H^1(\mathsf{P})\right]^2 \ : \boldsymbol{v}_{h|\partial\mathsf{P}} \in \left[\mathbb{B}\left(\partial\mathsf{P}\right)\right]^2, \mathrm{div}\,\boldsymbol{v}_h \in \mathbb{P}_0(\mathsf{P}), -\Delta\boldsymbol{v}_h - \nabla s = \boldsymbol{g}^{\perp} \tag{11}$$

$$\text{for some } s \in L^2_0(\mathsf{P}) \text{ and } \boldsymbol{g}^{\perp} \in \mathcal{G}_2^{\perp}\left(\mathsf{P}\right) \Big\}. \tag{12}$$

Then, we define the elliptic projection operator $\Pi_{\mathsf{P}}^{\nabla} : \mathbf{U}^h(\mathsf{P}) \to \left[\mathbb{P}_2(\mathsf{P})\right]^2$ that associates every vector-valued field $\boldsymbol{v}_h$ in $\mathbf{U}^h$ with $\Pi_{\mathsf{P}}^{\nabla}\boldsymbol{v}_h$, which is the solution of the variational problem:

$$\int_{\mathsf{P}} \nabla \Pi^{\nabla}_{\mathsf{P}} \boldsymbol{v}_h \cdot \nabla \boldsymbol{q}\, dV = \int_{\mathsf{P}} \nabla \boldsymbol{v}_h \cdot \nabla \boldsymbol{q}\, dV \quad \forall \boldsymbol{q} \in \left[\mathbb{P}_2(\mathsf{P})\right]^2 \tag{13a}$$

$$\sum_{\mathsf{V}} \Pi^{\nabla}_{\mathsf{P}} \boldsymbol{v}_h(\mathsf{V}) = \sum_{\mathsf{V}} \boldsymbol{v}_h(\mathsf{V}), \tag{13b}$$

where the sum above is taken over the vertices of P and the midpoints of every edge in P. The projector $\Pi^{\nabla}_{\mathsf{P}}$ can be computed using only the degrees of freedom $(\mathbf{Dv_1})$-$(\mathbf{Dv_2})$ (the details can be found in [14]). Then, we introduce the polynomial vector space

$$\mathcal{G}_2^{\perp}(\mathsf{P})/\mathbb{R}^2 := \left\{ \left(g_1, g_2\right)^T \in \mathcal{G}_2^{\perp}(\mathsf{P}) : \int_{\mathsf{P}} g_i dV = 0 \quad i = 1, 2 \right\}, \tag{14}$$

and we define the virtual element space $\mathcal{TV}_h(\mathsf{P})$ as the subspace of $\mathbf{U}^h$ such that:

$$\mathcal{TV}_h(\mathsf{P}) := \left\{ \boldsymbol{v}_h \in \mathbf{U}^h(\mathsf{P}) : \forall \boldsymbol{g}^{\perp} \in \mathcal{G}_2^{\perp}(\mathsf{P})/\mathbb{R}^2 \quad \left(\boldsymbol{v}_h - \Pi^{\nabla}_{\mathsf{P}} \boldsymbol{v}_h, \boldsymbol{g}^{\perp}\right) = 0 \right\}. \tag{15}$$

The unisolvency of the the degrees of freedom $(\mathbf{Dv_1})$-$(\mathbf{Dv_2})$ in $\mathcal{TV}_h(\mathsf{P})$ is proved in [35]. On this virtual element space we define the L^2-orthogonal projection $\Pi^0 : \mathcal{TV}_h(\mathsf{P}) \to [\mathbb{P}_2(\mathsf{P})]^2$, which associates every vector-valued field $\boldsymbol{v}_h \in \mathbf{U}^h$ with $\Pi^0 \boldsymbol{v}_h \in \left[\mathbb{P}_2(\mathsf{P})\right]^2$, which is the solution of the variational problem:

$$\int_{\mathsf{P}} \Pi^0 \boldsymbol{v}_h \cdot \boldsymbol{q} dV = \int_{\mathsf{P}} \boldsymbol{v}_h \cdot \boldsymbol{q} dV \quad \forall \boldsymbol{q} \in \left[\mathbb{P}_2(\mathsf{P})\right]^2.$$

The polynomial projection $\Pi^0 \boldsymbol{v}_h$ is computable using only the degrees of freedom $(\mathbf{Dv_1})$-$(\mathbf{Dv_2})$ of $\boldsymbol{v}_h$ (see, again, Ref. [35]).

Using the orthogonal projection Π^0, we define the inner product and the semi-inner product on $\mathcal{TV}_h(\mathsf{P})$ by

$$\begin{aligned}
&\forall \boldsymbol{u}_h, \boldsymbol{v}_h \in \mathcal{TV}_h(\mathsf{P}) : \\
&\quad \left(\boldsymbol{u}_h, \boldsymbol{v}_h\right)_{\mathcal{TV}_h(\mathsf{P})} = \left(\Pi^0 \boldsymbol{u}_h, \Pi^0 \boldsymbol{v}_h\right) + \mathcal{S}_{\mathsf{P}}^{\mathcal{TV}_h}\left((\mathrm{I} - \Pi^0 \boldsymbol{u}_h, (\mathrm{I} - \Pi^0)\boldsymbol{v}_h\right), \\
&\quad \left[\boldsymbol{u}_h, \boldsymbol{v}_h\right]_{\mathcal{TV}_h(\mathsf{P})} = \left(\nabla \Pi^{\nabla}_{\mathsf{P}} \boldsymbol{u}_h, \nabla \Pi^{\nabla}_{\mathsf{P}} \boldsymbol{v}_h\right) + \mathcal{T}_{\mathsf{P}}^{\mathcal{TV}_h}\left(\nabla(\mathrm{I} - \Pi^{\nabla}_{\mathsf{P}})\boldsymbol{u}_h, \nabla(\mathrm{I} - \Pi^{\nabla}_{\mathsf{P}})\boldsymbol{v}_h\right),
\end{aligned}$$

where I is the identity matrix and $\mathcal{S}_{\mathsf{P}}^{\mathcal{TV}_h}$ and $\mathcal{T}_{\mathsf{P}}^{\mathcal{TV}_h}$ can be any bilinear form that satisfies the following conditions:

$$\begin{aligned}
&\exists\, s_*,\, s^* > 0 \text{ such that } \forall \boldsymbol{v}_h \in \mathcal{TV}_h(\mathsf{P}) \cap \ker\Pi^0 : \; s_* \|\boldsymbol{v}_h\|^2_{0,\Omega} \leq \mathcal{S}_P^{\mathcal{TV}_h}(\boldsymbol{v}_h, \boldsymbol{v}_h) \leq s^* \|\boldsymbol{v}_h\|^2_{0,\Omega}, \\
&\exists\, t_*,\, t^* > 0 \text{ such that } \forall \boldsymbol{v}_h \in \mathcal{TV}_h(\mathsf{P}) \cap \ker\Pi^{\nabla}_{\mathsf{P}} : \; t_* \|\nabla \boldsymbol{v}_h\|^2_{0,\Omega} \leq \mathcal{T}_P^{\mathcal{TV}_h}(\nabla \boldsymbol{v}_h, \nabla \boldsymbol{v}_h) \leq t^* \|\nabla \boldsymbol{v}_h\|^2_{0,\Omega}.
\end{aligned} \tag{17}$$

Different choices of $\mathcal{S}_{\mathsf{P}}^{\mathcal{TV}_h}$ and $\mathcal{T}_{\mathsf{P}}^{\mathcal{TV}_h}$ are possible and examples can be found in [16,30]. The definitions in (16) provide symmetric bilinear forms that satisfy two fundamental properties: the **polynomial consistency** and the **stability**. These two properties are settled in the following lemma.

Lemma 4.1 *Let $\left(\cdot,\cdot\right)_{\mathcal{TV}_h(P)}$ and $\left[\cdot,\cdot\right]_{\mathcal{TV}_h(P)}$ be teh two inner and semi-inner products defined in* (16). *The following two properties hold:*

- ***polynomial consistency**: for every $\boldsymbol{v}_h \in \mathcal{TV}_h(P)$ and vectr polynomial $\boldsymbol{q} \in \mathbb{P}_2(P)$ it holds that:*

$$\left(\boldsymbol{v}_h, \boldsymbol{q}\right)_{\mathcal{TV}_h(P)} = \left(\boldsymbol{v}_h, \boldsymbol{q}\right), \quad \left[\boldsymbol{v}_h, \boldsymbol{q}\right]_{\mathcal{TV}_h(P)} = \left(\nabla \boldsymbol{v}_h, \nabla \boldsymbol{q}\right). \tag{18}$$

- ***stability**: there exists two pairs of positive real constants (α_*, α^*) and (γ_*, γ^*), which ar independent of h, such that for any $\boldsymbol{v}_h \in \mathcal{TV}_h(P)$ it holds that:*

$$\alpha_* \|\boldsymbol{v}_h\|^2_{0,P} \leq \left(\boldsymbol{v}_h, \boldsymbol{v}_h\right)_{\mathcal{TV}_h(P)} \leq \alpha^* \|\boldsymbol{v}_h\|^2_{0,P} \tag{19}$$

and

$$\gamma_* \|\nabla \boldsymbol{v}_h\|^2_{0,P} \leq \left[\boldsymbol{v}_h, \boldsymbol{v}_h\right]_{\mathcal{TV}_h(P)} \leq \alpha^* \|\gamma \boldsymbol{v}_h\|^2_{0,P}. \tag{20}$$

$$\tag{21}$$

Proof.
(i). The polynomial consistency is an immediate consequence of the definitions in (16) and the fact that $\Pi^{\nabla}_{\mathsf{P}} \boldsymbol{q} = \boldsymbol{q}$ and $\Pi^0_{\mathsf{P}} \boldsymbol{q} = qv$ for every vector polynomial $\boldsymbol{q} \in \mathbb{P}_2(\mathsf{P})$. Indeed, we first note that $\mathcal{S}_{\mathsf{P}}^{\mathcal{TV}_h}(\boldsymbol{v}_h, \boldsymbol{q}) = \mathcal{T}_{\mathsf{P}}^{\mathcal{TV}_h}(\boldsymbol{v}_h, \boldsymbol{q}) = 0$. Then, from the definition of Π^0_{P} and $\Pi^{\nabla}_{\mathsf{P}}$, we then see that for every vector polynomial $\boldsymbol{q} \in \mathbb{P}_2(\mathsf{P})$ it holds that

$$\begin{aligned}\big(\Pi^0 \boldsymbol{v}_h, \Pi^0 \boldsymbol{q}\big) &= \big(\Pi^0 \boldsymbol{v}_h, \boldsymbol{q}\big) = \big(\boldsymbol{v}_h, \boldsymbol{q}\big),\\ \big(\nabla\Pi^{\nabla}_{\mathsf{P}} \boldsymbol{v}_h, \nabla\Pi^{\nabla}_{\mathsf{P}} \boldsymbol{q}\big) &= \big(\nabla\Pi^{\nabla}_{\mathsf{P}} \boldsymbol{v}_h, \nabla \boldsymbol{q}\big) = \big(\nabla\boldsymbol{v}_h, \nabla\boldsymbol{q}\big).\end{aligned} \tag{22}$$

(ii). Since the proof of (20) follows from the same argument, we restrict the proof to the first inequality First, we note that

$$\begin{aligned}\|\boldsymbol{v}_h\|^2_{0,\mathsf{P}} = \big(\|\Pi^0\boldsymbol{v}_h\|_{0,\mathsf{P}} + \|I-\Pi^0\boldsymbol{v}_h\|_{0,\mathsf{P}}\big)^2 \leq \\ 2\left(\|\Pi^0\boldsymbol{v}_h\|^2_{0,\mathsf{P}} + \|I-\Pi^0\boldsymbol{v}_h\|^2_{0,\mathsf{P}}\right) \leq (\alpha_*)^{-1}\Big(\boldsymbol{v}_h,\boldsymbol{v}_h\Big)_{\mathcal{TV}_h(\mathsf{P})}\end{aligned}$$

where $\alpha_* = (\max\{s^*, 2\})^{-1}$. To attain the upper bound of (20) we use

$$\begin{aligned}\Big(\boldsymbol{v}_h,\boldsymbol{v}_h\Big)_{\mathcal{TV}_h(\mathsf{P})} &\leq \|\Pi^0\boldsymbol{v}_h\|^2_{0,\mathsf{P}} + s^*\|(I-\Pi^0)\boldsymbol{v}_h\|^2_{0,\mathsf{P}}\\ &\leq \|\Pi^0\|^2\|\boldsymbol{v}_h\|^2_{0,\mathsf{P}} + s^*\|I-\Pi^0\|^2\|\boldsymbol{v}_h\|^2_{0,\mathsf{P}}\\ &\leq \alpha^*\|\boldsymbol{v}_h\|^2_{0,\mathsf{P}},\end{aligned}$$

where $\alpha^* = \max\{\|\Pi^0\|^2, s^*\|I-\Pi^0\|^2\}$. □

Finally, we define the global virtual element spaces:

$$\mathcal{TV}_h = \Big\{\boldsymbol{v}_h \in \big[H^1(\Omega)\big]^2 : \forall \mathsf{P}\in\Omega_h \quad \boldsymbol{v}_{h|\mathsf{P}} \in \mathcal{TV}_h(\mathsf{P})\Big\} \quad \text{and} \quad \mathcal{TV}_{h,0} = \mathcal{TV}_h \cap \big[H^1_0(\Omega)\big]^2, \tag{23}$$

and extend the local bilinear forms in (16) to $\mathcal{TV}_h$ as follows:

$$\begin{aligned}\forall \boldsymbol{u}_h,\boldsymbol{v}_h\in\mathcal{TV}_h: \quad \big(\boldsymbol{u}_h,\boldsymbol{v}_h\big)_{\mathcal{TV}_h} &= \sum_{\mathsf{P}\in\Omega_h}\big(\boldsymbol{u}_h,\boldsymbol{v}_h\big)_{\mathcal{TV}_h(\mathsf{P})},\\ \big[\boldsymbol{u}_h,\boldsymbol{v}_h\big]_{\mathcal{TV}_h} &= \sum_{\mathsf{P}\in\Omega_h}\big[\boldsymbol{u}_h,\boldsymbol{v}_h\big]_{\mathcal{TV}_h(\mathsf{P})}.\end{aligned} \tag{24}$$

These forms induce the two norms and the seminorm on $\mathcal{TV}_h$ given by

$$|||\boldsymbol{v}_h|||^2_{\mathcal{TV}_h} = \big(\boldsymbol{v}_h,\boldsymbol{v}_h\big)_{\mathcal{TV}_h}, \quad \big|\boldsymbol{v}_h\big|^2_{\mathcal{TV}_h} = \big[\boldsymbol{v}_h,\boldsymbol{v}_h\big]_{\mathcal{TV}_h}, \tag{25a}$$

$$|||\boldsymbol{v}_h|||^2_{1,\mathcal{TV}_h} = |||\boldsymbol{v}_h|||^2_{\mathcal{TV}_h} + \big|\boldsymbol{v}_h\big|^2_{\mathcal{TV}_h}, \tag{25b}$$

and the norm in the topological dual space of $\mathcal{TV}_{h,0}$ denoted by $\mathcal{TV}'_{h,0}$:

$$|||\boldsymbol{f}_h|||_{-1,\mathcal{TV}_h} = \sup_{\boldsymbol{v}_h\in\mathcal{TV}_{h,0}} \frac{\big(\boldsymbol{f}_h,\boldsymbol{v}_h\big)_{\mathcal{TV}_h}}{\big|\boldsymbol{v}_h\big|_{\mathcal{TV}_h}} \qquad \forall \boldsymbol{f}_h\in\mathcal{TV}'_{h,0}. \tag{26}$$

These forms will inherit the local stability property as summarized in the following theorem.

Theorem 4.2 *The norms and semi-norm in* (25) *are equivalent to the* $[L^2(\Omega)]^2$ *and* $\big[H^1(\Omega)\big]^2$ *inner products and semi-inner product respectively. In other words, there exists* $\beta_*, \beta^* > 0$ *independent of the mesh characteristics such that for any* $\boldsymbol{v}_h\in\mathcal{TV}_h$ *it holds*

$$\beta_*\|\boldsymbol{v}_h\|^2_{0,\Omega} \leq |||\boldsymbol{v}_h|||_{\mathcal{TV}_h} \leq \beta^*\|\boldsymbol{v}_h\|^2_{0,\Omega}, \tag{27a}$$

$$\beta_*\|\nabla\boldsymbol{v}_h\|^2_{0,\Omega} \leq |||\boldsymbol{v}_h|||^{2,\nabla}_{\mathcal{TV}_h} \leq \beta^*\|\nabla\boldsymbol{v}_h\|^2_{0,\Omega}, \tag{27b}$$

$$\beta_*\|\boldsymbol{v}_h\|^2_{1,\Omega} \leq |||\boldsymbol{v}_h|||^2_{1,\mathcal{TV}_h} \leq \beta^*\|\boldsymbol{v}_h\|^2_{0,\Omega}. \tag{27c}$$

Proof. The three equivalences are a consequence of Lemma 4.1 and the fact the constants α_*, α^*, γ_* and γ^* are independent of h (and the mesh element), so we can simply take $\beta_* = \min(\alpha_*,\gamma_*)$ and $\beta^* = \min(\alpha^*,\gamma^*)$ to obtain the inequalities in (27). □

In order to embed functions into the space $\mathcal{TV}_h$, we define the Fortin operator $\mathcal{I}^{\mathcal{TV}_h} : [C^\infty(\mathsf{P})]^2 \subset \big[H^1(\mathsf{P})\big]^2 \to \mathcal{TV}_h(\mathsf{P})$ for any cell P in the mesh Ω_h by requiring that $\mathcal{I}^{\mathcal{TV}_h}(\boldsymbol{v}_h)_{|\mathsf{P}}$ and $\boldsymbol{v}_{h|\mathsf{P}}$ share the same degrees of freedom. Such an operator is well defined by the unisolvency condition on the space.

4.1.2. *The cell space and the stability condition*

For the local approximation of the pressure, we use the finite dimensional space of discontinuous constant functions defined on the elements $\mathsf{P} \in \Omega_h$ with zero average on Ω. Formally, we consider, as in the electromagnetics section, the elemental space:

$$\mathcal{P}_h(\mathsf{P}) = \mathbb{P}_0(\mathsf{P}) \qquad \forall \mathsf{P} \in \Omega_h, \tag{28}$$

and each piecewise constant function defined on a mesh Ω_h is uniquely identified by the set of costant values associated with the mesh elements. Correspondigly, we define the interpolation operator $\mathcal{I}^{\mathcal{P}_h} : L^2(\mathsf{P}) \to \mathbb{P}_0(\mathsf{P})$ as

$$\forall q \in L^2(\mathsf{P}) : \quad \mathcal{I}^{\mathcal{P}_h}(q) = \frac{1}{|\mathsf{P}|}\int_{\mathsf{P}} q. \tag{29}$$

The global space reads as

$$\mathcal{P}_{h,0} := \left\{ q_h \in L^2(\Omega) : q_{h|\mathsf{P}} \in \mathcal{P}_h(\mathsf{P}) \; \forall \mathsf{P} \in \Omega_h \text{ and } \int_\Omega q_h = 0, \right\} = \mathcal{P}_h \cap L^2_0(\Omega). \tag{30}$$

Equipped with the inner product

$$\forall q_h, p_h \in \mathcal{P}_{h,0} : \quad \big(q_h, p_h\big)_{\mathcal{P}_h} := \big(q_h, p_h\big) = \sum_{\mathsf{P}\in\Omega_h} |\mathsf{P}|(q_h p_h)_{|\mathsf{P}} \tag{31}$$

The spaces $\mathcal{TV}_h$ and $\mathcal{P}_{h,0}$ are selected to satisfy the inf-sup condition. This is proven in proposition 4.3 of [14].

Theorem 4.3 *There exists a projector* $\Pi_h : \left[H^1_0(\Omega)\right]^2 \to \mathcal{TV}_{h,0}$ *that satisfies*

$$\mathit{div}\,\Pi_h \boldsymbol{v} = \mathit{div}\,\boldsymbol{v} \quad \mathit{and} \quad |||\Pi_h \boldsymbol{v}|||_{1,\mathcal{TV}_h} \leq C_\pi \|\boldsymbol{v}\|_{1,\Omega}, \tag{32}$$

for every vector-valued field $\boldsymbol{v} \in \left[H^1_0(\Omega)\right]^2$ *and a real constant* $C_\pi > 0$ *that is independent of the mesh characteristics. stable inf-sup pair and satisfy the relation:*

$$\inf_{q_h\in\mathcal{P}_{h,0}} \sup_{\boldsymbol{v}_h\in\mathcal{TV}_{h,0}} \frac{\big(\mathit{div}\,\boldsymbol{v}_h, q_h\big)_{\mathcal{P}_h}}{|||\boldsymbol{v}_h|||_{1,\mathcal{TV}_h} |||q_h|||_{\mathcal{P}_h}} > 0. \tag{33}$$

4.2. *Electromagnetics*

In this section, we briefly describe the finite element spaces that we considered in [32] for the discretization of the electromagnetics of the MHD model. These spaces were originally proposed in the literature of virtual element methods in [4].

4.3. *Vertex Space*

The nodal space is given by

$$\mathcal{V}_h(\mathsf{P}) := \Big\{ D_h \in H(\mathbf{rot};\mathsf{P}) : \Delta D_h = 0 \text{ in } \mathsf{P},\ D_{h|\mathsf{e}} \in \mathbb{P}_1(\mathsf{e}) \; \forall \mathsf{e} \in \partial\mathsf{P} \Big\} \tag{34}$$

The virtual element functions in the nodal space are uniquely determined by their values at the elemental vertices, which we can take as the degrees of freedom. In the VEM we would ideally use the L^2 orthogonal projection of the nodal virtual element functions onto the space of linear polynomials to construct the mass matrices that represent the inner products in the MHD variational formulation in [**?**]. Unfortunately, the L^2 orthogonal projection is not directly computable from the degrees of freedon in $\mathcal{V}_h(\mathsf{P})$. Instead, we use a suitable reconstruction operator, which is denoted by $\Pi^{\mathcal{V}_h}_{\mathsf{P}} : \mathcal{V}_h(\mathsf{P}) \to \mathbb{P}_1(\mathsf{P})$ and required to satisfy the following set of criteria:

($\mathbf{V1}$) *(computability)* for any $D_h \in \mathcal{V}_h(\mathsf{P})$, the projector $\Pi^{\mathcal{V}_h}_{\mathsf{P}}$ is computable using only the degrees of freedom;

($\mathbf{V2}$) *($\mathbb{P}_1$-invariance)* for any polynomial $p \in \mathbb{P}_1(\mathsf{P})$, we have that $\Pi^{\mathcal{V}_h}_{\mathsf{P}} p = p$;

($\mathbf{V3}$) *(stability)* there exists a real constant $C > 0$ independent of the mesh characteristics such that

$$\|\Pi^{\mathcal{V}_h}_{\mathsf{P}} D_h\|_{0,\Omega} \leq C\|D_h\|_{0,\Omega} \quad \forall D_h \in \mathcal{V}_h(\mathsf{P}). \tag{35}$$

In the next section we propose three specific examples of such a projector. We can leverage $\Pi^{\mathcal{V}_h}_{\mathsf{P}}$ to define the local inner product as

$$\forall E_h, D_h \in \mathcal{V}_h(\mathsf{P}) : \quad \big(E_h, D_h\big)_{\mathcal{V}_h(\mathsf{P})} = \big(\Pi^{\mathcal{V}_h}_{\mathsf{P}} E_h, \Pi^{\mathcal{V}_h}_{\mathsf{P}} D_h\big) + \mathcal{S}^{\mathcal{V}_h}\big((1 - \Pi^{\mathcal{V}_h}_{\mathsf{P}})E_h, (1 - \Pi^{\mathcal{V}_h}_{\mathsf{P}})D_h\big). \tag{36}$$

Here, the bilinear form $\mathcal{S}_h^{\mathcal{V}}$ must satisfy the stability condition:

$$v_*\|D_h\|_{0,\Omega}^2 \leq \mathcal{S}^{\mathcal{V}_h}(D_h, D_h) \leq v^*\|D_h\|_{0,\Omega}^2 \quad \forall D_h \in \mathcal{V}_h(\mathsf{P}) \cap \ker\Pi_{\mathsf{P}}^{\mathcal{V}_h} : \tag{37}$$

for some pair of real positive constants $v_*, v^* > 0$, which are independent of h. Having defined the necessary local operations at the elemental level, we can extend the above mathematical entities to the full mesh. The global vertex space is defined as

$$\mathcal{V}_h = \Big\{ D_h \in H^1(\Omega) : D_{h|\mathsf{P}} \in \mathcal{V}_h(\mathsf{P}) \quad \forall \mathsf{P} \in \Omega_h \Big\}. \tag{38}$$

The inner product in this space is given by summing all local contributions:

$$\big(E_h, D_h\big)_{\mathcal{V}_h} = \sum_{\mathsf{P}\in\Omega_h} \big(E_h, D_h\big)_{\mathcal{V}_h(\mathsf{P})} \quad \forall D_h, E_h \in \mathcal{V}_h. \tag{39}$$

This inner product was first constructed in [32], where we proved its **consistency** with respect to linear polynomials and **stability**. This proof is similar to that of Lemma **??**. For the sake of completeness we present the result below.

Lemma 4.4 *For any two polynomials $p, q \in \mathbb{P}_0$ it follows that*

$$\big(p, q\big)_{\mathcal{V}_h} = \big(p, q\big). \tag{40}$$

Moreover, there exist two positive constants γ_* and γ^*, which are independent of h (and Δt), but may depend on the mesh regularity parameter ρ and the bounds on σ, such that

$$\gamma_*\|D_h\|_{0,\mathsf{P}}^2 \leq \big(D_h, D_h\big)_{\mathcal{V}_h(\mathsf{P})} \leq \gamma^*\|D_h\|_{0,\mathsf{P}}^2 \tag{41}$$

for every mesh element P.

Finally, we define a global interpolation operator $\mathcal{I}^{\mathcal{V}_h} : C^\infty(\Omega) \rightarrow \mathcal{V}_h$ in such a way that the D and $\mathcal{I}^{\mathcal{V}_h}D$ share the same degrees of freedom. This function is well defined by the unisolvency of such degrees of freedon in the finite element space $\mathcal{V}_h$.

4.3.1. *Construction of the projector $\Pi_{\mathsf{P}}^{\mathcal{V}_h}$*

We propose three alternatives for the projector $\Pi_{\mathsf{P}}^{\mathcal{V}_h}$. These projectors were proven to satisfy the conditions ($\mathbf{V1}$)-($\mathbf{V3}$), see the appendix in [32].

I. **Elliptic Projection Operator**(EP). This projector $\Pi_{\mathsf{P}}^{\nabla} : \mathcal{V}_h(\mathsf{P}) \rightarrow \mathbb{P}_1(\Omega)$ is given as the solution to

$$\forall q \in \mathbb{P}_1(\Omega) : \quad \int_{\mathsf{P}} \nabla\Pi_{\mathsf{P}}^{\nabla}E_h \cdot \nabla q = \int_{\mathsf{P}} \nabla E_h \cdot \nabla q \quad \text{in } \mathsf{P}, \tag{42a}$$

$$\sum_{\mathsf{v}} \big(\Pi_{\mathsf{P}}^{\nabla}E_h(\mathsf{v}) - E_h(\mathsf{v})\big) = 0. \tag{42b}$$

The sum above is taken over the vertices of V. To compute this projector note that

$$\int_{\mathsf{P}} \nabla E_h \cdot \nabla q = \int_{\mathsf{e}\in\partial\mathsf{P}} q\nabla E_h \cdot \boldsymbol{t} d\ell - \int_{\mathsf{P}} \Delta E_h q \tag{43}$$

the function $\nabla E_h \cdot \boldsymbol{t}$ is computable over the edges since E_h is a first degree polynomial over each edge giving a means of computing the boundary integral. The area integral vanishes since by construction $\Delta E_h = 0$.

II. **Least Squares reconstruction operator**(LS). An alternative to the elliptic projection operator and a second oblique projection is provided by the polynomial reconstruction $\Pi_{\mathsf{P}}^{LS}\boldsymbol{v}_h \in \mathbb{P}_1(\mathsf{P})$ for $\boldsymbol{v}_h \in \mathcal{TV}_h(\mathsf{P})$. This operator interpolates in the Least Squares sense the value of $\boldsymbol{v}_h$ at the elemental vertices:

$$\Pi_{\mathsf{P}}^{LS}\boldsymbol{v}_h(x_{\mathsf{V}}, y_{\mathsf{V}}) = \boldsymbol{v}_h(x_{\mathsf{V}}, y_{\mathsf{V}}) \quad \forall \mathsf{V} \in \partial\mathsf{P}. \tag{44}$$

The points $(x_{\mathsf{V}}, y_{\mathsf{V}})$ are the coordinate vectors of the vertices of the cell P. It is worth noting that on a triangular element this operator returns the standard linear interpolation.

III. **Galerkin Interpolator**(GI)

The third reconstruction operator, denoted by Π_{P}^{pw}, is the piecewise linear Galerkin interpolation on a patch of triangular subcells of element P. This construction is as follows. Our mesh assumptions implies that P is star-shaped with respect to some internal point $\boldsymbol{x}_{\mathsf{P}}*$, whose position vector is, thus, a convex combination of the vertices of P:

$$\boldsymbol{x}_{\mathsf{P}}^{*} = \sum_{\mathsf{v}\in\partial\mathsf{P}} \omega_{\mathsf{P},\mathsf{v}}\boldsymbol{x}_{\mathsf{v}}, \qquad \text{with} \quad 0 < \omega_{\mathsf{P},\mathsf{v}} < 1 \quad \text{and} \quad \sum_{\mathsf{v}\in\partial\mathsf{P}} \omega_{\mathsf{P},\mathsf{v}} = 1.$$

Using these weights, we can approximate the value of $D_h \in \mathcal{V}_h(\mathsf{P})$ at $\boldsymbol{x}*$

$$D_h(\boldsymbol{x}_{\mathsf{P}}^{*}) \approx D_h^{*} = \sum_{\mathsf{v}\in\partial\mathsf{P}} \omega_{\mathsf{P},\mathsf{v}} D_h(\boldsymbol{x}_{\mathsf{v}}).$$

We connect $\boldsymbol{x}_{\mathsf{P}}^{*}$ with each of the vertices in P to create a triangular partition of P. Thus, for any node in $\{\mathsf{v}\}\cup\{\mathsf{v}^{*}\}$ we can define ϕ_{v} such that ϕ_{v} is continuous and a linear polynomial over each triangle. Moreover, the evaluation of ϕ_{v} at $\boldsymbol{x}_{\mathsf{v}}$ is one and zero for the rest of the vertices. Finally, the projector is

$$\forall \boldsymbol{x} \in \mathsf{P}: \quad \Pi_{\mathsf{P}}^{pw} D_h(\boldsymbol{x}) = D_h^{*}\phi_{\mathsf{v}^{*}}(\boldsymbol{x}) + \sum_{\mathsf{v}\in\partial\mathsf{P}} D_h(\boldsymbol{x}_{\mathsf{v}})\phi_{\mathsf{v}}(\boldsymbol{x}),$$

4.4. *The edge space and the de Rham commuting diagram*

The local edge space is given by

$$\mathcal{E}_h(\mathsf{P}) := \Big\{ \boldsymbol{C}_h \in H(\mathrm{div};\mathsf{P}) \cap H(\mathrm{rot};\mathsf{P}) : \ \boldsymbol{C}_h \cdot \boldsymbol{n}_{|\mathsf{e}} \in \mathbb{P}_0(\mathsf{e}) \ \forall \mathsf{e} \in \partial\mathsf{P}, \\ \mathrm{div}\, \boldsymbol{C}_h \in \mathbb{P}_0(\mathsf{P}) \text{and} \ \ \mathrm{rot}\, \boldsymbol{C}_h = 0 \ \text{ in } \mathsf{P} \Big\}. \tag{45}$$

The degrees of freedom in this space are the normal fluxes across the elemental edges, i.e. the quantities

$$\int_{\mathsf{e}} \boldsymbol{C}_h \cdot \boldsymbol{n} d\ell \tag{46}$$

for $\boldsymbol{C}_h \in \mathcal{E}_h(\mathsf{P})$. In this space we define two different orthogonal projections that are computable from the degrees of freedom. The first one is the projection operator $\Pi_{\mathsf{P}}^{\mathcal{E}_h} : \mathcal{E}_h(\mathsf{P}) \to \big[\mathbb{P}_0(\mathsf{P})\big]^2$ and is such that $\Pi_{\mathsf{P}}^{\mathcal{E}_h}\boldsymbol{C}_h$ is the solution in $\big[\mathbb{P}_0(\mathsf{P})\big]^2$ of the variational problem:

$$\int_{\mathsf{P}} \Pi_{\mathsf{P}}^{\mathcal{E}_h}\boldsymbol{C}_h \cdot \boldsymbol{q} = \int_{\mathsf{P}} \boldsymbol{C}_h \cdot \boldsymbol{q} \qquad \forall \boldsymbol{q} \in \big[\mathbb{P}_0(\mathsf{P})\big]^2. \tag{47}$$

The computability of this operator is proved in [5]. The second one is the projection operator $\Pi_{\mathsf{P}}^{RT} : \mathcal{E}_h(\mathsf{P}) \to \mathrm{RT}_0(\mathsf{P})$, where $\mathrm{RT}_0(\mathsf{P})$ is the space of vector-valued functions of the form $\boldsymbol{q}(\boldsymbol{x}) = \boldsymbol{a} + c\boldsymbol{x}$ with $\boldsymbol{a} \in \mathbb{R}^2$ and $c \in \mathbb{R}$. This operator is such that $\Pi_{\mathsf{P}}^{RT}\boldsymbol{C}_h$ is the solution in $\mathrm{RT}_0(\mathsf{P})$, of the variational problem:

$$\int_{\mathsf{P}} \Pi_{\mathsf{P}}^{RT}\boldsymbol{C}_h \cdot \boldsymbol{q} = \int_{\mathsf{P}} \boldsymbol{C}_h \cdot \boldsymbol{q} \qquad \forall \boldsymbol{q} \in \mathrm{RT}_0(\mathsf{P}). \tag{48}$$

To compute this operator using the degrees of freedom we write a function $\boldsymbol{q} \in \mathrm{RT}_0(\mathsf{P})$ as $\boldsymbol{q} = \nabla p$, i.e., as the gradient the quadratic polynomial field $p(\boldsymbol{x}) = \boldsymbol{a} \cdot \boldsymbol{x} + b/2(x^2 + y^2)$. Then, an integration by parts yields:

$$\int_{\mathsf{P}} \boldsymbol{C}_h \cdot \nabla p = \int_{\partial\mathsf{P}} p\boldsymbol{C}_h \cdot \boldsymbol{n} d\ell - \int_{\mathsf{P}} p\mathrm{div}\, \boldsymbol{C}_h. \tag{49}$$

The normal components $\boldsymbol{C}_h \cdot \boldsymbol{n}$ are the edge degrees of freedom of $\boldsymbol{C}_h$. Using such degrees of freedom, we also compute the quantity $\mathrm{div}\, \boldsymbol{C}_h$, which is constant in each element, through the divergence theorem:

$$\mathrm{div}\, \boldsymbol{C}_h = \frac{1}{|\mathsf{P}|} \sum_{\mathsf{e}\in\partial\mathsf{P}} \int_{\mathsf{e}} \boldsymbol{C}_h \cdot \boldsymbol{n} d\ell. \tag{50}$$

We use the projector Π^{RT} to approximate the current density as evidenced in (6f) and $\Pi^{\mathcal{E}_h}$ to define the inner product in $\mathcal{E}_h(\mathsf{P})$ in accordance with the following definition:

$$\big(\boldsymbol{B}_h, \boldsymbol{C}_h\big)_{\mathcal{E}_h(\mathsf{P})} = \big(\Pi^{\mathcal{E}_h}\boldsymbol{B}_h, \Pi^{\mathcal{E}_h}\boldsymbol{C}_h\big) + \mathcal{S}^{\mathcal{E}_h}((\mathrm{I} - \Pi^{\mathcal{E}_h})\boldsymbol{B}_h, (\mathrm{I} - \Pi^{\mathcal{E}_h})\boldsymbol{C}_h) \qquad \forall \boldsymbol{B}_h, \boldsymbol{C}_h \in \mathcal{E}_h(\mathsf{P}). \tag{51}$$

In the definition above, the bilinear form $\mathcal{S}^{\mathcal{E}_h}$ satisfies the stability constraint:

$$\exists w^{*}, w_{*} > 0 \forall \boldsymbol{C}_h \in \mathcal{V}_h(\mathsf{P}) \cap \ker(\Pi_{\mathsf{P}}^{\mathcal{E}_h}): \quad w_{*}\|\boldsymbol{C}_h\|_{0,\Omega}^2 \le \mathcal{S}^{\mathcal{E}_h}(\boldsymbol{C}_h, \boldsymbol{C}_h) \le w^{*}\|\boldsymbol{C}_h\|_{0,\Omega}^2, \tag{52}$$

for some pair of real constants $w_{*}, w^{*} > 0$ that are independent of h. Dur to this property, it is immediate to verify that the inner product $\big(\cdot,\cdot\big)_{\mathcal{E}_h(\mathsf{P})}$ is characterized by the **constant polynomial consistency** and the **stability** properties. In fact, it holds that

– *(linear polynomial consistency)*: for every virtual element vector field $\boldsymbol{B}_h \in \mathcal{E}_h(\mathsf{P})$ it holds that:

$$\big(\boldsymbol{B}_h, \boldsymbol{q}\big)_{\mathcal{E}_h(\mathsf{P})} = \big(\boldsymbol{B}_h, \boldsymbol{q}\big) \qquad \forall \boldsymbol{q} \in \mathbb{P}_0(\mathsf{P}); \tag{53}$$

– *(stability)*: a pair of real positive constants δ_* and δ^* exists such that

$$\delta_* \|\boldsymbol{C}_h\|^2_{0,\mathsf{P}} \leq \mathcal{S}^{\mathcal{E}_h}(\boldsymbol{C}_h, \boldsymbol{C}_h) \leq \delta^* \|\boldsymbol{C}_h\|^2_{0,\mathsf{P}}. \qquad \forall \boldsymbol{C}_h \in \mathcal{E}_h(\mathsf{P}). \tag{54}$$

Having reviewed the local approximation spaces and relevant operators, the next step is to define their global counterparts. The space $\mathcal{E}_h$ is

$$\mathcal{E}_h = \big\{\boldsymbol{C}_h \in H(\mathrm{div};\Omega) : \boldsymbol{C}_{h|\mathsf{P}} \in \mathcal{E}_h(\mathsf{P}) \quad \forall \mathsf{P} \in \Omega_h\big\}, \tag{55}$$

and is endowed with the inner product

$$\big(\boldsymbol{B}_h, \boldsymbol{C}_h\big)_{\mathcal{E}_h} = \sum_{\mathsf{P}\in\Omega_h} \big(\boldsymbol{B}_h, \boldsymbol{C}_h\big)_{\mathcal{E}_h(\mathsf{P})} \qquad \forall \boldsymbol{B}_h, \boldsymbol{C}_h \in \mathcal{E}_h. \tag{56}$$

We can also extend the projector Π^{RT} by pasting together the local projectors Π^{RT}_{P}:

$$(\Pi^{RT}\boldsymbol{C}_h)_{|\mathsf{P}} = \Pi^{RT}_{\mathsf{P}}(\boldsymbol{C}_{h|\mathsf{P}}). \qquad \forall \boldsymbol{C}_h \in \mathcal{E}_h \forall \mathsf{P} \in \Omega_h. \tag{57}$$

Similarly to $\mathcal{TV}_h$ and $\mathcal{V}_h$, the unisolvency of the edge degrees of freedom in the finite element space $\mathcal{E}_h$ makes it possible to define a computable Fortin operator $\mathcal{I}^{\mathcal{E}_h} : H(\mathrm{div};\Omega) \to \mathcal{E}_h$.

A major property of the spaces $\mathcal{V}_h$, $\mathcal{E}_h$ and $\mathcal{P}_h$ (this latter being defined in Section 4.1.2) is that these space and the corresponding interpolation operators $\mathcal{I}^{\mathcal{V}_h}$, $\mathcal{I}^{\mathcal{E}_h}$ and $\mathcal{I}^{\mathcal{P}_h}$ satisfy the de Rham commuting diagram as summarized in Theorem 4.5 below.

Theorem 4.5 *The de Rham diagram*

$$\begin{array}{ccccc} H(\boldsymbol{rot};\Omega) & \xrightarrow{\ \mathbf{rot}\ } & H(div;\Omega) & \xrightarrow{\ div\ } & L^2(\Omega) \\ \big\downarrow \mathcal{I}^{\mathcal{V}_h} & & \big\downarrow \mathcal{I}^{\mathcal{E}_h} & & \big\downarrow \mathcal{I}^{\mathcal{P}_h} \\ \mathcal{V}_h & \xrightarrow{\ \mathbf{rot}\ } & \mathcal{E}_h & \xrightarrow{\ div\ } & \mathcal{P}_h \end{array}$$

is commutative and the chain

$$\mathcal{V}_h \xrightarrow{\ \mathbf{rot}\ } \mathcal{E}_h \xrightarrow{\ div\ } \mathcal{P}_h$$

is short and exact.

The proof of this theorem can be found in [4, 32].

restart from here

5. Energy Estimates

The conforming nature of VEM allows us to mimic many properties that are present in the continuous scenario. One of the more important is preserving certain types of energy estimates. These usually come about after testing the variational formulation against the exact solution and an application of Gronwall's Lemma. In this section we present an estimate of this type true for the continuous system (2) and its discrete counterpart (6). We begin by posing the decomposition

$$\boldsymbol{u} = \widehat{\boldsymbol{u}} + \boldsymbol{u}_b, \quad E = \widehat{E} + E_b, \tag{58}$$

where $\widehat{\boldsymbol{u}} \in \big[H^1_0(\Omega)\big]^2$ and $\widehat{E} \in H_0(\mathbf{rot};\Omega)$. The extension to the boundary condition on the velocity field is picked to satisfy

$$\mathrm{div}\,\boldsymbol{u}_b \equiv 0 \text{ in } \Omega, \quad \boldsymbol{u}_b(\boldsymbol{x}) = \boldsymbol{0} \text{ if } d(\boldsymbol{x}, \partial\Omega) \geq \epsilon. \tag{59}$$

For $h > \epsilon > 0$. We can do this by defining the domain $\Omega_\epsilon = \{\boldsymbol{x} \in \Omega : d(\boldsymbol{x}, \partial\Omega) < \epsilon\}$ and picking such an extension as the solution to

$$
\begin{aligned}
&-\triangle\widehat{\boldsymbol{u}}_b+\nabla s=\mathbf{0}\text{ in }\Omega_\epsilon, &\text{(60a)}\\
&\operatorname{div}\widehat{\boldsymbol{u}}_b=0\text{ in }\Omega_\epsilon, &\text{(60b)}\\
&\widehat{\boldsymbol{u}}_b=\boldsymbol{u}_b\text{ on }\partial\Omega, &\text{(60c)}\\
&\widehat{\boldsymbol{u}}_b=\mathbf{0}\text{ on }\partial(\Omega\setminus\Omega_\epsilon). &\text{(60d)}
\end{aligned}
$$

which is well-posed by the discussion in [6]. Finally we define

$$
\widehat{J}=\widehat{E}+\widehat{\boldsymbol{u}}\times\boldsymbol{B},\quad J_b=E_b+\boldsymbol{u}_b\times\boldsymbol{B}. \tag{61}
$$

We do this in order to reveal the boundary information. The following theorem gives the continuous energy estimate. Similar estimates are reported in [22, 26, 27].

Theorem 5.1 *Let* $(\boldsymbol{u},\boldsymbol{B},E,p)$ *solve the variational formulation* (5) *in the time interval* $[0,T]$ *then*

$$
\begin{aligned}
&\frac{1}{2}\frac{d}{dt}\|\widehat{\boldsymbol{u}}\|_{0,\Omega}^2+\frac{1}{2R_m}\frac{d}{dt}\|\boldsymbol{B}\|_{0,\Omega}^2+R_e^{-1}\|\nabla\widehat{\boldsymbol{u}}\|_{0,\Omega}^2+\|\widehat{J}\|_{0,\Omega}^2=\\
&\qquad=\Big(\boldsymbol{f},\widehat{\boldsymbol{u}}\Big)-\Big(\frac{\partial}{\partial t}\boldsymbol{u}_b,\widehat{\boldsymbol{u}}\Big)-R_e^{-1}\Big(\nabla\boldsymbol{u}_b,\nabla\widehat{\boldsymbol{u}}\Big)-R_m^{-1}\Big(\mathbf{rot}\,E_b,\boldsymbol{B}\Big)-\Big(J_b,\widehat{J}\Big). \qquad (62)
\end{aligned}
$$

And, as a consequence it must be true that

$$
\begin{aligned}
&\frac{e^{-T}}{2}\|\widehat{\boldsymbol{u}}(T)\|_{0,\Omega}^2+\frac{e^{-T}}{2R_m}\|\boldsymbol{B}(T)\|_{0,\Omega}^2+\int_0^T\left(\frac{e^{-t}}{2R_e}\|\nabla\widehat{\boldsymbol{u}}\|_{0,\Omega}^2+\frac{e^{-t}}{2}\|\widehat{J}\|_{0,\Omega}^2\right)dt\le\\
&\qquad\le\frac{e^{-T}}{2}\|\widehat{\boldsymbol{u}}(0)\|_{0,\Omega}^2+\frac{e^{-T}}{2R_m}\|\boldsymbol{B}(0)\|_{0,\Omega}^2+\\
&+\int_0^T\left(e^{-t}R_e\|\boldsymbol{f}\|_{-1,\Omega}^2+\frac{e^{-t}}{2}\frac{d}{dt}\|\boldsymbol{u}_b\|_{0,\Omega}^2+R_e^{-1}e^{-t}\|\nabla\boldsymbol{u}_b\|_{0,\Omega}^2+\frac{e^{-t}}{2R_m}\|\mathbf{rot}\,E_b\|_{0,\Omega}^2+\frac{e^{-t}}{2}\|J_b\|_{0,\Omega}^2\right)dt, \qquad (63)
\end{aligned}
$$

Proof. Taking the test function $(\boldsymbol{v},\boldsymbol{C},D,q)=(\widehat{\boldsymbol{u}},\boldsymbol{B},E,p)$ in the variational formulation (5) yields

$$
\begin{aligned}
&\frac{1}{2}\frac{d}{dt}\|\widehat{\boldsymbol{u}}\|_{0,\Omega}^2+R_e^{-1}\|\nabla\widehat{\boldsymbol{u}}\|_{0,\Omega}^2+\Big(\widehat{J},\widehat{\boldsymbol{u}}\times\boldsymbol{B}\Big)-\Big(\operatorname{div}\widehat{\boldsymbol{u}},p\Big)=\\
&=\Big(\boldsymbol{f},\widehat{\boldsymbol{u}}\Big)-\Big(\frac{\partial}{\partial t}\boldsymbol{u}_b,\widehat{\boldsymbol{u}}\Big)-R_e^{-1}\Big(\nabla\boldsymbol{u}_b,\nabla\widehat{\boldsymbol{u}}\Big)-\Big(J_b,\widehat{\boldsymbol{u}}\times\boldsymbol{B}\Big), &\text{(64a)}\\
&\Big(\operatorname{div}\widehat{\boldsymbol{u}},p\Big)=0, &\text{(64b)}\\
&\frac{1}{2R_m}\frac{d}{dt}\|\boldsymbol{B}\|_{0,\Omega}^2+R_m^{-1}\Big(\mathbf{rot}\,\widehat{E},\boldsymbol{B}\Big)=-R_m^{-1}\Big(\mathbf{rot}\,E_b,\boldsymbol{B}\Big), &\text{(64c)}\\
&\Big(\widehat{J},\widehat{E}\Big)-R_m^{-1}\Big(\boldsymbol{B},\mathbf{rot}\,\widehat{E}\Big)=-\Big(J_b,\widehat{E}\Big). &\text{(64d)}
\end{aligned}
$$

In the above we used the identities

$$
\Big(J\times\boldsymbol{B},\widehat{\boldsymbol{u}}\Big)=-\Big(J,\widehat{\boldsymbol{u}}\times\boldsymbol{B}\Big),\quad\operatorname{div}\boldsymbol{u}_b\equiv 0. \tag{65}
$$

Adding the equations in (64) we arrive at (62). To obtain (63) we use

$$
\begin{aligned}
&\left|\Big(\frac{\partial}{\partial t}\boldsymbol{u}_b,\widehat{\boldsymbol{u}}\Big)\right|\le\frac{d}{dt}\frac{1}{2}\|\boldsymbol{u}_b\|_{0,\Omega}^2+\frac{1}{2}\|\widehat{\boldsymbol{u}}\|_{0,\Omega}^2, &\text{(66a)}\\
&\left|\Big(\nabla\boldsymbol{u}_b,\nabla\widehat{\boldsymbol{u}}\Big)\right|\le\|\nabla\boldsymbol{u}_b\|_{0,\Omega}^2+\frac{1}{4}\|\nabla\widehat{\boldsymbol{u}}\|_{0,\Omega}^2, &\text{(66b)}\\
&\left|\Big(\boldsymbol{f},\widehat{\boldsymbol{u}}\Big)\right|\le\|\boldsymbol{f}\|_{-1,\Omega}\|\nabla\widehat{\boldsymbol{u}}_h\|_{0,\Omega}\le R_e\|\boldsymbol{f}\|_{-1,\Omega}^2+\frac{1}{4R_e}\|\nabla\widehat{\boldsymbol{u}}_h\|_{0,\Omega}^2 &\text{(66c)}\\
&\left|\Big(\mathbf{rot}\,E_b,\boldsymbol{B}\Big)\right|\le\frac{1}{2}\|\mathbf{rot}\,E_b\|_{0,\Omega}^2+\frac{1}{2}\|\boldsymbol{B}\|_{0,\Omega}^2, &\text{(66d)}\\
&\left|\Big(J_b,\widehat{J}\Big)\right|\le\frac{1}{2}\|J_b\|_{0,\Omega}^2+\frac{1}{2}\|\widehat{J}\|_{0,\Omega}^2, &\text{(66e)}
\end{aligned}
$$

which combined with (62) yields

$$\frac{d}{dt}\left(\frac{1}{2}\|\widehat{\boldsymbol{u}}\|_{0,\Omega}^2+\frac{1}{2R_m}\|\boldsymbol{B}\|_{0,\Omega}^2\right)-\left(\frac{1}{2}\|\widehat{\boldsymbol{u}}\|_{0,\Omega}^2+\frac{1}{2R_m}\|\boldsymbol{B}\|_{0,\Omega}^2\right)+\frac{1}{2R_e}\|\nabla\widehat{\boldsymbol{u}}\|_{0,\Omega}^2+\frac{1}{2}\|\widehat{J}\|_{0,\Omega}^2\leq$$

$$\leq R_e\|\boldsymbol{f}\|_{-1,\Omega}^2+\frac{1}{2}\frac{d}{dt}\|\boldsymbol{u}_b\|_{0,\Omega}^2+R_e^{-1}\|\nabla\boldsymbol{u}_b\|_{0,\Omega}^2+\frac{1}{2R_m}\|\mathbf{rot}\,E_b\|_{0,\Omega}^2+\frac{1}{2}\|J_b\|_{0,\Omega}^2, \quad (67)$$

Multiply by e^{-t} to get

$$\frac{d}{dt}(e^{-t})\left(\frac{1}{2}\|\widehat{\boldsymbol{u}}\|_{0,\Omega}^2+\frac{1}{2R_m}\|\boldsymbol{B}\|_{0,\Omega}^2\right)+\frac{e^{-t}}{2R_e}\|\nabla\widehat{\boldsymbol{u}}\|_{0,\Omega}^2+\frac{e^{-t}}{2}\|\widehat{J}\|_{0,\Omega}^2\leq$$

$$\leq e^{-t}R_e\|\boldsymbol{f}\|_{-1,\Omega}^2+\frac{e^{-t}}{2}\frac{d}{dt}\|\boldsymbol{u}_b\|_{0,\Omega}^2+e^{-t}R_e^{-1}\|\nabla\boldsymbol{u}_b\|_{0,\Omega}^2+\frac{e^{-t}}{2R_m}\|\mathbf{rot}\,E_b\|_{0,\Omega}^2+\frac{e^{-t}}{2}\|J_b\|_{0,\Omega}^2, \quad (68)$$

integration over the time domain $[0,T]$ will yield estimate (63). □

Next, we decompose

$$\forall 0\leq n\leq N-1: \quad E_h^{n+\theta}=\widehat{E}_h^{n+\theta}+\mathcal{I}^{\mathcal{V}_h}(E_b^{n+\theta}), \quad \boldsymbol{u}_h^{n+1}=\widehat{\boldsymbol{u}}_h^{n+1}+\mathcal{I}^{\mathcal{TV}_h}(\boldsymbol{u}_b^{n+1}). \quad (69)$$

where $(\widehat{E}_h^{n+\theta},\widehat{\boldsymbol{u}}_h^{n+\theta})\in\mathcal{V}_{h,0}\times\mathcal{TV}_{h,0}$ and $E_b,\boldsymbol{u}_b$ are picked such that its evaluations in $\Omega\backslash\Omega_\epsilon$ are identically zero. The condition on the boundary data is required to guarantee that the their degrees of freedom all lie along the boundary. Next, we define

$$\forall 1\leq n\leq N: \quad \widehat{J}_h^{n+\theta}=\widehat{E}_h^{n+\theta}+\mathcal{I}^{\mathcal{V}_h}(\widehat{\boldsymbol{u}}_h^{n+\theta}\times\Pi^{RT}\boldsymbol{B}_h^{n+\theta}),$$
$$J_{h,b}^{n+\theta}=\mathcal{I}^{\mathcal{V}_h}(E_b^{n+\theta})+\mathcal{I}^{\mathcal{V}_h}(\boldsymbol{u}_b^{n+\theta}\times\Pi^{RT}\boldsymbol{B}_h^{n+\theta}). \quad (70)$$

The next result is a discrete mimicry of Theorem 5.1.

Theorem 5.2 *Let* $\{(\boldsymbol{u}_h^n,\boldsymbol{B}_h^n)\}_{n=0}^N\subset\mathcal{TV}_h\times\mathcal{E}_h$ *and* $\{(E_h^{n+\theta},p_h^{n+\theta}))\}_{n=0}^{N-1}\subset\mathcal{V}_h\times\mathcal{P}_{h,0}$ *solve the formulation* (6)*. Then, it holds that*

$$(\mathbf{L1})+(\mathbf{L2})=(\mathbf{R}), \quad (71)$$

where

$$(\mathbf{L1})=\Delta t(\theta-1/2)\left(\frac{|||\widehat{\boldsymbol{u}}_h^{n+1}-\widehat{\boldsymbol{u}}_h^n|||_{\mathcal{TV}_h}^2}{\Delta t^2}+\frac{|||\boldsymbol{B}_h^{n+1}-\boldsymbol{B}_h^n|||_{\mathcal{E}_h}^2}{\Delta t^2R_m}\right)+$$
$$+\left(\frac{|||\widehat{\boldsymbol{u}}_h^{n+1}|||_{\mathcal{TV}_h}^2-|||\widehat{\boldsymbol{u}}_h^n|||_{\mathcal{TV}_h}^2}{2\Delta t}+\frac{|||\boldsymbol{B}_h^{n+1}|||_{\mathcal{E}_h}^2-|||\boldsymbol{B}_h^n|||_{\mathcal{E}_h}^2}{2\Delta tR_m}\right), \quad (72)$$

$$(\mathbf{L2})=R_e^{-1}\left|\widehat{\boldsymbol{u}}_h^{n+\theta}\right|_{\mathcal{TV}_h}^2+|||\widehat{J}_h^{n+\theta}|||_{\mathcal{V}_h}^2+\left(div\,\mathcal{I}^{\mathcal{TV}_h}\boldsymbol{u}_b^{n+\theta},p_h^{n+\theta}\right)_{\mathcal{P}_h}, \quad (73)$$

$$(\mathbf{R})=\left(\boldsymbol{f}_h,\widehat{\boldsymbol{u}}_h^{n+\theta}\right)_{\mathcal{TV}_h}-\left(\frac{\mathcal{I}^{\mathcal{TV}_h}\boldsymbol{u}_b^{n+1}-\mathcal{I}^{\mathcal{TV}_h}\boldsymbol{u}_b^n}{\Delta t},\widehat{\boldsymbol{u}}_h^{n+\theta}\right)_{\mathcal{TV}_h}-R_e^{-1}\left[\mathcal{I}^{\mathcal{TV}_h}\boldsymbol{u}_b^{n+\theta},\widehat{\boldsymbol{u}}_h^{n+\theta}\right]_{\mathcal{TV}_h}-$$
$$-\left(J_{h,b}^{n+\theta},\widehat{J}_h^{n+\theta}\right)_{\mathcal{V}_h}-R_m^{-1}\left(\mathbf{rot}\,\mathcal{I}^{\mathcal{V}_h}E_b^{n+\theta},\boldsymbol{B}_h^{n+\theta}\right)_{\mathcal{E}_h}. \quad (74)$$

In the case that $\theta\in[1/2,1]$ *then we can conclude that for any* $\epsilon>0$ *we have*

$$\alpha^N\left(|||\widehat{\boldsymbol{u}}_h^N|||_{\mathcal{TV}_h}^2+R_m^{-1}|||\boldsymbol{B}_h^N|||_{\mathcal{E}_h}^2\right)+\sum_{n=0}^N\gamma\alpha^n\left(R_e^{-1}\left|\widehat{\boldsymbol{u}}_h^{n+\theta}\right|_{\mathcal{TV}_h}^2+|||\widehat{J}_h^{n+\theta}|||_{\mathcal{V}_h}^2-2\epsilon|||p_h^{n+\theta}|||_{\mathcal{P}_h}^2\right)\Delta t\leq$$
$$\leq\left(|||\mathcal{I}^{\mathcal{TV}_h}(\boldsymbol{u}_0)|||_{\mathcal{TV}_h}^2+R_m^{-1}|||\mathcal{I}^{\mathcal{E}_h}(\boldsymbol{B}_0)|||_{\mathcal{E}_h}^2\right)+$$
$$+\sum_{n=0}^N\gamma\alpha^n\big(R_e|||\boldsymbol{f}_h|||_{-1,\mathcal{TV}_h}^2+\Delta t^{-1}|||\mathcal{I}^{\mathcal{TV}_h}(\boldsymbol{u}_b^{n+1}-\boldsymbol{u}_b^n)|||_{\mathcal{TV}_h}^2+R_e^{-1}\left|\mathcal{I}^{\mathcal{V}_h}\boldsymbol{u}_b^{n+\theta}\right|_{\mathcal{TV}_h}^2+\frac{\beta^*}{2\epsilon}\left(\int_{\partial\Omega}\left|\mathcal{I}^{\mathcal{TV}_h}\boldsymbol{u}_b^{n+\theta}\cdot\boldsymbol{n}\right|ds\right)^2+$$
$$+R_m^{-1}|||\mathbf{rot}\,\mathcal{I}^{\mathcal{V}_h}E_b^{n+\theta}|||_{\mathcal{E}_h}^2+|||J_{h,b}^{n+\theta}|||_{\mathcal{V}_h}^2\big)\Delta t, \quad (75)$$

where $\beta^*>0$ *is given in Theorem 4.2 and*

$$\alpha = \frac{\theta}{1+\theta}, \quad \gamma = \frac{1}{1+\theta}. \tag{76}$$

In the case that walls of the domain are non-penetrating, meaning $\boldsymbol{u}_b \cdot \boldsymbol{n} \equiv 0$ along $\partial\Omega$, then we obtain our final energy stability estimate

$$\alpha^N \left(|||\widehat{\boldsymbol{u}}_h^N|||^2_{\mathcal{TV}_h} + R_m^{-1} |||\boldsymbol{B}_h^N|||^2_{\mathcal{E}_h} \right) + \sum_{n=0}^{N} \gamma\alpha^n \left(R_e^{-1} \big| \widehat{\boldsymbol{u}}_h^{n+\theta} \big|^2_{\mathcal{TV}_h} + |||\widehat{J}_h^{n+\theta}|||^2_{\mathcal{V}_h} \right) \leq$$
$$\leq \left(|||\mathcal{I}^{\mathcal{TV}_h}(\boldsymbol{u}_0)|||^2_{\mathcal{TV}_h} + R_m^{-1} |||\mathcal{I}^{\mathcal{E}_h}(\boldsymbol{B}_0)|||^2_{\mathcal{E}_h} \right) +$$
$$+ \sum_{n=0}^{N} \gamma\alpha^n \big(R_e |||\boldsymbol{f}_h|||^2_{-1,\mathcal{TV}_h} + \Delta t^{-1} |||\mathcal{I}^{\mathcal{TV}_h}(\boldsymbol{u}_b^{n+1} - \boldsymbol{u}_b^n)|||^2_{\mathcal{TV}_h} + R_e^{-1} \big| \mathcal{I}^{\mathcal{V}_h} \boldsymbol{u}_b^{n+\theta} \big|^2_{\mathcal{TV}_h} +$$
$$+ R_m^{-1} |||\mathbf{rot}\, \mathcal{I}^{\mathcal{V}_h} E_b^{n+\theta}|||^2_{\mathcal{E}_h} + |||J_{h,b}^{n+\theta}|||^2_{\mathcal{V}_h} \big) \Delta t. \tag{77}$$

Proof. Testing the formulation (6) against $(\boldsymbol{v}_h, \boldsymbol{C}_h, D_h, q_h) = (\widehat{\boldsymbol{u}}_h^{n+\theta}, \boldsymbol{B}_h^{n+\theta}, \widehat{E}_h^{n+\theta}, p_h^{n+\theta})$ we obtain

$$\Big(\frac{\widehat{\boldsymbol{u}}_h^{n+1} - \widehat{\boldsymbol{u}}_h^n}{\Delta t}, \widehat{\boldsymbol{u}}_h^{n+\theta} \Big)_{\mathcal{TV}_h} + R_e^{-1} \big| \widehat{\boldsymbol{u}}_h^{n+\theta} \big|^2_{\mathcal{TV}_h} + \Big(\widehat{J}_h^{n+\theta}, \mathcal{I}^{\mathcal{V}_h}(\widehat{\boldsymbol{u}}_h^{n+\theta} \times \boldsymbol{B}_h^{n+\theta}) \Big)_{\mathcal{V}_h} -$$
$$- \Big(\operatorname{div} \widehat{\boldsymbol{u}}_h^{n+\theta}, p_h^{n+\theta} \Big)_{\mathcal{P}_h} = \Big(\boldsymbol{f}_h, \widehat{\boldsymbol{u}}_h^{n+\theta} \Big)_{\mathcal{TV}_h} - \Big(\frac{\mathcal{I}^{\mathcal{TV}_h} \boldsymbol{u}_b^{n+1} - \mathcal{I}^{\mathcal{TV}_h} \boldsymbol{u}_b^n}{\Delta t}, \widehat{\boldsymbol{u}}_h^{n+\theta} \Big)_{\mathcal{V}_h} - \tag{78a}$$
$$- R_e^{-1} \Big[\mathcal{I}^{\mathcal{TV}_h} \boldsymbol{u}_b^{n+\theta}, \widehat{\boldsymbol{u}}_h^{n+\theta} \Big]_{\mathcal{TV}_h} - \Big(J_{h,b}^{n+\theta}, \mathcal{I}^{\mathcal{V}_h}(\widehat{\boldsymbol{u}}_h^{n+\theta} \times \Pi^{RT} \boldsymbol{B}_h^{n+\theta}) \Big)_{\mathcal{TV}_h},$$

$$\Big(\operatorname{div} \widehat{\boldsymbol{u}}_h^{n+\theta}, q_h \Big)_{\mathcal{P}_h} = - \Big(\operatorname{div} \mathcal{I}^{\mathcal{TV}_h} \boldsymbol{u}_b^{n+\theta}, q_h \Big)_{\mathcal{P}_h}, \tag{78b}$$

$$R_m^{-1} \Big(\frac{\boldsymbol{B}_h^{n+1} - \boldsymbol{B}_h^n}{\Delta t}, \boldsymbol{B}_h^{n+\theta} \Big)_{\mathcal{E}_h} + R_m^{-1} \Big(\mathbf{rot}\, \widehat{E}_h^{n+\theta}, \boldsymbol{B}_h^{n+\theta} \Big)_{\mathcal{E}_h} = - R_m^{-1} \Big(\mathbf{rot}\, \mathcal{I}^{\mathcal{V}_h} E_b^{n+\theta}, \boldsymbol{B}_h^{n+\theta} \Big)_{\mathcal{E}_h}, \tag{78c}$$

$$\Big(\widehat{J}_h^{n+\theta}, \widehat{E}_h^{n+\theta} \Big)_{\mathcal{V}_h} - R_m^{-1} \Big(\boldsymbol{B}_h^{n+\theta}, \mathbf{rot}\, \widehat{E}_h^{n+\theta} \Big)_{\mathcal{E}_h} = - \Big(J_{h,b}, \widehat{E}_h^{n+\theta} \Big)_{\mathcal{V}_h}. \tag{78d}$$

Next, note that

$$\boldsymbol{B}_h^{n+\theta} = \Delta t \big(\theta - 1/2 \big) \frac{\boldsymbol{B}_h^{n+1} - \boldsymbol{B}_h^n}{\Delta t} + \frac{\boldsymbol{B}_h^{n+1} + \boldsymbol{B}_h^n}{2}, \tag{79}$$

immediately gives that

$$\Big(\frac{\boldsymbol{B}_h^{n+1} - \boldsymbol{B}_h}{\Delta t}, \boldsymbol{B}_h^{n+\theta} \Big)_{\mathcal{E}_h} = \Delta t \big(\theta - 1/2 \big) \frac{|||\boldsymbol{B}_h^{n+1} - \boldsymbol{B}_h^n|||^2_{\mathcal{E}_h}}{\Delta t^2} + \frac{|||\boldsymbol{B}_h^{n+1}|||^2_{\mathcal{E}_h} - |||\boldsymbol{B}_h^n|||^2_{\mathcal{E}_h}}{2\Delta t}. \tag{80}$$

An analogous argument will yield

$$\Big(\frac{\widehat{\boldsymbol{u}}_h^{n+1} - \boldsymbol{B}_h}{\Delta t}, \widehat{\boldsymbol{u}}_h^{n+\theta} \Big)_{\mathcal{TV}_h} = \Delta t \big(\theta - 1/2 \big) \frac{|||\widehat{\boldsymbol{u}}_h^{n+1} - \widehat{\boldsymbol{u}}_h^n|||^2_{\mathcal{TV}_h}}{\Delta t^2} + \frac{|||\widehat{\boldsymbol{u}}_h^{n+1}|||^2_{\mathcal{TV}_h} - |||\widehat{\boldsymbol{u}}_h^n|||^2_{\mathcal{TV}_h}}{2\Delta t}. \tag{81}$$

We can use the identities (80) and (81) to transform the left hand side of (78a) and (78c) then adding the resulting equations with (78b) and (78d) will yield (71). To verify the estimate in (75) note that $\theta \in [1/2, 1]$ guarantees

$$(\mathbf{L1}) \geq \frac{|||\widehat{\boldsymbol{u}}_h^{n+1}|||^2_{\mathcal{TV}_h} - |||\widehat{\boldsymbol{u}}_h^n|||^2_{\mathcal{TV}_h}}{2\Delta t} + \frac{|||\boldsymbol{B}_h^{n+1}|||^2_{\mathcal{E}_h} - |||\boldsymbol{B}_h^n|||^2_{\mathcal{E}_h}}{2\Delta t}. \tag{82}$$

Next we apply the following estimates to the terms in $(\mathbf{R})$,

$$-\Big(\frac{\mathcal{I}^{\mathcal{TV}_h}\boldsymbol{u}_b^{n+1}-\mathcal{I}^{\mathcal{TV}_h}\boldsymbol{u}_b^{n}}{\Delta t},\widehat{\boldsymbol{u}}_h^{n+\theta}\Big)_{\mathcal{TV}_h} \leq \frac{1}{2\Delta t}|||\mathcal{I}^{\mathcal{TV}_h}(\boldsymbol{u}_b^{n+1}-\boldsymbol{u}_b^{n})|||^2_{\mathcal{TV}_h}+\frac{1}{2}|||\widehat{\boldsymbol{u}}_h^{n+\theta}|||^2_{\mathcal{TV}_h}, \tag{83a}$$

$$-\Big[\mathcal{I}^{\mathcal{TV}_h}\boldsymbol{u}_b^{n+\theta},\widehat{\boldsymbol{u}}_h^{n+\theta}\Big]_{\mathcal{TV}_h} \leq \big|\mathcal{I}^{\mathcal{V}_h}\boldsymbol{u}_b^{n+\theta}\big|^2_{\mathcal{TV}_h}+\frac{1}{4}\big|\widehat{\boldsymbol{u}}_h^{n+\theta}\big|^2_{\mathcal{TV}_h}, \tag{83b}$$

$$\Big(\boldsymbol{f}_h,\widehat{\boldsymbol{u}}_h\Big)_{\mathcal{TV}_h} \leq R_e|||\boldsymbol{f}_h|||^2_{-1,\mathcal{TV}_h}+\frac{1}{4R_e}\big|\widehat{\boldsymbol{u}}_h\big|^2_{\mathcal{TV}_h}, \tag{83c}$$

$$-\Big(\operatorname{div}\mathcal{I}^{\mathcal{TV}_h}\boldsymbol{u}_b^{n+\theta},p^{n+\theta}\Big)_{\mathcal{P}_h} \leq \frac{1}{4\epsilon}|||\operatorname{div}\mathcal{I}^{\mathcal{TV}_h}\boldsymbol{u}_b^{n+\theta}|||^2_{\mathcal{P}_h}+\epsilon|||p^{n+\theta}|||^2_{\mathcal{P}_h}, \tag{83d}$$

$$-\Big(\mathbf{rot}\,\mathcal{I}^{\mathcal{V}_h}E_b^{n+\theta},\boldsymbol{B}_h^{n+\theta}\Big)_{\mathcal{E}_h} \leq \frac{1}{2}|||\mathbf{rot}\,\mathcal{I}^{\mathcal{V}_h}E_b^{n+\theta}|||^2_{\mathcal{E}_h}+\frac{1}{2}|||\boldsymbol{B}_h^{n+\theta}|||^2_{\mathcal{E}_h}, \tag{83e}$$

$$-\Big(J_{h,b}^{n+\theta},\widehat{J}_h^{n+\theta}\Big)_{\mathcal{V}_h} \leq \frac{1}{2}|||J_{h,b}^{n+\theta}|||^2_{\mathcal{V}_h}+\frac{1}{2}|||\widehat{J}_h^{n+\theta}|||^2_{\mathcal{V}_h}, \tag{83f}$$

$$|||\boldsymbol{B}_h^{n+\theta}|||^2_{\mathcal{E}_h} \leq \theta|||\boldsymbol{B}_h^{n}|||^2_{\mathcal{E}_h}+(1-\theta)|||\boldsymbol{B}_h^{n+1}|||^2_{\mathcal{E}_h}, \tag{83g}$$

$$|||\widehat{\boldsymbol{u}}_h^{n+\theta}|||^2_{\mathcal{TV}_h} \leq \theta|||\widehat{\boldsymbol{u}}_h^{n}|||^2_{\mathcal{TV}_h}+(1-\theta)|||\widehat{\boldsymbol{u}}_h^{n+1}|||^2_{\mathcal{TV}_h}. \tag{83h}$$

To estimate $(\mathbf{L2})$ use

$$-\Big(\operatorname{div}\boldsymbol{u}_b^{n+\theta},p_h^{n+\theta}\Big)_{\mathcal{P}_h} \leq \frac{1}{4\epsilon}|||\operatorname{div}\mathcal{I}^{\mathcal{TV}_h}\boldsymbol{u}_b^{n+\theta}|||^2_{\mathcal{P}_h}+\epsilon|||p_h^{n+\theta}|||^2_{\mathcal{P}_h}. \tag{84}$$

And, finally

$$\begin{aligned}
\Big|\Big|\Big|\operatorname{div}\mathcal{I}^{\mathcal{TV}_h}\boldsymbol{u}_b^{n+\theta}\Big|\Big|\Big|_{\mathcal{P}_h} &= \sum_{\mathsf{P}\in\partial\Omega_h}|||\operatorname{div}\mathcal{I}^{\mathcal{TV}_h}\boldsymbol{u}_b^{n+\theta}|||_{\mathcal{TV}_h(\mathsf{P})} && \mathcal{I}^{\mathcal{TV}_h}\boldsymbol{u}_b^{n+\theta}=\mathbf{0}\text{ away from }\partial\Omega,\\
&\leq \sqrt{\beta^*}\sum_{\mathsf{P}\in\partial\Omega_h}\big|\operatorname{div}\mathcal{I}^{\mathcal{TV}_h}\boldsymbol{u}_b^{n+\theta}\big|\,|\mathsf{P}| && \operatorname{div}\mathcal{I}^{\mathcal{TV}_h}\boldsymbol{u}_b^{n+\theta}\text{ is constant in every cell,}\\
&\leq \sqrt{\beta^*}\sum_{\mathsf{P}\in\partial\Omega_h}\Big|\int_{\mathsf{P}\cap\partial\Omega}\mathcal{I}^{\mathcal{TV}_h}\boldsymbol{u}_b^{n+\theta}\cdot\boldsymbol{n}ds\Big| && \text{apply the divergence theorem}\\
&\leq \sqrt{\beta^*}\sum_{\mathsf{P}\in\partial\Omega_h}\int_{\mathsf{P}\cap\partial\Omega}\big|\mathcal{I}^{\mathcal{TV}_h}\boldsymbol{u}_b^{n+\theta}\cdot\boldsymbol{n}\big|\,ds\\
&\leq \sqrt{\beta^*}\int_{\partial\Omega}\big|\mathcal{I}^{\mathcal{TV}_h}\boldsymbol{u}_b^{n+\theta}\cdot\boldsymbol{n}\big|\,ds
\end{aligned} \tag{85}$$

Where $\partial\Omega_h$ is defined as the set of elements that have an edge intersecting $\partial\Omega$ and the constant β^* is given by Theorem 4.2.

The result of applying estimates (82)-(85) is

$$\alpha\mathcal{A}^{n+1}(\widehat{\boldsymbol{u}}_h,\boldsymbol{B}_h)-\mathcal{A}^{n}(\widehat{\boldsymbol{u}}_h,\boldsymbol{B}_h)=\gamma\mathcal{F}^{n+\theta}(\widehat{\boldsymbol{u}}_h,\widehat{J}_h,p_h,\boldsymbol{u}_b,J_{h,b})\Delta t, \tag{86}$$

where

$$\alpha=\frac{\theta}{1+\theta},\quad \gamma=\frac{1}{1+\theta},\quad \mathcal{A}^n(\widehat{\boldsymbol{u}}_h,\boldsymbol{B}_h)=|||\widehat{\boldsymbol{u}}_h^n|||^2_{\mathcal{TV}_h}+R_m^{-1}|||\boldsymbol{B}_h^n|||^2_{\mathcal{E}_h} \tag{87}$$

and

$$\begin{aligned}
&\mathcal{F}^{n+\theta}(\widehat{\boldsymbol{u}}_h,\widehat{J}_h,p_h,\boldsymbol{u}_b,J_{h,b})= \\
&=R_e|||\boldsymbol{f}_h|||^2_{-1,\mathcal{TV}_h}+\frac{1}{\Delta t}|||\mathcal{I}^{\mathcal{TV}_h}(\boldsymbol{u}_b^{n+1}-\boldsymbol{u}_b^n)|||^2_{\mathcal{TV}_h}+\frac{1}{R_e}\big|\mathcal{I}^{\mathcal{V}_h}\boldsymbol{u}_b^{n+\theta}\big|^2_{\mathcal{TV}_h}+\frac{\beta^*}{2\epsilon}\left(\int_{\partial\Omega}\big|\mathcal{I}^{\mathcal{TV}_h}\boldsymbol{u}_b^{n+\theta}\cdot\boldsymbol{n}\big|\,ds\right)^2+\\
&+\frac{1}{R_m}|||\mathbf{rot}\,\mathcal{I}^{\mathcal{V}_h}E_b^{n+\theta}|||^2_{\mathcal{E}_h}+|||J_{h,b}^{n+\theta}|||^2_{\mathcal{V}_h}-\frac{1}{2R_e}\big|\widehat{\boldsymbol{u}}_h^{n+\theta}\big|^2_{\mathcal{TV}_h}-|||\widehat{J}_h^{n+\theta}|||^2_{\mathcal{V}_h}+2\epsilon|||p_h^{n+\theta}|||^2_{\mathcal{P}_h}.
\end{aligned} \tag{88}$$

When multiplying the inequalities (86) for $0\leq n\leq N$ by an appropriate power of $\alpha$and adding them together yields a telescoping sum, we illustrate this by writing the first 4 terms:

$$
\begin{array}{llll}
\text{for } n=0: & \alpha\mathcal{A}^1(\widehat{\boldsymbol{u}}_h,\boldsymbol{B}_h)\ -\mathcal{A}^0(\widehat{\boldsymbol{u}}_h,\boldsymbol{B}_h) & \le \gamma\mathcal{F}^{\theta}(\widehat{\boldsymbol{u}}_h,\widehat{J}_h,p_h,\boldsymbol{u}_b,J_{h,b})\Delta t & \big[\text{multiply by } 1\,\big],\\
\text{for } n=1: & \alpha^2\mathcal{A}^2(\widehat{\boldsymbol{u}}_h,\boldsymbol{B}_h)\ -\alpha\mathcal{A}^1(\widehat{\boldsymbol{u}}_h,\boldsymbol{B}_h) & \le \gamma\alpha\mathcal{F}^{1+\theta}(\widehat{\boldsymbol{u}}_h,\widehat{J}_h,p_h,\boldsymbol{u}_b,J_{h,b})\Delta t & \big[\text{multiply by } \alpha\,\big],\\
\text{for } n=2: & \alpha^3\mathcal{A}^3(\widehat{\boldsymbol{u}}_h,\boldsymbol{B}_h)\ -\alpha^2\mathcal{A}^2(\widehat{\boldsymbol{u}}_h,\boldsymbol{B}_h) & \le \gamma\alpha^2\mathcal{F}^{2+\theta}(\widehat{\boldsymbol{u}}_h,\widehat{J}_h,p_h,\boldsymbol{u}_b,J_{h,b})\Delta t & \big[\text{multiply by } \alpha^2\big],\\
\text{for } n=3: & \alpha^4\mathcal{A}^4(\widehat{\boldsymbol{u}}_h,\boldsymbol{B}_h)\ -\alpha^3\mathcal{A}^3(\widehat{\boldsymbol{u}}_h,\boldsymbol{B}_h) & \le \gamma\alpha^3\mathcal{F}^{3+\theta}(\widehat{\boldsymbol{u}}_h,\widehat{J}_h,p_h,\boldsymbol{u}_b,J_{h,b})\Delta t & \big[\text{multiply by } \alpha^3\big],\\
\quad \cdots\cdots & & &
\end{array}
$$

The result of this sum is (75). Finally, if we assume that $\boldsymbol{u}_b \cdot \boldsymbol{n} = 0$ along $\partial\Omega_h$ then since the quadrature is exact for constants

$$\int_{\partial\Omega} |\mathcal{I}^{\mathcal{V}_h}\boldsymbol{u}_b^{n+\theta}\cdot\boldsymbol{n}|ds = \int_{\partial\Omega} |\boldsymbol{u}_b^{n+\theta}\cdot\boldsymbol{n}|ds = 0, \tag{89}$$

This allows us to take $\epsilon \to 0$ in (75) to attain the final estability estimate (77). □

6. Linearization

6.1. *A Newton-Krylov approach*

This section takes inspiration from [9]. In this section we will mainly be concerned with the development of a solver for (6) at a single point in time. For this reason the values of $\theta > 0$ and n will remain fixed and thus we will omit them from the notation that we will introduce.

In practice, we will find arrays of degrees of freedom, to express this we will add a superscript I. This to say that, for example, $\boldsymbol{u}_h^I$ will refer to the array of degrees of freedom of $\boldsymbol{u}_h$. To begin let us introduce the space

$$\mathcal{X}_{h,0} = \left\{(\boldsymbol{v}_h^I, \boldsymbol{C}_h^I, D_h^I, q_h^I) : (\boldsymbol{v}_h, \boldsymbol{C}_h, D_h, q_h) \in \mathcal{TV}_{h,0} \times \mathcal{E}_h \times \mathcal{V}_{h,0} \times \mathcal{P}_{h,0}\right\}. \tag{90}$$

We will equip this space with the ℓ_2 inner product. We do this mainly to conform to much of the literature on linear and nonlinear methods. We seek to pose the formulation (6) in the space $\mathcal{X}_h$. To do this we first have to substitute (6c) with the equivalent expression

$$\theta R_m^{-1}\big(\frac{\boldsymbol{B}_h - \boldsymbol{B}_h^n}{\Delta t}, \boldsymbol{C}_h\big)_{\mathcal{E}_h} + \theta R_m^{-1}\big(\mathbf{rot}\, E_h, \boldsymbol{C}_h\big)_{\mathcal{E}_h} = 0 \tag{91}$$

and add it to (6a), (6b) and (6d). We define G in such a way that $G(\boldsymbol{x}_h)\cdot\boldsymbol{y}_h$ as the left hand side of the resulting expression. In doing this we are implying that $\boldsymbol{x}_h, \boldsymbol{y}_h \in \mathcal{X}_{h,0}$ with

$$\boldsymbol{x}_h = (\widehat{\boldsymbol{u}}_h^{n+1,I}, \boldsymbol{B}_h^{n+1,I}, \widehat{E}_h^{n+\theta,I}, p_h^{n+\theta,I}), \quad \boldsymbol{y}_h = (\boldsymbol{v}_h^I, \boldsymbol{C}_h^I, D_h^I, q_h^I). \tag{92}$$

Thus, solving the variational formulation (6) is equivalent to solving

Find $\boldsymbol{x}_h \in \mathcal{X}_h$ such that

$$G(\boldsymbol{x}_h) = \mathbf{0}. \tag{93}$$

Indeed, testing (93) against $\boldsymbol{y}_h = (\boldsymbol{v}_h, \mathbf{0}, 0, 0)$ we retrieve (6a), the three remaining equations can be attained similarly. This is the set up to apply a Jacobian-free Newton–Krylov method. This method is highly parallelizable and has optimal speed of convergence.

The Newton method will have us, at every iteration, update the estimate for the zeroes of G in accordance to

$$\boldsymbol{x}_h^0 = (\widehat{\boldsymbol{u}}_h^{n,I}, \boldsymbol{B}_h^{n,I}, \widehat{E}_h^{n-1+\theta,I}, p_h^{n-1+\theta,I}), \quad \boldsymbol{x}_h^{m+1} = \boldsymbol{x}_h^m + \delta\boldsymbol{x}_h^m, \quad \partial G(\boldsymbol{x}_h^m)\delta\boldsymbol{x}_h^m = -G(\boldsymbol{x}_h^m), \tag{94}$$

where $\partial G : \mathcal{X}_{h,0} \to \mathcal{L}(\mathcal{X}_{h,0})$ is the Jacobian of G, the space $\mathcal{L}(\mathcal{X}_{h,0})$ is the collection of linear operators from $\mathcal{X}_{h,0}$ to $\mathcal{X}_{h,0}'$. The reason we had to substitute (6c) with (91) is to attain some symmetry in the Jacobian matrix, this will be clear from the well-posedness analysis. This method, as described, will require that we compute and store the Jacobian matrix. This takes a good deal of memory and computational power. Instead, we will approximate the action of the Jacobian matrix onto vectors using the finite difference approximation

$$DG(\boldsymbol{x}_h)\delta\boldsymbol{x}_h = \frac{G(\boldsymbol{x}_h + \epsilon\delta\boldsymbol{x}_h) - G(\boldsymbol{x}_h)}{\epsilon}, \quad \epsilon = 10^{-7}. \tag{95}$$

The value of ϵ is selected as a "sweet-spot" value for epsilon that makes for stable float point arithmetic and approximation accuracy. suggested in page 80 of [24]. The algorithm we propose by provides updates in accordance to

$$\forall 0 \leq m \leq M-1: \quad \boldsymbol{x}_h^{m+1} = \boldsymbol{x}_h^m + \delta \boldsymbol{x}_h^m, \quad DG(\boldsymbol{x}_h^m)\delta \boldsymbol{x}^m = -G(\boldsymbol{x}_h^m), \tag{96a}$$

$$\boldsymbol{x}_h^0 = \begin{cases} \left(\widehat{\boldsymbol{u}}_h^{n,I}, \boldsymbol{B}_h^{0,I}, \widehat{E}_h^{n-1+\theta,I}, p_h^{n-1+\theta,I}\right), & n > 0, \\ \left(\widehat{\boldsymbol{u}}_h^{0,I}, \boldsymbol{B}_h^{0,I}, 0, 0\right), & n = 0. \end{cases} \tag{96b}$$

We define $(\widehat{\boldsymbol{u}}_h^{n+1}, \boldsymbol{B}_h^{n+1}, \widehat{E}_h^{n+\theta}, p_h^{n+\theta})$ such that its array degrees of freedom is $\boldsymbol{x}_h^M$ whereas intermediate steps will be denoted as

$$\boldsymbol{x}_h^k = \left(\widehat{\boldsymbol{u}}_h^{n+1,k,I}, \boldsymbol{B}_h^{n+1,k,I}, \widehat{E}_h^{n+\theta,k,I}, p_h^{n+\theta,k,I}\right). \tag{97}$$

The routine we use to solve the linear system in (96) is the GMRES algorithm. This Krylov method will require a tolerance input which will be fixed to satify

$$\|DG(\boldsymbol{x}_h^m)\delta \boldsymbol{x}^m + G(\boldsymbol{x}_h^m)\|_2 \leq \eta_m \|G(\boldsymbol{x}_h^m)\|_2, \tag{98a}$$

$$\eta_m = \min\left\{\eta_{\text{max}}, \max\left(\eta_m^B, \gamma \frac{\epsilon_t}{\|G(\boldsymbol{x}_h^m)\|_2}\right)\right\}, \tag{98b}$$

$$\eta_m^B = \min\left\{\eta_{\text{max}}, \max\left(\eta_m^A, \gamma \eta_{m-1}^\alpha\right)\right\}, \quad \eta_m^A = \gamma \left(\frac{\|G(\boldsymbol{x}_h^m)\|_2}{\|G(\boldsymbol{x}_h^{m-1})\|_2}\right)^\alpha. \tag{98c}$$

with $\alpha = 1.5, \gamma = 0.9, \eta_{\text{max}} = 0.8$. The value of ϵ_t is fixed to guarantee non-linear convergence has been achieved.

$$\|G(\boldsymbol{x}_h^m)\|_2 < \epsilon_a + \epsilon_r \|G(\boldsymbol{x}_h^0)\|_2 = \epsilon_t, \quad \epsilon_a = \sqrt{\#dof} \times 10^{-15}, \epsilon_r = 10^{-4}. \tag{99}$$

The particular choices for the constants are the same as in [9]. However, this strategy is much more general [19]. The guiding philosophy being a desire to guarantee super-linear convergence while simultaneously not over-solving with unnecessary GMRES iterations.

The non-linear nature of the inexact Newton steps may shed doubt as to whether or not this solver preserves the divergence free nature of the magnetic field. The following result arises from an understanding of how Faraday's Law is used to predict the magnetic field. The reality is that since this Law is linear then our finite difference approximation to its Jacobian will, in fact, be exact.

Theorem 6.1 *Suppose that $\delta \boldsymbol{x}_h$ solves*

$$DG(\boldsymbol{x}_h)\delta \boldsymbol{x}_h = -G(\boldsymbol{x}_h), \tag{100}$$

then

$$\textit{div}\, \delta \boldsymbol{B}_h = \textit{div}\, (\boldsymbol{B}_h^n - \boldsymbol{B}_h). \tag{101}$$

Proof. Testing (100) against $\boldsymbol{y}_h = (0, \boldsymbol{C}_h^I, 0, 0)$ yields

$$\Delta t^{-1}\left(\delta \boldsymbol{B}_h, \boldsymbol{C}_h\right)_{\mathcal{E}_h} + \left(\mathbf{rot}\, \delta \widehat{E}_h, \boldsymbol{C}_h\right)_{\mathcal{E}_h} = -\left(\frac{\boldsymbol{B}_h - \boldsymbol{B}_h^n}{\Delta t}, \boldsymbol{C}_h\right)_{\mathcal{E}_h} - \Delta t\left(\mathbf{rot}\, \widehat{E}_h, \boldsymbol{C}_h\right)_{\mathcal{E}_h} \tag{102}$$

since $\boldsymbol{C}_h$ can be selected arbitrarily the above is equivalent to

$$\Delta t^{-1}\left[\delta \boldsymbol{B}_h + \boldsymbol{B}_h - \boldsymbol{B}_h^n\right] = \mathbf{rot}\, \left(\delta \widehat{E}_h + \widehat{E}_h\right). \tag{103}$$

Taking divergence on both sides yields (101). □

Corollary 6.2 *If the initial conditions on the magnetic field $\boldsymbol{B}_0$ satisfy that div $\boldsymbol{B}_0 = 0$ then updates defined by* (96) *will satisfy that*

$$\forall 0 \leq n \leq N, 0 \leq m \leq M: \quad \textit{div}\, \boldsymbol{B}_h^{n,m} = 0. \tag{104}$$

Proof. The divergence of the initial estimate can be computed using the commuting property of the diagram in Theorem 4.5. Indeed:

$$\text{div}\, \boldsymbol{B}_h^0 = \text{div}\, \mathcal{I}^{\mathcal{E}_h}(\boldsymbol{B}_0) = \mathcal{I}^{\mathcal{P}_h}(\text{div}\, \boldsymbol{B}_0) = 0 \tag{105}$$

Next, suppose that div ${}_h\boldsymbol{B}_h^n = 0$ then by definition div $\boldsymbol{B}_h^{n+1,0} = 0$. For the inductive step we can further assume that div $\boldsymbol{B}_h^{n+1,m} = 0$ thus from Theorem 6.1 we have that

$$\text{div}\, \boldsymbol{B}_h^{n+1,m+1} = \text{div}\, \boldsymbol{B}_h^{n+1,m} + \text{div}\, \delta \boldsymbol{B}_h^{n+1,m} = \text{div}\, (2\boldsymbol{B}_h^{n+1,m} - \boldsymbol{B}_h^n) = 0. \tag{106}$$

□

6.2. *Well-posedness*

In this section we will study the wellposedness of each linear solve in the proposed Newton-Krylov method. To this end we define the space

$$\mathfrak{X}_h = \mathcal{TV}_{h,0} \times \mathcal{E}_h \times \mathcal{V}_{h,0} \tag{107}$$

And, $a_h : \mathfrak{X}_h \times \mathfrak{X}_h \to \mathbb{R}$ whose evaluation at $\delta\boldsymbol{\xi}_h = (\delta\widehat{\boldsymbol{u}}_h, \delta\boldsymbol{B}_h, \delta\widehat{E}_h)$, $\boldsymbol{\eta}_h = (\boldsymbol{v}_h, \boldsymbol{C}_h, D_h)$ is given by $a(\delta\boldsymbol{\xi}_h, \boldsymbol{\eta}_h) = \ell_1(\boldsymbol{v}_h) + \ell_2(\boldsymbol{C}_h) + \ell_3(D_h)$ for

$$\ell_1(\boldsymbol{v}_h) = \Delta t^{-1}\Big(\delta\widehat{\boldsymbol{u}}_h, \boldsymbol{v}_h\Big)_{\mathcal{TV}_h} + \theta R_e^{-1}\Big[\delta\widehat{\boldsymbol{u}}_h, \boldsymbol{v}_h\Big]_{\mathcal{TV}_h} + \theta\Big(\widehat{E}_h, \mathcal{I}^{\mathcal{V}_h}(\boldsymbol{v}_h \times \Pi^{RT}\delta\boldsymbol{B}_h)\Big)_{\mathcal{V}_h} + \tag{108a}$$

$$\theta\Big(\delta\widehat{E}_h, \mathcal{I}^{\mathcal{V}_h}(\boldsymbol{v}_h \times \Pi^{RT}\boldsymbol{B}_h)\Big)_{\mathcal{V}_h} + \theta^3\Big(\mathcal{I}^{\mathcal{V}_h}(\widehat{\boldsymbol{u}}_h \times \Pi^{RT}\boldsymbol{B}_h), \mathcal{I}^{\mathcal{V}_h}(\boldsymbol{v}_h \times \Pi^{RT}\delta\boldsymbol{B}_h)\Big)_{\mathcal{V}_h} +$$

$$\theta^3\Big(\mathcal{I}^{\mathcal{V}_h}(\widehat{\boldsymbol{u}}_h \times \Pi^{RT}\delta\boldsymbol{B}_h), \mathcal{I}^{\mathcal{V}_h}(\boldsymbol{v}_h \times \Pi^{RT}\boldsymbol{B}_h)\Big)_{\mathcal{V}_h} + \theta^3\Big(\mathcal{I}^{\mathcal{V}_h}(\widehat{\boldsymbol{u}}_h \times \Pi^{RT}\delta\boldsymbol{B}_h), \mathcal{I}^{\mathcal{V}_h}(\boldsymbol{v}_h \times \Pi^{RT}\boldsymbol{B}_h)\Big)_{\mathcal{V}_h},$$

$$\ell_2(\boldsymbol{C}_h) = \theta R_m^{-1}\Delta t^{-1}\Big(\delta\boldsymbol{B}_h, \boldsymbol{C}_h\Big)_{\mathcal{E}_h} + \theta R_m^{-1}\Big(\mathbf{rot}\,\delta E_h, \boldsymbol{C}_h\Big)_{\mathcal{E}_h}, \tag{108b}$$

$$\ell_3(D_h) = \Big(\delta\widehat{E}_h + \theta\mathcal{I}^{\mathcal{V}_h}(\widehat{\boldsymbol{u}}_h \times \Pi^{RT}\delta\boldsymbol{B}_h + \delta\widehat{\boldsymbol{u}}_h \times \Pi^{RT}\boldsymbol{B}_h), \boldsymbol{D}_h\Big)_{\mathcal{V}_h} - R_m^{-1}\theta\big(\delta\boldsymbol{B}_h, \mathbf{rot}\,_h D_h\big)_{\mathcal{E}_h}. \tag{108c}$$

Here, and for the remainder of the section, we have fixed the value of $\boldsymbol{x}_h = (\widehat{\boldsymbol{u}}_h^I, \boldsymbol{B}_h^I, \widehat{E}_h^I)$. With these definitions we can pose the problem of finding $\delta\boldsymbol{x}_h$ satisfying $\partial G(\boldsymbol{x}_h)\delta\boldsymbol{x}_h = -G(\boldsymbol{x}_h)$ as
Find $(\delta\boldsymbol{\xi}_h, \delta p_h) \in \mathfrak{X}_h \times \mathcal{P}_{h,0}$ *such that for all* $(\boldsymbol{\eta}_h, q_h) \in \mathfrak{X}_h \times \mathcal{P}_{h,0}$ *it holds that*

$$a_h(\delta\boldsymbol{\xi}_h, \boldsymbol{\eta}_h) - b_h(\boldsymbol{v}_h, \delta p_h) = f(\boldsymbol{\eta}_h), \tag{109a}$$

$$b_h(\delta\widehat{\boldsymbol{u}}_h, q_h) = g(q_h). \tag{109b}$$

Where $f \in \mathfrak{X}_h'$ and $g \in \mathcal{P}_{h,0}'$ are some appropriate bounded linear functionals and

$$b_h(\boldsymbol{v}_h, q_h) = \Big(\mathrm{div}\,\boldsymbol{v}_h, q_h\Big)_{\mathcal{P}_h} \tag{110}$$

The study of well posedness of (109) will have us introduce the next auxiliary problem
Find $(\delta\boldsymbol{\xi}_h, \delta p_h) \in \mathfrak{X}_h \times \mathcal{P}_{h,0}$ *such that for all* $(\boldsymbol{\eta}_h, q_h) \in \mathfrak{X}_h \times \mathcal{P}_{h,0}$ *it holds that*

$$a_{h,0}(\delta\boldsymbol{\xi}_h, \boldsymbol{\eta}_h) - b_h(\boldsymbol{v}_h, \delta p_h) = f_h(\boldsymbol{\eta}_h), \tag{111a}$$

$$b_h(\delta\widehat{\boldsymbol{u}}_h, q_h) = g_h(q_h). \tag{111b}$$

The difference lies in that

$$a_{h,0}(\delta\boldsymbol{\xi}_h, \boldsymbol{\eta}_h) = a_h(\delta\boldsymbol{\xi}_h, \boldsymbol{\eta}_h) + \theta R_m^{-1}\Big(\mathrm{div}\,\delta\boldsymbol{B}_h, \mathrm{div}\,\boldsymbol{C}_h\Big)_{\mathcal{P}_h}. \tag{112}$$

Therefore, the first result we need to establish is the equivalency between (109) and (111).
Proposition 6.3 *Let* $\delta\boldsymbol{\xi}_h = (\delta\widehat{\boldsymbol{u}}_h, \delta\boldsymbol{B}_h, \delta\widehat{E}_h) \in \mathfrak{X}_h$ *and* $p_h \in \mathcal{P}_{h,0}$ *solve* (111) *should the initial conditions on the magnetic field be divergence free then div* $\delta\boldsymbol{B}_h = 0$.

Proof. Testing (111) against $q_h = 0$, and $\eta = (\mathbf{0}, \boldsymbol{C}_h, 0)$ yields

$$\Delta t^{-1}\Big(\delta\boldsymbol{B}_h + \mathbf{rot}\,\delta E_h, \boldsymbol{C}_h\Big)_{\mathcal{E}_h} + \Big(\mathrm{div}\,\delta\boldsymbol{B}_h, \mathrm{div}\,\boldsymbol{C}_h\Big)_{\mathcal{P}_h} = -\Big(\frac{\boldsymbol{B}_h - \boldsymbol{B}_h^n}{\Delta t} + \mathbf{rot}\,E_h, \boldsymbol{C}_h\Big)_{\mathcal{E}_h} \tag{113}$$

or equivalently

$$\Delta t^{-1}\Big(\delta\boldsymbol{B}_h + \mathbf{rot}\,\delta E_h + \frac{\boldsymbol{B}_h^{n,m} - \boldsymbol{B}_h^n}{\Delta t} + \mathbf{rot}\,E_h, \boldsymbol{C}_h\Big)_{\mathcal{E}_h} = -\Big(\mathrm{div}\,\delta\boldsymbol{B}_h, \mathrm{div}\,\boldsymbol{C}_h\Big)_{\mathcal{E}_h}. \tag{114}$$

Therefore, making

$$\boldsymbol{C}_h = \delta\boldsymbol{B}_h + \mathbf{rot}\,\delta E_h + \frac{\boldsymbol{B}_h^{n,m} - \boldsymbol{B}_h^n}{\Delta t} + \mathbf{rot}\,E_h \tag{115}$$

we find that, since by Corollary 6.2, the divergence of most terms in our choice of $\boldsymbol{C}_h$ are zero yielding

$$\Delta t^{-1}|||\boldsymbol{C}_h|||_{\mathcal{E}_h}^2 = -|||\mathrm{div}\,\delta\boldsymbol{B}_h|||_{\mathcal{P}_h}^2 \tag{116}$$

As a consequence the only solution is that div $\delta\boldsymbol{B}_h = 0$. □

The result of proposition 6.3 implies that if $\delta\xi$ and p_h solve (109) then

$$a(\delta\xi,\eta) = a_0(\delta\xi,\eta). \tag{117}$$

Providing the evidence we needed to guarantee that (109) and (111) are equivalent. Finally, we can present the well-posedness of (111). In the spirit of [22] we introduce the following norm on $\boldsymbol{\xi}_h = (\boldsymbol{u}_h, \boldsymbol{B}_h, E_h) \in \mathfrak{X}_{h,0}$ as

$$|||\boldsymbol{\xi}_h|||^2_{\mathfrak{X}_{h,0}} := |||\boldsymbol{v}_h|||^2_{\Delta t,\nabla} + |||E_h|||^2_{\Delta t,\mathbf{rot}} + |||\boldsymbol{B}_h|||^2_{\Delta t,\mathrm{div}}\,, \tag{118a}$$

$$|||\boldsymbol{u}_h|||^2_{\Delta t,\nabla} := \Delta t^{-1}|||\boldsymbol{u}_h|||^2_{\mathcal{TV}_h} + \left|\boldsymbol{u}_h\right|^2_{\mathcal{TV}_h} + \Delta t^{-1}|||\mathrm{div}\,\boldsymbol{u}_h|||^2_{\mathcal{P}_h}\,, \tag{118b}$$

$$|||\boldsymbol{B}_h|||^2_{\Delta t,\mathrm{div}} := \Delta t^{-1}|||\boldsymbol{B}_h|||^2_{\mathcal{E}_h} + |||\mathrm{div}\,\boldsymbol{B}_h|||^2_{\mathcal{P}_h}\,, \tag{118c}$$

$$|||E_h|||^2_{\Delta t,\mathbf{rot}} := |||E_h|||^2_{\mathcal{V}_h} + \Delta t|||\mathbf{rot}\,E_h|||^2_{\mathcal{E}_h}\,. \tag{118d}$$

Well-posedness relies on the LBB theorem, the following two lemmas prove that (111) satisfies its hypothesis.

Lemma 6.4 *Suppose that $\Delta t^{1/2}\widehat{\boldsymbol{u}}_h, \widehat{\boldsymbol{u}}_h, \boldsymbol{B}_h \in [L^\infty(\Omega)]^2$ and $\widehat{E}_h \in L^\infty(\Omega)$ then bilinear form $a_{h,0}$ is continuous in the norms defined in* (118a)*.*

Proof. Let $\xi = (\boldsymbol{u}_h, \boldsymbol{B}_h, E_h)$ and $\eta = (\boldsymbol{v}_h, \boldsymbol{C}_h, E_h)$ be arbitrary elements in $\mathfrak{X}_h$. A series of applications of the Cauchy-Schwartz inequality yields that

$$\Delta t^{-1}\Big(\delta\boldsymbol{u}_h,\boldsymbol{v}_h\Big)_{\mathcal{TV}_h} \le \Delta t^{-1/2}|||\delta\boldsymbol{u}_h|||_{\mathcal{TV}_h}\Delta t^{-1/2}|||\boldsymbol{v}_h|||_{\mathcal{TV}_h} \le |||\delta\boldsymbol{u}_h|||_{\Delta t,\nabla}|||\boldsymbol{v}_h|||_{\Delta t,\nabla}\,, \tag{119}$$

$$\Big[\delta\boldsymbol{u}_h,\boldsymbol{v}_h\Big]_{\mathcal{TV}_h} \le \left|\delta\boldsymbol{u}_h\right|_{\mathcal{TV}_h}\left|\boldsymbol{v}_h\right|_{\mathcal{TV}_h} \le |||\delta\boldsymbol{u}_h|||_{\Delta t,\nabla}|||\boldsymbol{v}_h|||_{\Delta t,\nabla} \tag{120}$$

$$\Delta t^{-1}\big(\delta\boldsymbol{B}_h,\boldsymbol{C}_h\big)_{\mathcal{E}_h} \le \Delta t^{-\frac{1}{2}}|||\delta\boldsymbol{B}_h|||_{\mathcal{E}_h}\,\Delta t^{-\frac{1}{2}}|||\boldsymbol{C}_h|||_{\mathcal{E}_h} \le |||\delta\boldsymbol{B}_h|||_{\Delta t,\mathrm{div}}\,|||\boldsymbol{C}_h|||_{\Delta t,\mathrm{div}}\,, \tag{121}$$

$$\big(\mathbf{rot}\,\delta E_h,\boldsymbol{C}_h\big)_{\mathcal{E}_h} \le \Delta t^{\frac{1}{2}}|||\mathbf{rot}\,\delta E_h|||_{\mathcal{E}_h}\,\Delta t^{-\frac{1}{2}}|||\boldsymbol{C}_h|||_{\mathcal{E}_h} \le |||\delta E_h|||_{\Delta t,\mathbf{rot}}\,|||\boldsymbol{C}_h|||_{\Delta t,\mathrm{div}}\,, \tag{122}$$

$$\big(\delta E_h, D_h\big)_{\mathcal{V}_h} \le |||\delta E_h|||_{\mathcal{V}_h}\,|||D_h|||_{\mathcal{V}_h} \le |||\delta E_h|||_{\Delta t,\mathbf{rot}}\,|||D_h|||_{\Delta t,\mathbf{rot}}\,, \tag{123}$$

$$\big(\mathrm{div}\,\delta\boldsymbol{B}_h,\mathrm{div}\,\boldsymbol{C}_h\big)_{\mathcal{P}_h} \le |||\mathrm{div}\,\delta\boldsymbol{B}_h|||_{\mathcal{P}_h}\,|||\mathrm{div}\,\boldsymbol{w}_h|||_{\mathcal{P}_h} \le |||\delta\boldsymbol{B}_h|||_{\Delta t,\mathrm{div}}\,|||\boldsymbol{C}_h|||_{\Delta t,\mathrm{div}}\,. \tag{124}$$

Continuity of the coupling terms comes about by similar arguments. Here, two representative terms. They rely on the Friedrichs-Poincaré inequality, recall that $\|E_h\|_{0,\Omega} \le C\|\nabla E_h\|_{0,\Omega} = \|\mathbf{rot}\,E_h\|_{0,\Omega}$ and $\|\boldsymbol{v}_h\|_{0,\Omega} \le C\|\nabla\boldsymbol{v}_h\|_{0,\Omega}$ holds for every $E_h \in \mathcal{V}_{h,0} \subset H^1_0(\Omega)$ and $\boldsymbol{v}_h \in \mathcal{TV}_{h,0} \subset H^1_0$ respectively. Thus,

$$\begin{aligned}
\big(\mathcal{I}^{\mathcal{V}_h}\big(\widehat{\boldsymbol{u}}_h \times \Pi^{RT}\delta\boldsymbol{B}_h\big), D_h\big)_{\mathcal{V}_h} &\le C\|\mathcal{I}^{\mathcal{V}_h}\big(\widehat{\boldsymbol{u}}_h \times \Pi^{RT}\delta\boldsymbol{B}_h\big)\|_{0,\Omega}\|D_h\|_{0,\Omega}\\
&\le C\|\widehat{\boldsymbol{u}}_h\|_\infty\|\delta\boldsymbol{B}_h\|_{0,\Omega}\|D_h\|_{0,\Omega}\\
&\le C\|\widehat{\boldsymbol{u}}_h\|_\infty\|\delta\boldsymbol{B}_h\|_{0,\Omega}\|\mathbf{rot}\,D_h\|_{0,\Omega}\\
&\le C\|\widehat{\boldsymbol{u}}_h\|_\infty\Delta t^{-1/2}|||\delta\boldsymbol{B}_h|||_{\mathcal{E}_h}\Delta t^{1/2}|||\mathbf{rot}\,D_h|||_{\mathcal{E}_h}\\
&\le \widetilde{C}|||\delta\boldsymbol{B}_h|||_{\Delta t,\mathrm{div}}\,|||D_h|||_{\Delta t,\mathbf{rot}}\,.
\end{aligned}$$

Finally, continuity of the second coupling term follows by

$$\begin{aligned}
\Big(\mathcal{I}^{\mathcal{V}_h}(\widehat{\boldsymbol{u}}_h \times \Pi^{RT}\delta\boldsymbol{B}_h), \mathcal{I}^{\mathcal{V}_h}(\boldsymbol{v}_h \times \Pi^{RT}\boldsymbol{B}_h)\Big)_{\mathcal{V}_h} &\le C\|\mathcal{I}^{\mathcal{V}_h}(\widehat{\boldsymbol{u}}_h \times \Pi^{RT}\delta\boldsymbol{B}_h)\|_{0,\Omega}\|\mathcal{I}^{\mathcal{V}_h}(\boldsymbol{v}_h \times \Pi^{RT}\boldsymbol{B}_h)\|_{0,\Omega}\\
&\le C\|\widehat{\boldsymbol{u}}_h\|_\infty\|\Pi^{RT}\boldsymbol{B}_h\|_\infty\|\delta\boldsymbol{B}_h\|_{0,\Omega}\|\boldsymbol{v}_h\|_{0,\Omega}\\
&\le C\|\Delta t^{1/2}\widehat{\boldsymbol{u}}_h\|_\infty\|\Pi^{RT}\boldsymbol{B}_h\|_\infty\Delta t^{-1/2}\|\delta\boldsymbol{B}_h\|_{0,\Omega}\|\nabla\boldsymbol{v}_h\|_{0,\Omega}\\
&\le \widetilde{C}\|\Delta t^{1/2}\widehat{\boldsymbol{u}}_h\|_\infty\|\Pi^{RT}\boldsymbol{B}_h\|_\infty\Delta t^{-1/2}|||\delta\boldsymbol{B}_h|||_{\mathcal{E}_h}\left|\boldsymbol{v}_h\right|_{\mathcal{TV}_h}\\
&\le \widetilde{C}|||\delta\boldsymbol{B}_h|||_{\Delta t,\mathrm{div}}\,|||\boldsymbol{v}_h|||_{\Delta t,\nabla}\,.
\end{aligned}$$

□

Next, we present a proof of the so-called inf-sup condition.

Lemma 6.5 *Let $\theta > 0$, and $\widehat{\boldsymbol{u}}_h, \boldsymbol{B}_h \in [L^\infty(\Omega)]^2$ and $\widehat{E}_h \in L^\infty(\Omega)$ In this case, for Δt is small enough then*

$$\inf_{\delta\boldsymbol{\xi}_h \in \mathfrak{X}_{h,0}}\sup_{\boldsymbol{\eta}_h \in \mathfrak{X}_{h,0}}\frac{a_{h,0}(\delta\boldsymbol{\xi}_h,\boldsymbol{\eta}_h)}{|||\delta\boldsymbol{\xi}_h|||_{\mathfrak{X}_h}|||\boldsymbol{\eta}_h|||_{\mathfrak{X}_h}} \ge C > 0, \quad \textit{where} \quad \mathfrak{X}_{h,0} = \{(\boldsymbol{v}_h,\boldsymbol{B}_h,E_h) : \mathit{div}\,\boldsymbol{v}_h = 0\}\,. \tag{125}$$

Where C does not depend on h nor Δt.

Proof. Select $\boldsymbol{\xi}_h = (\delta\boldsymbol{u}_h, \delta\boldsymbol{B}_h, \delta E_h) \in \mathfrak{X}_{h,0}$ arbitrarily, proof of (125) would follow if we can show that there exists $\boldsymbol{\eta}_h \in \mathfrak{X}_{h,0}$ satisfying

$$a_{h,0}(\delta\boldsymbol{\xi}_h,\boldsymbol{\eta}_h)\geq C|||\delta\boldsymbol{\xi}_h|||_{\mathfrak{X}_h}|||\boldsymbol{\eta}_h|||_{\mathfrak{X}_h}. \tag{126}$$

We will do this by decomposing $a_{h,0}$ into

$$a_{h,0}(\delta\boldsymbol{\xi}_h,\boldsymbol{\eta}_h)=\ell_1(\boldsymbol{v}_h)+\ell_2^*(\boldsymbol{C}_h)+\ell_3(D_h), \tag{127}$$

where ℓ_1 and ℓ_3 are defined in (108) and

$$\ell_2^*(\boldsymbol{C}_h)=\ell_2(\boldsymbol{C}_h)+\Big(\operatorname{div}\delta\boldsymbol{B}_h,\operatorname{div}\boldsymbol{C}_h\Big). \tag{128}$$

Let us pick $\eta=(\boldsymbol{v}_h,\boldsymbol{C}_h,D_h)$ for

$$\boldsymbol{v}_h=\delta\widehat{\boldsymbol{u}}_h,\quad \boldsymbol{C}_h=\frac{1}{2}(\delta\boldsymbol{B}_h+\Delta t\,\mathbf{rot}\,\delta E_h),\quad D_h=\delta\widehat{E}_h. \tag{129}$$

Then,

$$\begin{aligned}\ell_1(\boldsymbol{v}_h)&=\Delta t^{-1}|||\delta\widehat{\boldsymbol{u}}_h|||_{\mathcal{TV}_h}+R_e^{-1}\big|\delta\widehat{\boldsymbol{u}}_h\big|_{\mathcal{TV}_h}+\theta\Big(\widehat{E}_h,\mathcal{I}^{\mathcal{V}_h}(\delta\widehat{\boldsymbol{u}}_h\times\Pi^{RT}\delta\boldsymbol{B}_h)\Big)_{\mathcal{V}_h}+\\&+\theta^3\Big(\delta\widehat{E}_h,\mathcal{I}^{\mathcal{V}_h}(\delta\widehat{\boldsymbol{u}}_h\times\Pi^{RT}\boldsymbol{B}_h)\Big)_{\mathcal{V}_h}+\theta^3\Big(\mathcal{I}^{\mathcal{V}_h}(\widehat{\boldsymbol{u}}_h\times\Pi^{RT}\boldsymbol{B}_h),\mathcal{I}^{\mathcal{V}_h}(\delta\widehat{\boldsymbol{u}}_h\times\Pi^{RT}\delta\boldsymbol{B}_h)\Big)_{\mathcal{V}_h}+\\&+\theta^3\Big(\mathcal{I}^{\mathcal{V}_h}(\widehat{\boldsymbol{u}}_h\times\Pi^{RT}\delta\boldsymbol{B}_h),\mathcal{I}^{\mathcal{V}_h}(\delta\boldsymbol{u}_h\times\Pi^{RT}\boldsymbol{B}_h)\Big)_{\mathcal{V}_h}+\theta^3\Big(\mathcal{I}^{\mathcal{V}_h}(\delta\widehat{\boldsymbol{u}}_h\times\Pi^{RT}\boldsymbol{B}_h),\mathcal{I}^{\mathcal{V}_h}(\delta\widehat{\boldsymbol{u}}_h\times\Pi^{RT}\boldsymbol{B}_h)\Big)_{\mathcal{V}_h},\end{aligned}$$

$$\begin{aligned}\ell_2^*(\boldsymbol{C}_h)=\theta R_m^{-1}\frac{\Delta t^{-1}}{2}|||\delta\boldsymbol{B}_h|||^2_{\mathcal{E}_h}+\theta\frac{R_m^{-1}}{2}|||\operatorname{div}\delta\boldsymbol{B}_h|||^2_{\mathcal{E}_h}+\theta\frac{R_m^{-1}\Delta t}{2}|||\mathbf{rot}\,\delta\widehat{E}_h|||^2_{\mathcal{E}_h}+\\+\theta R_m^{-1}\Big(\delta\boldsymbol{B}_h,\mathbf{rot}\,\delta\widehat{E}_h\Big)_{\mathcal{E}_h},\end{aligned}$$

$$\begin{aligned}\ell_3(D_h)=|||\delta\widehat{E}_h|||^2_{\mathcal{V}_h}+\theta\Big(\mathcal{I}^{\mathcal{V}_h}(\widehat{\boldsymbol{u}}_h\times\Pi^{RT}\delta\boldsymbol{B}_h),\delta\widehat{E}_h\Big)_{\mathcal{V}_h}+\theta\Big(\mathcal{I}^{\mathcal{V}_h}(\delta\widehat{\boldsymbol{u}}_h\times\Pi^{RT}\boldsymbol{B}_h),\delta\widehat{E}_h\Big)_{\mathcal{V}_h}-\\-\theta R_m^{-1}\big(\delta\boldsymbol{B}_h,\mathbf{rot}_h\delta\widehat{E}_h\big)_{\mathcal{E}_h}.\end{aligned}$$

Using

$$\begin{aligned}&\theta\Big(\widehat{E}_h,\mathcal{I}^{\mathcal{V}_h}(\delta\widehat{\boldsymbol{u}}_h\times\Pi^{RT}\delta\boldsymbol{B}_h)\Big)_{\mathcal{V}_h}+\theta^3\Big(\mathcal{I}^{\mathcal{V}_h}(\widehat{\boldsymbol{u}}_h\times\Pi^{RT}\boldsymbol{B}_h),\mathcal{I}^{\mathcal{V}_h}(\delta\widehat{\boldsymbol{u}}_h\times\Pi^{RT}\delta\boldsymbol{B}_h)\Big)_{\mathcal{V}_h}+\\&\theta^3\Big(\mathcal{I}^{\mathcal{V}_h}(\widehat{\boldsymbol{u}}_h\times\Pi^{RT}\delta\boldsymbol{B}_h,\mathcal{I}^{\mathcal{V}_h}(\delta\boldsymbol{u}_h\times\Pi^{RT}\boldsymbol{B}_h)\Big)_{\mathcal{V}_h}+\theta^3\Big(\mathcal{I}^{\mathcal{V}_h}(\delta\widehat{\boldsymbol{u}}_h\times\Pi^{RT}\boldsymbol{B}_h),\mathcal{I}^{\mathcal{V}_h}(\delta\widehat{\boldsymbol{u}}_h\times\Pi^{RT}\boldsymbol{B}_h)\Big)_{\mathcal{V}_h}\geq\\&\geq-\widetilde{C}\Delta t\left(\Delta t^{-1}|||\delta\boldsymbol{B}_h|||^2_{\mathcal{E}_h}+\Delta t^{-1}|||\delta\widehat{\boldsymbol{u}}_h|||^2_{\mathcal{TV}_h}\right)\end{aligned}$$

where $\widetilde{C}>0$ depends on $\theta,\|\widehat{\boldsymbol{u}}_h\|_\infty,\|\boldsymbol{B}_h\|_\infty$ and $\|\widehat{E}_h\|_\infty$. And,

$$\begin{aligned}&2\theta\Big(\delta\widehat{E}_h,\mathcal{I}^{\mathcal{V}_h}(\delta\widehat{\boldsymbol{u}}_h\times\Pi^{RT}\boldsymbol{B}_h)\Big)_{\mathcal{V}_h}+\theta\Big(\mathcal{I}^{\mathcal{V}_h}(\widehat{\boldsymbol{u}}_h\times\Pi^{RT}\delta\boldsymbol{B}_h),\delta\widehat{E}_h\Big)_{\mathcal{V}_h}\geq\\&\geq-C_1\Delta t(\Delta t^{-1}|||\delta\widehat{\boldsymbol{u}}_h|||_{\mathcal{TV}_h})-C_2\Delta t(\Delta t^{-1}|||\delta\boldsymbol{B}_h|||_{\mathcal{E}_h})-\frac{1}{2}|||\delta\widehat{E}_h|||^2_{\mathcal{V}_h}\end{aligned}$$

here C_1 depends on $\|\Pi^{RT}\boldsymbol{B}_h\|_\infty$ and C_2 depends on $\|\widehat{\boldsymbol{u}}_h\|_\infty$. Putting these together we find that

$$\begin{aligned}a_{h,0}(\boldsymbol{\xi}_h,\boldsymbol{\eta}_h)&\geq(1-\widetilde{C}\Delta t-C_1\Delta t)\Delta t^{-1}|||\delta\widehat{\boldsymbol{u}}_h|||_{\mathcal{TV}_h}+R_e^{-1}\big|\delta\widehat{\boldsymbol{u}}_h\big|_{\mathcal{TV}_h}+\\&+\left(\frac{R_m^{-1}}{2}-\widetilde{C}\Delta t-C_2\Delta t\right)\Delta t^{-1}|||\delta\boldsymbol{B}_h|||^2_{\mathcal{E}_h}+|||\operatorname{div}\delta\boldsymbol{B}_h|||^2_{\mathcal{E}_h}+\frac{R_m^{-1}\Delta t}{2}|||\mathbf{rot}\,\delta\widehat{E}_h|||^2_{\mathcal{E}_h}+\frac{1}{2}|||\widehat{E}_h|||^2_{\mathcal{V}_h}\end{aligned}$$

We pick Δt in such a way that

$$1-\widetilde{C}\Delta t-C_1\Delta t\geq\frac{1}{2},\quad\frac{R_m^{-1}}{2}-\widetilde{C}\Delta t-C_2\Delta t\geq\frac{R_m^{-1}}{4}.$$

This gives

$$a_{h,0}(\boldsymbol{\xi}_h, \boldsymbol{\eta}_h) \geq \min\left\{\frac{1}{2}, R_e^{-1}\right\} |||\delta\widehat{\boldsymbol{u}}_h|||^2_{\Delta t,\nabla} + \min\left\{\frac{R_m^{-1}}{4}, 1\right\} |||\delta \boldsymbol{B}_h|||^2_{\Delta t,\mathrm{div}} + \\ + \min\left\{\frac{R_m^{-1}}{2}, \frac{1}{2}\right\} |||\delta\widehat{E}_h|||^2_{\Delta t,\mathbf{rot}} \geq \min\left\{\frac{1}{2}, R_e^{-1}, \frac{R_m^{-1}}{4}\right\} |||\boldsymbol{\xi}_h|||^2_{\mathfrak{X}_h},$$

To finish, note that

$$\begin{aligned}
|||\eta_\xi|||^2_{\mathcal{X}_h} &= |||(\theta/2)\left(\boldsymbol{B}_h + \Delta t\,\mathbf{rot}\,E_h\right)|||^2_{\Delta t,\mathrm{div}} + |||E_h|||^2_{\Delta t,\mathbf{rot}} \\
&= \frac{\theta^2}{4}\left(\Delta t^{-1}|||\boldsymbol{B}_h + \Delta t\mathbf{rot}\,E_h|||^2_{\mathcal{E}_h} + \|\mathrm{div}\,\boldsymbol{B}_h\|^2_{0,\Omega}\right) + |||E_h|||^2_{\Delta t,\mathbf{rot}} \\
&= \frac{\theta^2}{4}\left(\Delta t^{-1}|||\boldsymbol{B}_h|||^2_{\mathcal{E}_h} + \Delta t|||\mathbf{rot}\,E_h|||^2_{\mathcal{E}_h} + 2\Big(\boldsymbol{B}_h, \mathbf{rot}\,E_h\Big)_{\mathcal{E}_h} + \|\mathrm{div}\,\boldsymbol{B}_h\|^2_{0,\Omega}\right) + |||E_h|||^2_{\Delta t,\mathbf{rot}} \\
&= \frac{\theta^2}{4}\left(\Delta t^{-1}|||\boldsymbol{B}_h|||^2_{\mathcal{E}_h} + \|\mathrm{div}\,\boldsymbol{B}_h\|^2_{0,\Omega} + 2\Big(\Delta t^{-1/2}\boldsymbol{B}_h, \Delta t^{1/2}\mathbf{rot}\,E_h\Big)_{\mathcal{E}_h} + \Delta t|||\mathbf{rot}\,E_h|||^2_{\mathcal{E}_h}\right) + |||E_h|||^2_{\Delta t,\mathbf{rot}} \\
&\leq \frac{\theta^2}{4}\left(2\Delta t^{-1}|||\boldsymbol{B}_h|||^2_{\mathcal{E}_h} + \|\mathrm{div}\,\boldsymbol{B}_h\|^2_{0,\Omega} + 2\Delta t|||\mathbf{rot}\,E_h|||^2_{\mathcal{E}_h}\right) + |||E_h|||^2_{\Delta t,\mathbf{rot}} \\
&\leq \frac{\theta^2}{2}|||\boldsymbol{B}_h|||^2_{\Delta t,\mathrm{div}} + \left(1 + \frac{\theta^2}{2}\right)|||E_h|||^2_{\Delta t,\mathbf{rot}} \\
&\leq \left(1 + \frac{\theta^2}{2}\right)|||\xi|||^2_{\mathcal{X}_h}.
\end{aligned}$$

□

Finally, we present the main result of this sub section.

Theorem 6.6 *Both problems* (109) *and* (111) *are well-posed.*

Proof. Lemmas 6.4,6.5 and Theorem (4.3) prove that the hypothesis of the BBL theorem are satisfied yielding as a conclusion that (111) is well-posed. Since, as a consequence of Proposition 6.3, problems (109) and (111) are equivalent, the well posedness of one will imply the well-posedness of both. □

We note that this wellposedness result exposes the saddle-point nature of the linear system. This result can be leveraged to come up with efficient preconditioner following the framework laid out in [28]. This was done for a similar MHD system in [29] using a Picard fixed point iteration as the choice of linearization.

6.2.1. *The Exact Jacobian*

The strategy for preconditioning involved requires that we have an expression for the Jacobian $\partial G(\boldsymbol{x}_h)\delta\boldsymbol{x}_h$. To do this, we can select a direction $\boldsymbol{y}_h \in \mathcal{X}_{h,0}$ and use

$$[\partial G(\boldsymbol{x}_h)\delta\boldsymbol{x}_h]\cdot\boldsymbol{y}_h = \lim_{\epsilon\to 0}\frac{G(\boldsymbol{x}_h + \epsilon\delta\boldsymbol{x}_h)\cdot\boldsymbol{y}_h - G(\boldsymbol{x}_h)\cdot\boldsymbol{y}_h}{\epsilon}. \tag{130}$$

This process yields

$$[\partial G(\boldsymbol{x}_h)\delta\boldsymbol{x}_h]\cdot\boldsymbol{y}_h = \ell_1(\boldsymbol{y}_h) + \ell_2(\boldsymbol{y}_h) + \ell_3(\boldsymbol{y}_h) + \ell_4(\boldsymbol{y}_h), \tag{131a}$$

$$\boldsymbol{x}_h = (\widehat{\boldsymbol{u}}_h^I, \boldsymbol{B}_h^I, \widehat{E}_h^I, p_h^I), \quad \delta\boldsymbol{x}_h = (\delta\widehat{\boldsymbol{u}}_h^I, \delta\boldsymbol{B}_h^I, \delta\widehat{E}_h^I, \delta p_h^I), \quad \boldsymbol{y}_h = (\boldsymbol{v}_h^I, \boldsymbol{C}_h^I, D_h^I, q_h^I), \tag{131b}$$

$$\ell_1(\boldsymbol{y}_h) = \Delta t^{-1}\Big(\delta\widehat{\boldsymbol{u}}_h, \boldsymbol{v}_h\Big)_{\mathcal{T}\mathcal{V}_h} + \theta R_e^{-1}\Big[\delta\widehat{\boldsymbol{u}}_h, \boldsymbol{v}_h\Big]_{\mathcal{T}\mathcal{V}_h} + \theta\Big(\widehat{E}_h, \mathcal{I}^{\mathcal{V}_h}(\boldsymbol{v}_h \times \Pi^{RT}\delta\boldsymbol{B}_h)\Big)_{\mathcal{V}_h} + \\ + \theta\Big(\delta\widehat{E}_h, \mathcal{I}^{\mathcal{V}_h}(\boldsymbol{v}_h \times \Pi^{RT}\boldsymbol{B}_h)\Big)_{\mathcal{V}_h} - \Big(\mathrm{div}\,\boldsymbol{v}_h, p_h\Big)_{\mathcal{P}_h}, \tag{131c}$$

$$\ell_2(\boldsymbol{y}_h) = \theta\Big(\mathrm{div}\,\delta\widehat{\boldsymbol{u}}_h, q_h\Big)_{\mathcal{P}_h}, \quad \ell_3(\boldsymbol{y}_h) = \Delta t^{-1}\Big(\delta\boldsymbol{B}_h, \boldsymbol{C}_h\Big)_{\mathcal{E}_h} + \Big(\mathbf{rot}\,\delta E_h, \boldsymbol{C}_h\Big)_{\mathcal{E}_h}, \tag{131d}$$

$$\ell_4(\boldsymbol{y}_h) = \Big(\delta\widehat{E}_h + \theta\mathcal{I}^{\mathcal{V}_h}(\widehat{\boldsymbol{u}}_h \times \Pi^{RT}\delta\boldsymbol{B}_h + \delta\widehat{\boldsymbol{u}}_h \times \Pi^{RT}\boldsymbol{B}_h), \boldsymbol{D}_h\Big)_{\mathcal{V}_h} + R_m^{-1}\theta\big(\delta\boldsymbol{B}_h, \mathbf{rot}_h D_h\big)_{\mathcal{E}_h}. \tag{131e}$$

The process of preconditioning will be done at the discrete level. The Jacobian is

$$\partial G(\boldsymbol{x}_h)\delta\boldsymbol{x}_h = \left[\begin{pmatrix} \mathbb{A} & 0 & \mathbb{B} & \mathbb{C} \\ 0 & \mathbb{D} & \mathbb{E} & 0 \\ \mathbb{B}^T & \mathbb{E}^T & \mathbb{F} & 0 \\ \mathbb{C}^T & 0 & 0 & 0 \end{pmatrix} + \begin{pmatrix} 0 & \mathbb{G}+\mathbb{I} & 0 & 0 \\ 0 & 0 & 0 & 0 \\ 0 & \mathbb{H} & 0 & 0 \\ 0 & 0 & 0 & 0 \end{pmatrix}\right] \begin{pmatrix} \delta\widehat{\boldsymbol{u}}_h^I \\ \delta\boldsymbol{B}_h^I \\ \delta\widehat{E}_h^I \\ \delta p_h^I \end{pmatrix} \tag{132}$$

for

$$\mathbb{A} = \Delta t^{-1}\mathbb{M}_{\mathcal{TV}_h} + \theta R_e^{-1}\$_{\mathcal{TV}_h} + \theta^3\mathbb{M}_{\boldsymbol{B}}^T\mathbb{M}_{\mathcal{V}_h}\mathbb{M}_{\boldsymbol{B}}, \quad \mathbb{B} = \theta\mathbb{M}_{\boldsymbol{B}}^T\mathbb{M}_{\mathcal{V}_h}, \quad \mathbb{C} = \operatorname{div}_h^T\mathbb{M}_{\mathcal{P}_h}, \tag{133a}$$

$$\mathbb{D} = \theta R_m^{-1}\Delta t^{-1}\mathbb{M}_{\mathcal{E}_h}, \quad \mathbb{E} = \theta R_m^{-1}\mathbb{M}_{\mathcal{E}_h}\mathbf{rot}_h, \quad \mathbb{F} = \mathbb{M}_{\mathcal{V}_h}, \quad \mathbb{H} = \theta\mathbb{M}_{\mathcal{V}_h}\mathbb{M}_{\boldsymbol{u}}, \tag{133b}$$

$$\mathbb{I} = \theta^3\mathbb{M}_{\boldsymbol{B}}^T\mathbb{M}_{\mathcal{V}_h}\mathbb{M}_{\boldsymbol{u}} \tag{133c}$$

where

$$\boldsymbol{v}_h^I\cdot\mathbb{M}_{\mathcal{TV}_h}\boldsymbol{u}_h^I = \Big(\boldsymbol{u}_h, \boldsymbol{v}_h\Big)_{\mathcal{TV}_h}, \quad \boldsymbol{v}_h^I\cdot\$_{\mathcal{TV}_h}\boldsymbol{u}_h^I = \Big[\boldsymbol{v}_h, \boldsymbol{u}_h\Big]_{\mathcal{TV}_h}, \quad q_h^I\cdot\mathbb{M}_{\mathcal{P}_h}p_h^I = \Big(q_h, p_h\Big)_{\mathcal{P}_h} \tag{134a}$$

$$\boldsymbol{C}_h^I\cdot\mathbb{M}_{\mathcal{E}_h}\boldsymbol{B}_h^I = \Big(\boldsymbol{C}_h, \boldsymbol{B}_h\Big)_{\mathcal{E}_h}, \quad D_h^I\cdot\mathbb{M}_{\mathcal{V}_h}E_h^I = \Big(D_h, E_h\Big)_{\mathcal{V}_h}, \quad \mathbf{rot}_h E_h^I = [\mathbf{rot}\, E_h]^I, \tag{134b}$$

$$\operatorname{div}_h\boldsymbol{u}_h^I = [\operatorname{div}_h\boldsymbol{u}_h]^I, \quad \mathbb{M}_{\boldsymbol{u}}\boldsymbol{B}_h^I = [\mathcal{I}^{\mathcal{TV}_h}(\widehat{\boldsymbol{u}}_h\times\Pi^{RT}\boldsymbol{B}_h)]^I, \mathbb{M}_{\boldsymbol{B}}\boldsymbol{u}_h^I = [\mathcal{I}^{\mathcal{TV}_h}(\widehat{\boldsymbol{u}}_h\times\Pi^{RT}\boldsymbol{B}_h)]^I \tag{134c}$$

The matrix $\mathbb{G}$ can be computed by selecting a basis consistent with the degrees of freedom for $\mathcal{TV}_{h,0}$ and onether for $\mathcal{E}_h$, say $\{\boldsymbol{v}_h^j\}$ and $\{\boldsymbol{C}_h^i\}$ respectively then

$$\mathbb{G}_{i,j} = \theta\Big(\widehat{E}_h, \mathcal{I}^{\mathcal{V}_h}(\boldsymbol{v}_h^i\times\Pi^{RT}\boldsymbol{C}_h^j)\Big)_{\mathcal{V}_h} + \theta^3\Big(\mathcal{I}^{\mathcal{V}_h}(\widehat{\boldsymbol{u}}_h\times\Pi^{RT}\boldsymbol{B}_h), \mathcal{I}^{\mathcal{V}_h}(\boldsymbol{v}_h^i\times\Pi^{RT}\boldsymbol{C}_h^j)\Big)_{\mathcal{V}_h}. \tag{135}$$

The matrix $\mathbb{G}$ can be computed by selecting a basis consistent with the degrees of freedom for $\mathcal{TV}_{h,0}$ and onether for $\mathcal{E}_h$, say $\{\boldsymbol{v}_h^j\}$ and $\{\boldsymbol{C}_h^i\}$ respectively then

$$\mathbb{G}_{i,j} = \Big(\widehat{E}_h, \mathcal{I}^{\mathcal{V}_h}(\boldsymbol{v}_h^j\times\Pi^{RT}\boldsymbol{C}_h^j)\Big)_{\mathcal{V}_h} \tag{136}$$

$$DG(\boldsymbol{x}_h)\delta\boldsymbol{x}_h = \partial G(\boldsymbol{x}_h)\delta\boldsymbol{x}_h + \epsilon(\boldsymbol{x}_h)\delta\boldsymbol{x}_h \tag{137}$$

7. Numerical Experiments

7.1. *Convergence Analysis*

The first experiment we perform involves assessing the convergence of the numerical method. To this end we set source terms, initial and boundary conditions in accordance with the exact solution given by

$$\boldsymbol{u}(x,y,t) = \begin{pmatrix} e^t\cos y \\ 0 \end{pmatrix}, \quad \boldsymbol{B}(x,y,t) = \begin{pmatrix} 0 \\ \sin t\cos x \end{pmatrix}, \quad E(x,y,t) = \sin x, \quad p(x,y,t) = -x\cos y.$$

This convergence test was proposed in [29]. To check the generality of the method we will the three different types of geometries described in figure 1

7.2. *The Driven Cavity Problem*

The driven cavity problem is a classic benchmark from computational fluid mechanics. In this experiment we consider an electrically conducting fluid that is entirely trapped inside a container with hard walls. The container, in our simulations, will be the square $\Omega = [-1,1]^2$. This fluid is subjected to an external magnetic field given by the initial conditions

$$\boldsymbol{B}_0(x,y) = (1,0). \tag{138}$$

We borrow the set up from [21]. The source term in the momentum equation is neglected i.e. $\boldsymbol{f}\equiv\mathbf{0}$. The initial and boundary conditions on the velocity field are given by

$$\boldsymbol{u}_0(x,y) = \boldsymbol{u}_b(x,y,t) = (0, v(x,y)) \tag{139}$$

where $v\in C^1[-1,1]$ is any function satisfying

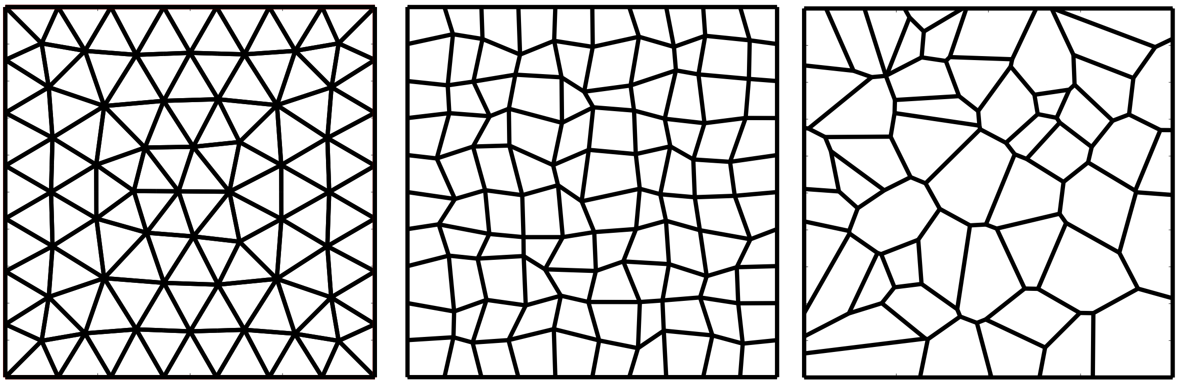

Fig. 1. Illustration of the meshes used for testing the rate of convergence: triangular mesh (left panel), perturbed square mesh (central panel) and Voronoi tesselation (right panel).

$$v(x,y) = \begin{cases} 1 & y = 1 \\ 0 & -1 \leq y \leq 1-h \end{cases} \tag{140}$$

Where $2 > h > 0$ is the mesh-size. Finally, we will consider the walls of our cavity to be made from a perfect conductor. This is reflected in the boundary conditions on the electric field

$$E_b(x,y,t) = 0 \tag{141}$$

7.3. *Magnetic Reconnection*

The next experiment we will perform involves a characteristic feature of resistive MHD, the phenomenon of magnetic reconnection. At very large scales, usually in space physics, the behaviour of plasmas can be well-approximated using ideal MHD. In this case, the magnetic field lines will advect with the fluid. This is often referred to as the ”frozen-in” condition on the magnetic field and it is the statement of Alfven’s Theorem. In certain regions of the earth’s magnetosphere, namely the magnetopause and magnetotail, this process will lead to very thin current sheets that separate regions across which the magnetic field changes substantially. In this test we consider one Harris sheet constrained to the computational domain $\Omega = [-1,1]^2$. The magnetic field in this domain is given by

$$\boldsymbol{B}_0(x,y) = (\tanh y, 0). \tag{142}$$

The above expression will be the initial conditions on the magnetic field. This profile for the magnetic field was introduced in [20]. Its simplicity has made it a common choice in modelling magnetic reconnection. We will further assume that the particles in this sheet are subjected by some external agent to a flow described by

$$\boldsymbol{u}_b(x,y,t) = \boldsymbol{u}_0(x,y) = (-x, y). \tag{143}$$

The above are, mathematically speaking, the initial and boundary conditions on the velocity field. This flow will force the magnetic field lines together at a single point making the current density grow. A tearing instability is formed and magnetic reconnection happens as a response. This process is described in detail in [25, 33]. We close this model by imposing the boundary conditions

$$\forall t > 0: \quad E_b(t) \in \mathbb{P}_0(\partial\Omega), \quad \text{and} \quad \int_{\partial\Omega} \boldsymbol{B}_b(t) \cdot \boldsymbol{n} \, d\ell = 0 \tag{144}$$

8. Conclusions

We have designed a VEM to come up with approximations to the solution to the system of MHD (2). Our analysis shows that the approximations satisfy a set of desirable energy estimates as shown in Theorem 5.2. Moreover, we have also developed a linearization strategy that is easier to implement than the more classical Newton method while simultaneously preserving the rate of convergence. Our well-posedness study shows that each linear solve should be stable. We have also identified three numerical experiments that are of interest. The first will allow us to verify the rate of convergence of the method. The expectation is that such a rate is quadratic, linear, quadratic and linear for the velocity field, pressure, electric field and magnetic field respectively. The second experiment is related to the fluid flow. In a sealed square cavity we push a magnetized fluid tangential to the top wall. The fluid should begin to follow spirals, the number and size of these spirals depend on the magnetic and viscous Reynolds numbers. The final experiment is a model for magnetic reconnection. This phenomenon is characteristic of MHD and a feature in several settings involving plasma physics including space weather and tokemaks. Further work is necessary to complete these numerical experiments.

Acknowledgements.
S. Naranjo Alvarez's work was supported by the National Science Foundation (NSF) grant #1545188, "*NRT-DESE: Risk and uncertainty quantification in marine science and policy*", which provided a one year fellowship and internship support at Los Alamos National Laboratory. S. Naranjo Alvarez also received graduate research funding from V. A. Bokil's DMS grant #1720116, an INTERN supplemental award to Professor Bokil's DMS grant # 1720116 for a second internship at Los Alamos National Laboratory, and teaching support from the Department of Mathematics at Oregon State University. In addition, S. Naranjo Alvarez was also supported by the DOE-ASCR AM (Applied Math) base program grant for a summer internship.

Professor V. A. Bokil is partially supported by NSF funding from the DMS grants # 1720116 and # 2012882. Dr. V. Gyrya and Dr. G. Manzini were supported by the Laboratory Directed Research and Development - Exploratory Research (LDRD-ER) Program of Los Alamos National Laboratory under project number 20180428ER.

The authors would like to thank Dr. K. Lipnikov and Dr. L Chacon, T-5 Group, Theoretical Division, Los Alamos National Laboratory, for their advice during the writing of this article. Los Alamos National Laboratory is operated by Triad National Security, LLC, for the National Nuclear Security Administration of U.S. Department of Energy (Contract No. 89233218CNA000001).

References

[1] B. Ahmad, A. Alsaedi, F. Brezzi, L. D. Marini, and A. Russo, *Equivalent projectors for virtual element methods*, Computers & Mathematics with Applications, 66 (2013), pp. 376–391.

[2] L. Beirão da Veiga, C. Lovadina, and A. Russo, *Stability analysis for the virtual element method*, Mathematical Models and Methods in Applied Sciences, 27 (2017), pp. 2557–2594.

[3] L. Beirao da Veiga, F. Brezzi, L. D. Marini, and A. Russo, *The hitchhiker's guide to the virtual element method*, Mathematical models and methods in applied sciences, 24 (2014), pp. 1541–1573.

[4] L. Beirao da Veiga, F. Brezzi, L. D. Marini, and A. Russo, *H(div) and H(curl)-conforming VEM*, Numerische Mathematik, 133 (2016), pp. 303–332.

[5] ———, *Mixed virtual element methods for general second order elliptic problems on polygonal meshes*, ESAIM: Mathematical Modelling and Numerical Analysis, 50 (2016), pp. 727–747.

[6] D. Boffi, F. Brezzi, M. Fortin, et al., *Mixed finite element methods and applications*, vol. 44, Springer, 2013.

[7] J. U. Brackbill and D. C. Barnes, *The effect of nonzero Div B on the numerical solution of the magnetohydrodynamic equations*, Journal of Computational Physics, 35 (1980), pp. 426–430.

[8] S. C. Brenner and L.-Y. Sung, *Virtual element methods on meshes with small edges or faces*, Mathematical Models and Methods in Applied Sciences, 28 (2018), pp. 1291–1336.

[9] L. Chacón, *An optimal, parallel, fully implicit newton–krylov solver for three-dimensional viscoresistive magnetohydrodynamics*, Physics of Plasmas, 15 (2008), p. 056103.

[10] E. C. Cyr, J. N. Shadid, R. S. Tuminaro, R. P. Pawlowski, and L. Chacón, *A new approximate block factorization preconditioner for two-dimensional incompressible (reduced) resistive mhd*, SIAM Journal on Scientific Computing, 35 (2013), pp. B701–B730.

[11] L. B. da Veiga, F. Brezzi, F. Dassi, L. Marini, and A. Russo, *Virtual element approximation of 2d magnetostatic problems*, Computer Methods in Applied Mechanics and Engineering, 327 (2017), pp. 173–195.

[12] L. B. da Veiga, F. Brezzi, F. Dassi, L. Marini, and A. Russo, *A family of three-dimensional virtual elements with applications to magnetostatics*, SIAM Journal on Numerical Analysis, 56 (2018), pp. 2940–2962.

[13] L. B. da Veiga, K. Lipnikov, and G. Manzini, *The mimetic finite difference method for elliptic problems*, vol. 11, Springer, 2014.

[14] L. B. da Veiga, C. Lovadina, and G. Vacca, *Divergence free virtual elements for the stokes problem on polygonal meshes*, ESAIM: Mathematical Modelling and Numerical Analysis, 51 (2017), pp. 509–535.

[15] L. B. da Veiga, C. Lovadina, and G. Vacca, *Virtual elements for the navier–stokes problem on polygonal meshes*, SIAM Journal on Numerical Analysis, 56 (2018), pp. 1210–1242.

[16] F. Dassi and L. Mascotto, *Exploring high-order three dimensional virtual elements: bases and stabilizations*, Comput. Math. Appl., 75 (2018), pp. 3379–3401.

[17] P. A. Davidson, *An introduction to magnetohydrodynamics*, 2002.

[18] J. Ding and Y. Yang, *Low-dispersive FDTD on hexagon revisited*, Electronics Letters, 53 (2017), pp. 834–835.

[19] S. C. Eisenstat and H. F. Walker, *Choosing the forcing terms in an inexact newton method*, SIAM Journal on Scientific Computing, 17 (1996), pp. 16–32.

[20] E. G. Harris, *On a plasma sheath separating regions of oppositely directed magnetic field*, Il Nuovo Cimento (1955-1965), 23 (1962), pp. 115–121.

[21] R. Hiptmair, L. Li, S. Mao, and W. Zheng, *A fully divergence-free finite element method for magnetohydrodynamic equations*, Mathematical Models and Methods in Applied Sciences, 28 (2018), pp. 659–695.

[22] K. Hu, Y. Ma, and J. Xu, *Stable finite element methods preserving div B = 0 exactly for mhd models*, Numerische Mathematik, 135 (2017), pp. 371–396.

[23] M. Joaquim and S. Scheer, *Finite-difference time-domain method for three-dimensional grid of hexagonal prisms*, Wave Motion, 63 (2016), pp. 32–54.

[24] C. T. KELLEY, *Iterative methods for linear and nonlinear equations*, vol. 16, Siam, 1995.
[25] M. G. KIVELSON, M. G. KIVELSON, AND C. T. RUSSELL, *Introduction to space physics*, Cambridge university press, 1995.
[26] J. G. LIU AND W. C. WANG, *An energy-preserving mac–yee scheme for the incompressible mhd equation*, Journal of Computational Physics, 174 (2001), pp. 12–37.
[27] J. G. LIU AND W. C. WANG, *Energy and helicity preserving schemes for hydro-and magnetohydro-dynamics flows with symmetry*, Journal of Computational Physics, 200 (2004), pp. 8–33.
[28] D. LOGHIN AND A. J. WATHEN, *Analysis of preconditioners for saddle-point problems*, SIAM Journal on Scientific Computing, 25 (2004), pp. 2029–2049.
[29] Y. MA, K. HU, X. HU, AND J. XU, *Robust preconditioners for incompressible mhd models*, Journal of Computational Physics, 316 (2016), pp. 721–746.
[30] L. MASCOTTO, *Ill-conditioning in the virtual element method: stabilizations and bases*, Numer. Methods Partial Differential Equations, 34 (2018), pp. 1258–1281.
[31] R. J. MOREAU, *Magnetohydrodynamics*, vol. 3, Springer Science & Business Media, 2013.
[32] N. A. S, B. V. A, G. V, AND M. G, *A virtual element method for magnetohydrodynamics*, arXiv preprint arXiv:2004.11467, (2020).
[33] K. SCHINDLER, *Physics of space plasma activity*, Cambridge University Press, 2006.
[34] M. A. TAYLOR, B. A. WINGATE, AND L. P. BOS, *Several new quadrature formulas for polynomial integration in the triangle*, arXiv preprint math/0501496, (2005).
[35] G. VACCA, *An H^1-conforming virtual element for darcy and brinkman equations*, Mathematical Models and Methods in Applied Sciences, 28 (2018), pp. 159–194.

9. Constructing The Inner Product Matrices in $\mathcal{TV}_h$

Let P be a cell in the mesh Ω_h. In this section we will assume that, for a bilinear form a_h which will either represent the inner product or semi inner product in $\mathcal{TV}_h$. They are

$$a_h(\boldsymbol{u},\boldsymbol{v}) = \Big(\boldsymbol{u},\boldsymbol{v}\Big), \quad \text{or} \quad a_h(\boldsymbol{u},\boldsymbol{v}) = (\nabla\boldsymbol{u},\nabla\boldsymbol{v}) \tag{145}$$

We assume that we already have a means, using only the degrees of freedom, of computing the quantities

$$a_h(\boldsymbol{x},\boldsymbol{q}), \quad \boldsymbol{x}\in\mathcal{TV}_h, \;\; \boldsymbol{q}\in[\mathbb{P}_2(\mathsf{P})]^2. \tag{146}$$

Let $\Phi := \{\boldsymbol{v}_k\}$ be a basis that is consistent with the degrees of freedom of $\mathcal{TV}_h$ and $Q := \{\boldsymbol{q}_0,...,\boldsymbol{q}_\ell\}$ a basis for $[\mathbb{P}_2(\mathsf{P})]^2$. Then, if we define the matrix G and B whose entries are defined by

$$G_{i,j} = a_h(\boldsymbol{q}_i,\boldsymbol{q}_j) \quad \text{and} \quad B_{i,k} = a_h(\boldsymbol{q}_i,\varphi_k) \quad \text{for} \quad \boldsymbol{q}_{i,j}\in Q, \varphi_k\in\Phi \tag{147}$$

then right multiplication by $\Pi_* := G^{-1}B$ to a vector that carries the degrees of freedom of a function in will yield the coefficients of the expansion of the projection onto the basis Q. We note that in the case that $a_h(\boldsymbol{u},\boldsymbol{v}) = \Big(\nabla\boldsymbol{u},\nabla\boldsymbol{v},\Big)$, the matrix G described above is singular. We fix this by annexing two more equations. We mention this in the section 10.

In the end we are much more concerned with knowing the degrees of freedom of the projection rather than the coefficients in its expansion. Right multiplication by $\Pi = D\Pi^*$ will yield the necessary degrees of freedom, the entries in the matrix D are

$$D_{i,j} = \mathrm{dof}_i(\boldsymbol{q}_j), \quad \boldsymbol{q}_j\in Q. \tag{148}$$

Where $\mathrm{dof}_i(\boldsymbol{q})$ represents the $i-$th degree of freedom of the function $\boldsymbol{q}$. Finally, the inner product matrix is given by

$$M = \Pi_*^T H \Pi_* + |P|(I-\Pi)^T(I-\Pi). \tag{149}$$

where the entries of H are given by

$$H_{i,j} = a_h(\boldsymbol{q}_i,\boldsymbol{q}_j). \tag{150}$$

In this manuscript we will considered the following ordered basis for $[\mathbb{P}_2(\mathsf{P})]^2$.

$$\boldsymbol{q}_1 = \begin{pmatrix}1\\0\end{pmatrix}, \quad \boldsymbol{q}_2 = \begin{pmatrix}0\\1\end{pmatrix}, \quad \boldsymbol{q}_3 = \begin{pmatrix}x\\0\end{pmatrix}, \quad \boldsymbol{q}_4 = \begin{pmatrix}0\\x\end{pmatrix}, \tag{151a}$$

$$\boldsymbol{q}_5 = \begin{pmatrix}y\\0\end{pmatrix}, \quad \boldsymbol{q}_6 = \begin{pmatrix}0\\y\end{pmatrix}, \quad \boldsymbol{q}_7 = \begin{pmatrix}x^2\\0\end{pmatrix}, \quad \boldsymbol{q}_8 = \begin{pmatrix}0\\x^2\end{pmatrix}, \tag{151b}$$

$$\boldsymbol{q}_9 = \begin{pmatrix}y^2\\0\end{pmatrix}, \quad \boldsymbol{q}_{10} = \begin{pmatrix}0\\y^2\end{pmatrix}, \quad \boldsymbol{q}_{11} = \begin{pmatrix}xy\\0\end{pmatrix}, \quad \boldsymbol{q}_{12} = \begin{pmatrix}0\\xy\end{pmatrix}. \tag{151c}$$

10. The semi-inner product in $\mathcal{TV}_h(\mathsf{P})$

We want to approximate the bilinear form

$$a(\boldsymbol{u},\boldsymbol{v}) = \Big(\nabla\boldsymbol{u},\nabla\boldsymbol{v}\Big) \tag{152}$$

First we need to compute $\operatorname{div}\boldsymbol{u}_h$ for $\boldsymbol{u}_h \in \mathcal{TV}_h(\mathsf{P})$. By definition $\operatorname{div}\boldsymbol{u}_h \in \mathbb{P}_0(\mathsf{P})$. Thus, in one hand

$$\int_{\mathsf{P}} \operatorname{div}\boldsymbol{u}_h = \operatorname{div}\boldsymbol{u}_h|\mathsf{P}|. \tag{153}$$

In the other hand

$$\begin{aligned}\int_{\mathsf{P}} \operatorname{div}\boldsymbol{u}_h = \int_{\partial\mathsf{P}} \boldsymbol{u}_h\cdot\boldsymbol{n}d\ell = \sum_{\mathsf{e}\in\partial\mathsf{P}}\int_{\mathsf{e}} \boldsymbol{u}_h\cdot\boldsymbol{n}d\ell = \\ = \sum_{\mathsf{e}\in\partial\mathsf{P}} \frac{|\mathsf{e}|}{6}\left(\boldsymbol{u}_h\cdot\boldsymbol{n}(\mathsf{v}_\mathsf{e}^1) + 4\boldsymbol{u}_h\cdot\boldsymbol{n}(\frac{\mathsf{v}_\mathsf{e}^2+\mathsf{v}_\mathsf{e}^1}{2}) + \boldsymbol{u}_h\cdot\boldsymbol{n}(\mathsf{v}_\mathsf{e}^1)\right)\end{aligned} \tag{154}$$

Where, the edge e has endpoints at the vertices v_e^1 and v_e^2. The above uses a quadrature exact for quadratic polynomials, recall that $\forall\mathsf{e}\in\partial\mathsf{P}: \quad \boldsymbol{u}_h \in [\mathbb{P}_2(\mathsf{e})]^2$. Therefore,

$$\operatorname{div}\boldsymbol{u}_h = \frac{1}{|\mathsf{P}|}\sum_{\mathsf{e}\in\partial\mathsf{P}} \frac{|\mathsf{e}|}{6}\left(\boldsymbol{u}_h\cdot\boldsymbol{n}(\mathsf{v}_\mathsf{e}^1) + 4\boldsymbol{u}_h\cdot\boldsymbol{n}(\frac{\mathsf{v}_\mathsf{e}^2+\mathsf{v}_\mathsf{e}^1}{2}) + \boldsymbol{u}_h\cdot\boldsymbol{n}(\mathsf{v}_\mathsf{e}^1)\right) \tag{155}$$

10.1. *The matrix B*

The structure for the matrix B is taken from [3].

$$B = \begin{pmatrix} P_0(\boldsymbol{v}_1)\dots P_0(\boldsymbol{v}_N) \\ \Big(\nabla\boldsymbol{q}_3,\nabla\boldsymbol{v}_1\Big)\dots\Big(\nabla\boldsymbol{q}_3,\nabla\boldsymbol{v}_N\Big) \\ \vdots\ddots\vdots \\ \Big(\nabla\boldsymbol{q}_{12},\nabla\boldsymbol{v}_1\Big)\dots\Big(\nabla\boldsymbol{q}_{12},\nabla\boldsymbol{v}_N\Big)\end{pmatrix} \tag{156}$$

where we define

$$P_0(\boldsymbol{v}) = \sum_{\mathsf{v}} \boldsymbol{v}(\mathsf{v}). \tag{157}$$

To compute each the rest of the internal entries we use

$$\int_P \nabla\boldsymbol{q}_i\cdot\nabla\boldsymbol{v}_k = \int_{\partial\mathsf{P}} \boldsymbol{v}_k\nabla\boldsymbol{q}_i\boldsymbol{n}d\ell - \int_P \triangle\boldsymbol{q}_i\cdot\boldsymbol{v}_k \tag{158}$$

Note that for any $\boldsymbol{q}_i$ it is the case that $\triangle\boldsymbol{q}_i \in [\mathbb{P}_0(\mathsf{P})]^2$ so we can find $g_i \in \mathbb{P}_1(\mathsf{P})$ such that $\triangle\boldsymbol{q}_i = \nabla g_i$. Then,

$$\begin{aligned}\int_{\mathsf{P}} \nabla\boldsymbol{q}_i\cdot\nabla\boldsymbol{v}_k &= \int_{\partial\mathsf{P}} \boldsymbol{v}_k\cdot\nabla\boldsymbol{q}_i\boldsymbol{n}d\ell - \int_P \triangle\boldsymbol{q}_i\cdot\boldsymbol{v}_k = \\ &= \int_{\partial\mathsf{P}} \boldsymbol{v}_k\cdot\nabla\boldsymbol{q}_i\boldsymbol{n}d\ell + \int_{\mathsf{P}} g_i\operatorname{div}\boldsymbol{v}_k - \int_{\partial\mathsf{P}} g_i\boldsymbol{v}_k\cdot\boldsymbol{n}d\ell = \\ &= (\mathbf{T1}) + (\mathbf{T2}) - (\mathbf{T3})\end{aligned} \tag{159}$$

Now we separate into cases depending on which term we are computing.

10.1.1. *The Term T1*

A formula for T1 will require that we compute the gradient of each of the polynomials, they are:

$$\nabla \boldsymbol{q}_3 = \begin{pmatrix} 1 & 0 \\ 0 & 0 \end{pmatrix}, \quad \nabla \boldsymbol{q}_4 = \begin{pmatrix} 0 & 0 \\ 1 & 0 \end{pmatrix}, \quad \nabla \boldsymbol{q}_5 = \begin{pmatrix} 0 & 1 \\ 0 & 0 \end{pmatrix}, \quad \nabla \boldsymbol{q}_6 = \begin{pmatrix} 0 & 0 \\ 0 & 1 \end{pmatrix}, \quad \nabla \boldsymbol{q}_7 = \begin{pmatrix} 2x & 0 \\ 0 & 0 \end{pmatrix}, \tag{160}$$

$$\nabla \boldsymbol{q}_8 = \begin{pmatrix} 0 & 0 \\ 2x & 0 \end{pmatrix}, \nabla \boldsymbol{q}_9 = \begin{pmatrix} 0 & 2y \\ 0 & 0 \end{pmatrix}, \quad \nabla \boldsymbol{q}_{10} = \begin{pmatrix} 0 & 0 \\ 0 & 2y \end{pmatrix} \quad \nabla \boldsymbol{q}_{11} = \begin{pmatrix} y & x \\ 0 & 0 \end{pmatrix}, \quad \nabla \boldsymbol{q}_{12} = \begin{pmatrix} 0 & 0 \\ y & x \end{pmatrix}. \tag{161}$$

We use Simpson's Rule to compute the integrals that come up. We note that Simpson's Rule is exact for cubic polynomials.

$$\int_{\partial \mathsf{P}} \boldsymbol{v}_k \cdot \nabla \boldsymbol{q}_3 \boldsymbol{n} d\ell = \sum_{\mathsf{e} \in \partial \mathsf{P}} \frac{|\mathsf{e}| n_x}{6} \left(v_{k,x}(\mathsf{v}_1^{\mathsf{e}}) + 4 v_{k,x}(\mathsf{v}_{3/2}^{\mathsf{e}}) + v_{k,x}(\mathsf{v}_2^{\mathsf{e}}) \right),$$

$$\int_{\partial \mathsf{P}} \boldsymbol{v}_k \cdot \nabla \boldsymbol{q}_4 \boldsymbol{n} d\ell = \sum_{\mathsf{e} \in \partial \mathsf{P}} \frac{|\mathsf{e}| n_x}{6} \left(v_{k,y}(\mathsf{v}_1^{\mathsf{e}}) + 4 v_{k,y}(\mathsf{v}_{3/2}^{\mathsf{e}}) + v_{k,y}(\mathsf{v}_2^{\mathsf{e}}) \right),$$

$$\int_{\partial \mathsf{P}} \boldsymbol{v}_k \cdot \nabla \boldsymbol{q}_5 \boldsymbol{n} d\ell = \sum_{\mathsf{e} \in \partial \mathsf{P}} \frac{|\mathsf{e}| n_y}{6} \left(v_{k,x}(\mathsf{v}_1^{\mathsf{e}}) + 4 v_{k,x}(\mathsf{v}_{3/2}^{\mathsf{e}}) + v_{k,x}(\mathsf{v}_2^{\mathsf{e}}) \right),$$

$$\int_{\partial \mathsf{P}} \boldsymbol{v}_k \cdot \nabla \boldsymbol{q}_6 \boldsymbol{n} d\ell = \sum_{\mathsf{e} \in \partial \mathsf{P}} \frac{|\mathsf{e}| n_y}{6} \left(v_{k,y}(\mathsf{v}_1^{\mathsf{e}}) + 4 v_{k,y}(\mathsf{v}_{3/2}^{\mathsf{e}}) + v_{k,y}(\mathsf{v}_2^{\mathsf{e}}) \right),$$

$$\int_{\partial \mathsf{P}} \boldsymbol{v}_k \cdot \nabla \boldsymbol{q}_7 \boldsymbol{n} d\ell = \sum_{\mathsf{e} \in \partial \mathsf{P}} \frac{|\mathsf{e}| n_x}{3} \left(\mathsf{v}_1^{\mathsf{e},x} v_{k,x}(\mathsf{v}_1^{\mathsf{e}}) + 4 \mathsf{v}_{3/2}^{\mathsf{e},x} v_{k,x}(\mathsf{v}_{3/2}^{\mathsf{e}}) + \mathsf{v}_2^{\mathsf{e},x} v_{k,x}(\mathsf{v}_2^{\mathsf{e}}) \right),$$

$$\int_{\partial \mathsf{P}} \boldsymbol{v}_k \cdot \nabla \boldsymbol{q}_8 \boldsymbol{n} d\ell = \sum_{\mathsf{e} \in \partial \mathsf{P}} \frac{|\mathsf{e}| n_x}{3} \left(\mathsf{v}_1^{\mathsf{e},x} v_{k,y}(\mathsf{v}_1^{\mathsf{e}}) + 4 \mathsf{v}_{3/2}^{\mathsf{e},x} v_{k,y}(\mathsf{v}_{3/2}^{\mathsf{e}}) + \mathsf{v}_2^{\mathsf{e},x} v_{k,y}(\mathsf{v}_2^{\mathsf{e}}) \right),$$

$$\int_{\partial \mathsf{P}} \boldsymbol{v}_k \cdot \nabla \boldsymbol{q}_9 \boldsymbol{n} d\ell = \sum_{\mathsf{e} \in \partial \mathsf{P}} \frac{|\mathsf{e}| n_y}{3} \left(\mathsf{v}_1^{\mathsf{e},y} v_{k,x}(\mathsf{v}_1^{\mathsf{e}}) + 4 \mathsf{v}_{3/2}^{\mathsf{e},y} v_{k,x}(\mathsf{v}_{3/2}^{\mathsf{e}}) + \mathsf{v}_2^{\mathsf{e},y} v_{k,x}(\mathsf{v}_2^{\mathsf{e}}) \right),$$

$$\int_{\partial \mathsf{P}} \boldsymbol{v}_k \cdot \nabla \boldsymbol{q}_{10} \boldsymbol{n} d\ell = \sum_{\mathsf{e} \in \partial \mathsf{P}} \frac{|\mathsf{e}| n_y}{3} \left(\mathsf{v}_1^{\mathsf{e},y} v_{k,y}(\mathsf{v}_1^{\mathsf{e}}) + 4 \mathsf{v}_{3/2}^{\mathsf{e},y} v_{k,y}(\mathsf{v}_{3/2}^{\mathsf{e}}) + \mathsf{v}_2^{\mathsf{e},y} v_{k,y}(\mathsf{v}_2^{\mathsf{e}}) \right),$$

$$\int_{\partial \mathsf{P}} \boldsymbol{v}_k \cdot \nabla \boldsymbol{q}_{11} \boldsymbol{n} d\ell = \sum_{\mathsf{e} \in \partial \mathsf{P}} \frac{|\mathsf{e}|}{6} \left(v_{k,x}(\mathsf{v}_1^{\mathsf{e}})(\mathsf{v}_1^{\mathsf{e},y} n_x + \mathsf{v}_1^{\mathsf{e},x} n_y) + 4 v_{k,x}(\mathsf{v}_{3/2}^{\mathsf{e}})(\mathsf{v}_{3/2}^{\mathsf{e},y} n_x + \mathsf{v}_{3/2}^{\mathsf{e},x} n_y) + v_{k,x}(\mathsf{v}_2^{\mathsf{e}}(\mathsf{v}_2^{\mathsf{e},y} n_x + \mathsf{v}_2^{\mathsf{e},x} n_y)) \right),$$

$$\int_{\partial \mathsf{P}} \boldsymbol{v}_k \cdot \nabla \boldsymbol{q}_{12} \boldsymbol{n} d\ell = \sum_{\mathsf{e} \in \partial \mathsf{P}} \frac{|\mathsf{e}|}{6} \left(v_{k,y}(\mathsf{v}_1^{\mathsf{e}})(\mathsf{v}_1^{\mathsf{e},y} n_x + \mathsf{v}_1^{\mathsf{e},x} n_y) + 4 v_{k,x}(\mathsf{v}_{3/2}^{\mathsf{e}})(\mathsf{v}_{3/2}^{\mathsf{e},y} n_x + \mathsf{v}_{3/2}^{\mathsf{e},x} n_y) + v_{k,y}(\mathsf{v}_2^{\mathsf{e}}(\mathsf{v}_2^{\mathsf{e},y} n_x + \mathsf{v}_2^{\mathsf{e},x} n_y)) \right).$$

10.1.2. *Terms T2 and T3*

To compute the two remaining terms we need the corresponding g_i. First we note that $\triangle \boldsymbol{q}_i = \boldsymbol{0}$ for $i = 2, 3, 4, 5, 6, 11, 12$, we can pick the corresponding value of g_i to be exactly 0. For the rest of the polynomials we have

$$\triangle \boldsymbol{q}_7 = \begin{pmatrix} 2 \\ 0 \end{pmatrix} = \nabla(2x) = \nabla g_7, \quad \triangle \boldsymbol{q}_8 = \begin{pmatrix} 0 \\ 2 \end{pmatrix} = \nabla(2y) = \nabla g_8,$$
$$\triangle \boldsymbol{q}_9 = \begin{pmatrix} 2 \\ 0 \end{pmatrix} = \nabla(2x) = \nabla g_9, \quad \triangle \boldsymbol{q}_{10} = \begin{pmatrix} 0 \\ 2 \end{pmatrix} = \nabla(2y) = \nabla g_{10}.$$

Thus, to compute $(\mathbf{T2})$ we can use

$$\int_{\mathsf{P}} g_7 \mathrm{div}\, \boldsymbol{v}_k = \int_{\mathsf{P}} g_9 \mathrm{div}\, \boldsymbol{v}_k = 2|\mathsf{P}|(\mathrm{div}\, \boldsymbol{v}_k)(x_{\mathsf{P}}),$$
$$\int_{\mathsf{P}} g_8 \mathrm{div}\, \boldsymbol{v}_k = \int_{\mathsf{P}} g_{10} \mathrm{div}\, \boldsymbol{v}_k = 2|\mathsf{P}|(\mathrm{div}\, \boldsymbol{v}_k)(y_{\mathsf{P}}).$$

Here, $(x_{\mathsf{P}}, y_{\mathsf{P}})$ is the centroid of P. Finally, to compute $(\mathbf{T3})$ we use

$$\int_{\partial \mathsf{P}} g_7 \boldsymbol{v}_k \cdot \boldsymbol{n} d\ell = \int_{\partial \mathsf{P}} g_9 \boldsymbol{v}_k \cdot \boldsymbol{n} d\ell = \sum_{\mathsf{e}\in\partial\mathsf{P}} \frac{|\mathsf{e}|}{3} \left(\mathsf{v}_1^{\mathsf{e},x} \boldsymbol{v}_k \cdot \boldsymbol{n}(\mathsf{v}_1^{\mathsf{e}}) + 4\mathsf{v}_{3/2}^{\mathsf{e},x} \boldsymbol{v}_k \cdot \boldsymbol{n}(\mathsf{v}_{3/2}^{\mathsf{e}}) + \mathsf{v}_2^{\mathsf{e},x} \boldsymbol{v}_k \cdot \boldsymbol{n}(\mathsf{v}_2^{\mathsf{e}})\right)$$

$$\int_{\partial \mathsf{P}} g_8 \boldsymbol{v}_k \cdot \boldsymbol{n} d\ell = \int_{\partial \mathsf{P}} g_{10} \boldsymbol{v}_k \cdot \boldsymbol{n} d\ell = \sum_{\mathsf{e}\in\partial\mathsf{P}} \frac{|\mathsf{e}|}{3} \left(\mathsf{v}_1^{\mathsf{e},y} \boldsymbol{v}_k \cdot \boldsymbol{n}(\mathsf{v}_1^{\mathsf{e}}) + 4\mathsf{v}_{3/2}^{\mathsf{e},y} \boldsymbol{v}_k \cdot \boldsymbol{n}(\mathsf{v}_{3/2}^{\mathsf{e}}) + \mathsf{v}_2^{\mathsf{e},y} \boldsymbol{v}_k \cdot \boldsymbol{n}(\mathsf{v}_2^{\mathsf{e}})\right)$$

10.2. *The Matrix G and H*

In the case where we consider

$$a_h(\boldsymbol{u}, \boldsymbol{v}) = \Big(\nabla \boldsymbol{u}, \nabla \boldsymbol{v}\Big)$$

The matrices G and H are

$$G = \begin{pmatrix} P_0(\boldsymbol{q}_1) & P_0(\boldsymbol{q}_2) & P_0(\boldsymbol{q}_3) & \dots & P_0(\boldsymbol{q}_{12}) \\ 0 & 0 & \Big(\nabla \boldsymbol{q}_3, \nabla \boldsymbol{q}_3\Big) & \dots & \Big(\nabla \boldsymbol{q}_3, \nabla \boldsymbol{q}_{12}\Big) \\ \vdots & \vdots & \ddots & \vdots & \\ 0 & 0 & \Big(\nabla \boldsymbol{q}_{12}, \nabla \boldsymbol{q}_3\Big) & \dots & \Big(\nabla \boldsymbol{q}_{12}, \nabla \boldsymbol{q}_{12}\Big) \end{pmatrix}, \quad H = \begin{pmatrix} 0 & 0 & 0 & \dots & 0 \\ 0 & 0 & 0 & \dots & 0 \\ 0 & 0 & \Big(\nabla \boldsymbol{q}_3, \nabla \boldsymbol{q}_3\Big) & \dots & \Big(\nabla \boldsymbol{q}_3, \nabla \boldsymbol{q}_{12}\Big) \\ \vdots & \vdots & \ddots & \vdots & \\ 0 & 0 & \Big(\nabla \boldsymbol{q}_{12}, \nabla \boldsymbol{q}_3\Big) & \dots & \Big(\nabla \boldsymbol{q}_{12}, \nabla \boldsymbol{q}_{12}\Big) \end{pmatrix}.$$

In order to compute the quantities $\Big(\nabla \boldsymbol{q}_i, \nabla \boldsymbol{q}_j\Big)$ we can divide each element P into triangles and we apply

$$\int_T f(x,y) dA = \frac{|T|}{3} \left(f(\mathsf{v}_{1/2}) + f(\mathsf{v}_{3/2}) + f(\mathsf{v}_{5/2})\right)$$

the evaluations are done at the midpoint of edges. We note that the above quadrature is exact for up to quadratic polynomial.

11. The Mass Matrix in $\mathcal{TV}_h(\mathsf{P})$

The first step in computing the mass matrix is to come up with a method to compute integrals of the form

$$\int_{\mathsf{P}} \boldsymbol{v}_h \cdot \boldsymbol{q}, \tag{162}$$

for $\boldsymbol{q} \in [\mathbb{P}_2(\mathsf{P})]^2$ and $\boldsymbol{v}_h \in \mathcal{V}_h(\mathsf{P})$. First, note that in the case that $\boldsymbol{q} \in [\mathbb{P}_0(\mathsf{P})]^2$, then we can find $g \in \mathbb{P}_1(0)$ such that $\nabla g = \boldsymbol{q}$. Applying an integration by parts formula.

$$\int_{\mathsf{P}} \boldsymbol{v}_h \cdot \boldsymbol{q} = \int_{\partial \mathsf{P}} g \boldsymbol{v}_h \cdot \boldsymbol{n} d\ell - \operatorname{div} \boldsymbol{v}_h \int_{\mathsf{P}} g, \tag{163}$$

In the case where we have a general polynomial $\boldsymbol{q} \in [\mathbb{P}_2(\mathsf{P})]^2$. Then, by construction $\boldsymbol{q} - \boldsymbol{c} \in \mathcal{G}_2^{\perp}(\mathsf{P})/\mathbb{R}^2$ for $\boldsymbol{c} = \int_{\mathsf{P}} \boldsymbol{q}$ implying that

$$\int_{\mathsf{P}} \boldsymbol{v}_h \cdot \boldsymbol{q} = \int_{\mathsf{P}} \boldsymbol{v}_h \cdot (\boldsymbol{q} - \boldsymbol{c}) + \int_{\mathsf{P}} \boldsymbol{v}_h \cdot \boldsymbol{c}. \tag{164}$$

We already know how to compute $\int_{\mathsf{P}} \boldsymbol{v}_h \cdot \boldsymbol{c}$. And, by definition of $\mathcal{TV}_h(\mathsf{P})$ we have that

$$\int_{\mathsf{P}} \boldsymbol{v}_h \cdot (\boldsymbol{q} - \boldsymbol{c}) = \int_{\mathsf{P}} \Pi_{\mathsf{P}}^{\nabla} \boldsymbol{v}_h \cdot (\boldsymbol{q} - \boldsymbol{c}) \tag{165}$$

In order to compute many of the integrals that will arise we will need a quadrature formula exact for quartic polynomials. We borrow this quadrature from [34]. However, we need To apply a transformation that maps the triangle T_0 with vertices at $(0,1), (1,0)$ and $(0,0)$ to the triangle T with vertices at $(x_0, y_0), (x_1, y_1)$ and (x_2, y_2). Such a transformation is

$$L(x,y) = \begin{pmatrix} x_1 - x_0 & x_2 - x_0 \\ y_1 - y_0 & y_2 - y_0 \end{pmatrix} \begin{pmatrix} x \\ y \end{pmatrix} + \begin{pmatrix} x_0 \\ y_0 \end{pmatrix} \tag{166}$$

Thus, we will use the following integration formula

$$\int_T f = [(x_1 - x_0)(y_2 - y_0) - (x_2 - x_0)(y_1 - y_0)] \int_{T_0} f \circ L \tag{167}$$

We will use the quadrature rule presented in [34].

12. Computing G

The variational formulation is given by

$$\begin{aligned}
&\Big(\frac{\boldsymbol{u}_h^{n+1} - \boldsymbol{u}_h^n}{\Delta t}, \boldsymbol{v}_h\Big)_{\mathcal{TV}_h} + R_e^{-1}\Big[\boldsymbol{u}_h^{n+\theta}, \boldsymbol{v}_h\Big]_{\mathcal{TV}_h} + \Big(J_h^{n+\theta}, \mathcal{I}^{\mathcal{V}_h}(\boldsymbol{v}_h \times \Pi^{RT}\boldsymbol{B}_h^{n+\theta})\Big)_{\mathcal{V}_h} \\
&- \Big(\operatorname{div}\boldsymbol{v}_h, p_h^{n+\theta}\Big)_{\mathcal{P}_h} = \Big(\boldsymbol{f}_h, \boldsymbol{v}_h\Big)_{\mathcal{TV}_h}, && (168a)\\
&\Big(\operatorname{div}\boldsymbol{u}_h^{n+\theta}, q_h\Big)_{\mathcal{P}_h} = 0, && (168b)\\
&\left(\frac{\boldsymbol{B}_h^{n+1} - \boldsymbol{B}_h^n}{\Delta t}, \boldsymbol{C}_h\right)_{\mathcal{E}_h} + \Big(\mathbf{rot}\, E_h^{n+\theta}, \boldsymbol{C}_h\Big)_{\mathcal{E}_h} = 0, && (168c)\\
&\big(J_h^{n+\theta}, D_h\big)_{\mathcal{V}_h} - R_m^{-1}\big(\boldsymbol{B}_h^{n+\theta}, \mathbf{rot}\, D_h\big)_{\mathcal{E}_h} = 0, && (168d)\\
&\boldsymbol{u}_h^{n+\theta} = (1-\theta)\boldsymbol{u}_h^n + \theta\boldsymbol{u}_h^{n+1}, \quad \boldsymbol{B}_h^{n+\theta} = (1-\theta)\boldsymbol{B}_h^n + \theta\boldsymbol{B}_h^{n+1}, && (168e)\\
&J_h^{n+\theta} = E_h^{n+\theta} + \mathcal{I}^{\mathcal{V}_h}(\boldsymbol{u}_h^{n+\theta} \times \Pi^{RT}\boldsymbol{B}_h^{n+\theta}), && (168f)
\end{aligned}$$

We want to compute $G(\boldsymbol{x})$ which is defined in such a way that $G(\boldsymbol{x}) \cdot \boldsymbol{y}$ is the sum of (168a)-(168d). To recall

$$\boldsymbol{x} = (\widehat{\boldsymbol{u}}_h^{n+1,I}, \boldsymbol{B}_h^{n+1,I}, \widehat{E}_h^{n+\theta,I}, p_h^{n+\theta,I}), \quad \boldsymbol{y} = (\boldsymbol{v}_h^I, \boldsymbol{C}_h^I, D_h^I, q_h^I) \tag{169}$$

If we wanted to know the first entry in $G(\boldsymbol{x})$ we could test against

$$\boldsymbol{y} = (\boldsymbol{e}_1, \mathbf{0}, \mathbf{0}, \mathbf{0}) \tag{170}$$

This works as long $\boldsymbol{e}_1 \in (\mathcal{TV}_{h,0})^I$, and $\mathbf{0} \in (\mathcal{V}_{h,0})^I, (\mathcal{E}_h)^I, (\mathcal{V}_{h,0})^I, (\mathcal{P}_{h,0})^I$. This works well for the spaces $(\mathcal{TV}_{h,0})^I, (\mathcal{E}_h)^I, (\mathcal{V}_{h,0})^I$ do contain a basis that is consistent with the degrees of freedom. Unfortunately, this is not the case for $\mathcal{P}_{h,0}$, note that by construction it must be the case that

$$\sum_i (q_h^I)_i = 0. \tag{171}$$

Next we will propose a solution to this problem. Let us consider $\{\mathsf{P}_i : 1 \le i \le N\}$ as the set of cells in the mesh Ω_h. Moreover, let us consider

$$q_h^I = ((q_h^I)_1, \dots, (q_h^I)_{N-1}) \tag{172}$$

This is to say that we are going to ignore the last entry in the test function. When the information is necessary we will use the identity

$$(q_h^I)_N = -\sum_{i=1}^{N-1} (q_h^I)_i \tag{173}$$

In this case we can find a basis that is consistent with respect to the degrees of freedom. We need to note that the outcome of this process should only yield

$$p_h^I = ((p_h^I)_1, \dots, (p_h^I)_{N-1}) \tag{174}$$

the final entry can be found as before. Mathematically speaking what we are doing is considering a basis for $\mathcal{P}_{h,0}$. In term we are writing the arrays as

$$\begin{pmatrix} q_1 \\ \vdots \\ q_N \end{pmatrix} = q_1 \begin{pmatrix} 1 \\ 0 \\ \vdots \\ -1 \end{pmatrix} + q_2 \begin{pmatrix} 0 \\ 1 \\ \vdots \\ -1 \end{pmatrix} + \cdots + q_{N-1} \begin{pmatrix} 0 \\ \vdots \\ 1 \\ -1 \end{pmatrix}. \tag{175}$$

The first step is to compute the projector $\Pi^0 : \mathcal{TV}_h(\mathsf{P}) \to \big[\mathbb{P}_2(\mathsf{P})\big]^2$ defined by

$$\int_{\mathsf{P}} \Pi^0 \boldsymbol{v}_h \cdot \boldsymbol{q} dV = \int_{\mathsf{P}} \boldsymbol{v}_h \cdot \boldsymbol{q} dV \quad \forall \boldsymbol{q} \in \left[\mathbb{P}_2(\mathsf{P})\right]^2.$$